Univerzita Karlova
Přírodovědecká fakulta

Vývojová a buněčná biologie

Mgr. Lívia Uličná

Function of nuclear phosphoinositides and their binding partners in gene expression
Funkce jaderných fosfoinozitidů a jejich vazebných partnerů v genové expresi

Disertační práce

Školitel: Prof. RNDr. Pavel Hozák, DrSc.

Praha 2018

Prohlášení:

Prohlašuji, že jsem závěrečnou práci zpracovala samostatně a že jsem uvedla všechny použité informační zdroje a literaturu. Tato práce ani její podstatná část nebyla předložena k získání jiného nebo stejného akademického titulu.

V Praze, 16.02.2018

Podpis

At the first place, I would like to thank my supervisor Prof. Pavel Hozak who allowed me do my PhD study in his lab. During these years, he prepared me for the tough life of a scientist and taught me how to be an independent researcher.

I am very grateful to Bětka Krausová and Janka Rohožková, wonderfull friends and colleagues and last but not least great scientists, for their kindness, support, and friendship. They surely did my PhD life easier.

I would like to thank Tomáš Venit and Pavel Marášek whose attitude help me adjust and feel welcome in the lab. I always look forward to our meetings and sharing crazy life stories.

I am thankful to Sara E. E. Lopes and Míla Manínová for moral support and fruitful discussions, which constantly cheered me up during this last year.

I would like to thank all former and present members of the Hozak lab for their help and creating a nice friendly environment.

Last but not least, I would like to thank from all of my heart my family, especially to beloved Filip, for endless support and help.

Thank you!

ABBREVIATIONS

Akt, protein kinase B

Arp, actin-related protein

ATX, Arabidopsis homolog of trithorax

BASP1, brain acid soluble protein 1

BRG-1, Brahma-related gene 1

DAG, diacylglycerol

EBP1, ErbB3 binding protein-1

EN-actin, EYEP-NLS actin

ENTH, epsin N-terminal homology domain

F-actin, filamentous actin

FERM, 4.1/ezrin/radixin/moesin domain

FYVE, Fab1/YOTB/Vac1/EEA domain

G-actin, globular actin

GAL1, galactokinase 1

HDAC1, histone deacetylase 1

IMPK, inositol multiphosphate kinase

ING2, ihibitor of growth protein 2

IP3, inositol 1,4,5-trisphosphate

Jmjd-1.1, PHD and JmjC domain-containing protein 1.1

Jmjd-1.2, PHD and JmjC domain-containing protein 1.2

K/R rich motif, lysine/ariginine rich motif

MARCKS, Myristoylated Alanine Rich Protein Kinase C

PH, pleckstrin homology domain

PHD, plant homeodomain

PHF8, plant homeodomain finger protein 8

PI, phosphatidylinositol

PIs, phosphoinositides

PI-PLC, phosphatidylinositol-specific phospholipase C

PIPTs, PI transfer proteins

PI(3)P, phosphatidylinositol 3-phosphate

PI(3,4)P2, phosphatidylinositol 3,4-bisphosphate

PI(3,4,5)P3, phosphatidylinositol 3,4,5-trisphosphate

PI(3,5)P2, phosphatidylinositol 3,5-bisphosphate

PI(4)P, phosphatidylinositol 4-phosphate

PI(4,5)P2 4-Ptase I, phosphatidylinositol 4,5-bisphosphate 4-phosphatase

PI(4,5)P2, phosphatidylinositol 4,5-bisphosphate

PI(5)P, phosphatidylinositol 5-phosphate

PKCδ, protein kinase C δ

PI3KC2α, phosphatidylinositol 3-kinase type IIα

PI3KC2β, phosphatidylinositol 3-kinase type IIβ

PI3Kβ, phosphatidylinositol 3-kinase type Iβ

PI3Kγ, phosphatidylinositol 3-kinase type Iγ

PI4Kα, phosphatidylinositol 4-kinase α

PI4Kβ, phosphatidylinositol 4-kinase β

PIKfyve, FYVE finger-containing phosphoinositide kinase

PIP4KIIα, phosphatidylinositol 5-phosphate 4-kinase type IIα

PIP4KIIβ, phosphatidylinositol 5-phosphate 4-kinase type IIβ

PIP5KIα, phosphatidylinositol 4-phosphate 5-kinase type Iα

PIP5KIγ, phosphatidylinositol 4-phosphate 5-kinase I γ

PIP5KIγ_i4, phosphatidylinositol 4-phosphate 5-kinase type Iγ_i4

PTEN, phosphatase and tensin homolog

PX, phox homology domain

RING finger domain, really interesting new gene finger domain

RNA Pol I and II, RNA polymerase I and II

SARA, Smad anchor for receptor activation

SF-1, steroidogenic factor 1

SL1, promoter selectivity factor 1

SMO, Smoothened

SHIP-1, Src-homology 2-containing inositol 5-phosphatase 1

SHIP-2, Src-homology 2-containing inositol 5-phosphatase 2

UBF, upstream binding factor 1

UHFR1, ubiquitin-like PHD and RING finger domain-containing protein 1

ABSTRAKT (ČESKÝ)

Fosfoinozitidy jsou negativně nabité fosfolipidy s inositolovou hlavičkou, která může být fosforylovaná. Fosforylací inositolu vzniká sedm různě fosforylovaných forem fosfoinozitidů, které mohou být mono-, bis- nebo tris-fosforylované. Role cytoplasmatických fosfoinozitidů byly popsané v regulaci dynamiky buněčných membrán a cytoskeletu, v transportu membránových váčků, v funkci iontových kanálů a transportérů a produkci druhých poslů. Jaderné fosfoinozitidy se podílejí na posttranskripčních úpravách a exportu pre-mRNA, DNA transkripci a remodelování chromatinu. Zatímco cytoplasmatické funkce jsou dobře popsané, molekulární mechanizmy jaderných fosfoinozitidů v těchto jaderných procesech nebyly doposud dostatečně prozkoumány. V této práci jsme si kladli za cíl popsat lokalizaci fosfoinozitidů v jednotlivých funkčních kompartmentech jádra, což nám napomůže objasnit zapojení fosfoinozitidů do jaderných procesů. Dále jsme se zaměřili na identifikaci jaderných fosfoinozitidů zapojených do regulace genové exprese a objasnení detailního mechanismu interakce PI(4,5)P2 a PHF8 v regulaci transkripce ribozomálních genů.

Dvěma nezávislými metodami jsme popsali lokalizaci fosfoinozitidů na jaderné membráně, v jaderných škvrnách, nukleoplasmě a jadérku. Tato rozšířená jaderná lokalizace naznačuje a i potvrzuje jejich zapojení do procesů jako signalizace a tvorba sekundárních poslů, přepis a sestřih genů.

Známý PI(4,5)P2 vazebným proteinem zapojeným do regulace transkripce je aktin, který může být v buňce přítomný ve dvou formách, a to monomerní a fibrilární. Avšak přítomnost fibrilárního aktinu v jádře prozatím není dobře popsaná. V této práci ukazujeme, že aktin v buněčném jádře tvoří vlákna, která kolokalizují se známými aktin vazobnými proteiny, jako je kofilín a aktín příbuzný protein 3 (Arp3). Tvorba aktinových vláken v jádře zvýšuje transkripci v S fázi buněčného cyklu a na druhé straně snižuje buněčnou proliferaci a způsobuje aberantní mitózu.

Navíc zde popisujeme přímou interakci mezi PI(4,5)P2 a lyzín-specifickou histon demetylázou PHF8, která demetyluje H3K9me2/1, H3K27me2 a H4K20me1. Přes tuto interakci PI(4,5)P2 snižuje PHF8 aktivitu jako aktivátora transkripce ribozomálních genů. Proto je PI(4,5)P2 důležitým regulátorem genové exprese ribosomálních genů na epigenetické úrovni.

Využitím modelu *Caenorhabditis elegans* jsme ukázali, že samotný PI(4,5)P2 je důležitá molekula zapojená do různých jaderných procesů, jako je, párování chromozomů, apoptóza způsobená poškozením DNA nebo stav chromatinu v zárodečných buňkách.

ABSTRACT (ENGLISH)

Phosphoinositides (PIs) are negatively charged glycerol-based phospholipids with inositol head (ring) which can be phosphorylated. Inositol ring phosphorylation yields in seven different PIs species which can be mono-, bis,- or tris-phosphorylated. Roles of cytoplasmic PIs have been extensively studied in for membrane and cytoskeletal dynamics, vesicular trafficking, ion channels and transporters and generating of second messengers. Nuclear PIs have been implicated in posttranscriptional processing of pre-mRNA, DNA transcription and chromatin remodelling. While cytoplasmic functions are very well described, the molecular mechanism of their nuclear functions are still poorly understood. In this study we focus on description of localization of nuclear PIs in particular functional nuclear compartments, which enable us to reveal PIs involvement in nuclear processes. We also focused on identification of nuclear PIs involved in the regulation of genes transcription and revealed detailed mechanism of PI(4,5)P2 a PHF8 interaction in the regulation of ribosomal genes transcription.

By two independent approaches, we have described PIs localization to the nuclear membrane, nuclear speckles, small foci in the nucleoplasm, and the nucleolus. This spread nuclear localization suggests and confirms PI´s involvement in various processes such as signalling, production of secondary messengers, splicing and transcription.

Known PI(4,5)P2 binding protein involved in the regulation of transcription is actin which can be present in the cell in two forms, as monomeric or filamentous. However, the presence of filamentous actin in the cell nucleus is not well described. Here we show that actin can form filaments in the cell nucleus and these filaments col-localize with known actin binding proteins, such as cofilin and actin related protein 3 (Arp3). The presence of nuclear filamentous actin increases transcription in S-phase and on the other hand decreases cell proliferation and aberrant mitosis.

Moreover, we demonstrated a direct interaction of PI(4,5)P2 with histone lysine demethylase PHF8 (PHF8), enzyme that demethylates H3K9me2/1, H3K27me2, H4K20me1. Through this interaction PI(4,5)P2 represses PHF8 function as rRNA genes transcription activator. Therefore, is PI(4,5)P2 an important regulator at the epigenetic level and contributes to the fine-tuning of rRNA genes expression.

Using *Caenorhabditis elegans* as s model organism, we showed that PI(4,5)P2 itself is involved in various nuclear processes such as chromosome pairing, DNA-damage driven apoptosis or chromatin shape in germ cells.

1 INTRODUCTION

1.1 Localization and function of phosphoinositides

Phosphoinositides (PIs) are phosphorylated derivatives of phosphatidylinositol, a glycerol based phospholipid. In detailed description, phosphoinositides are amphipathic molecules formed by hydrophilic inositol head (ring) and hydrophobic acyl tail, generated by a number of kinases and phosphatases. The inositol ring can be phosphorylated at three different positions: -3, -4, -5 and a combination of these phosphorylations gives rise to the seven known PIs: PI(3)P, PI(4)P, PI(5)P, PI(3,4)P2, PI(3,5)P2, PI(4,5)P2, PI(3,4,5)P3. Phosphorylation occurs at the -OH groups of the inositol ring of PIs that is linked to the diacylglycerol (DAG) backbone. The inositol ring and DAG backbone are connected via a phosphodiester linkage utilizing the -OH group of the ring at the D1 position. The tail of most PIs has 1-stearoyl-2 arachidonyl form (Fig. 1).

Phosphoinositides are very well known cytoplasmic molecules present in cellular membranes with various important roles in cellular processes (reviewed in Balla, 2013). Even though phosphoinositides represent a small (less than 5%) proportion of the total cell phospholipids, they were identified among the first families of phospholipids in the nucleus. They play crucial roles in the regulation of cell metabolism through their involvement in intracellular signaling events (Hammond et al. 2004) but their nuclear functions are not described in such detail as the cytoplasmic ones (Osborne et al. 2001; Shah et al. 2013).

1.1.1 PI(3)P

PI(3)P localizes predominantly to the plasma membrane (Ivetac et al. 2005), endosomes (Ivetac et al. 2005; Slessareva et al. 2006) smooth endoplasmic reticulum, and the Golgi apparatus (Sarkes and Rameh 2010). PI(3)P acts as an activator of many effector proteins. Almost all effectors contain FYVE (Fab1/YOTB/Vac1/EEA1) domain (Gaullier et al. 1998; Patki et al. 1998) and phox homology (PX) domain (Xu et al. 2001; Ellson et al. 2001; Kanai et al. 2001; Cheever et al. 2001). Recently, Su et al. (2017) showed that the PX domain of zebrafish sorting nexin 25 (zSNX25-PX) is capable of binding to PI3P only in dimeric form of PX domain.

In yeast, PI(3)P attaches serine/threonine protein kinase Atg21 to the preautophagosomal structure, recruits ubiquitin-like Atg8 and the E3 ligase complex Atg12~Atg5/Atg16 and arranges them for efficient lipidation of Atg8 (Juris et al. 2015).

Moreover, PI(3)P has been detected in nucleoli of human fibroblasts and baby hamster kidney cells (Gillooly et al. 2000). Its nucleolar function remains however unknown.

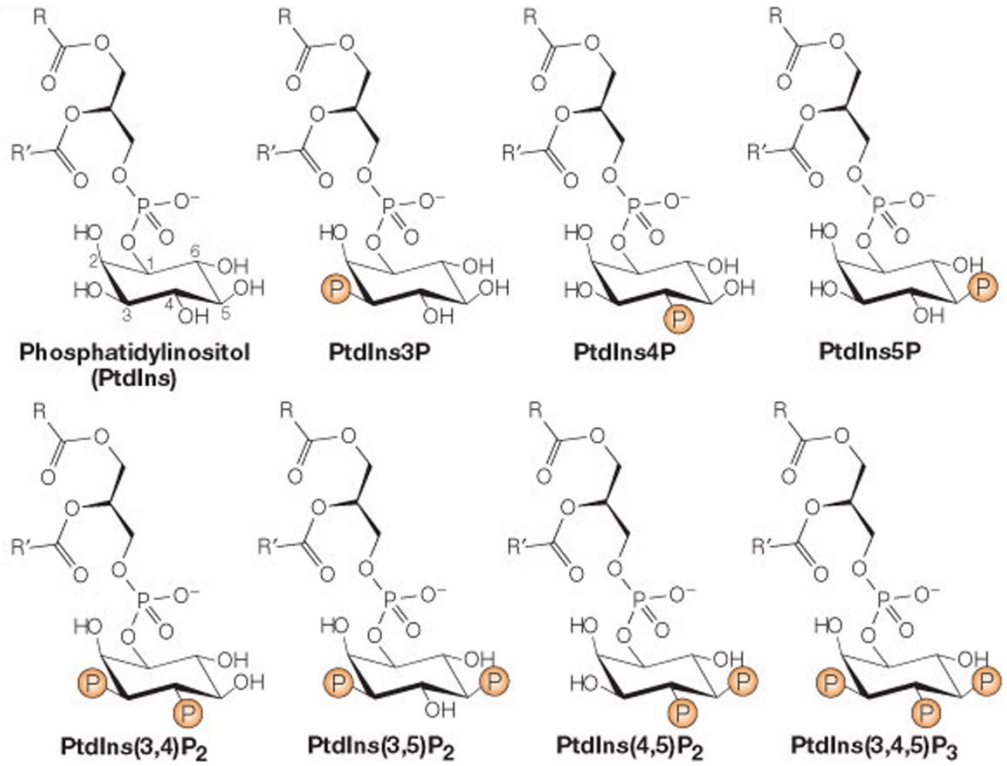

Fig. 1 Schematic representation of phosphatidylinositol (PI) and seven differently phosphorylated form of PIs. PI can be phosphorylated at 3', 4' and 5' positions yielding in PI(3)P, PI(4)P, PI(5)P,PI(3,4)P2, PI(3,5)P2, PI(4,5)P2 and PI(3,4,5)P3. Orange circle depicts position of phosphorylation on the inositol ring (head). The head is linked to the DAG backbone and further connected to fatty-acid tail.

1.1.2 PI(4)P

PI(4)P is one of the most abundant PIs species and is mostly present in Golgi apparatus, at plasma membrane and in endosomes (reviewed in Viaud et al. 2015). It regulates vesicular transport between these compartments (Mills et al. 2003; Wang et al. 2003; Godi et al. 2004).

Jiang et al. (2016) showed that hedgehog (Hh) signaling activity promotes increased levels of PI(4)P, whereas decreased levels of PI(4)P inhibit Hh signaling. Authors found that PI(4)P binds directly to Smoothened (Smo) through an arginine rich motif, and this binding then triggers Smo phosphorylation and activation. Moreover, the pleckstrin homology (PH) domain of G protein-coupled receptor kinase 2 (Gprk2) is an essential component for elevation of PI(4)P and facilitating Smo activation.

1.1.3 PI(5)P

PI(5)P is the phosphoinositide of the lowest abundance – its level reaches only approximately 1-2% of PI(4)P levels. The majority of PI(5)P localizes at the plasma membrane but is also present in the smooth endoplasmic reticulum, and the Golgi apparatus (Sarkes and Rameh 2010), thus serving as a regulator of endosome to lysosome trafficking (reviewed in Viaud et al. 2014). A new role has been identified for PI(5)P – it acts as a positive regulator of cell migration, probably by facilitating actin cytoskeletal rearrangements (Oppelt et al. 2013)

PI(5)P levels have been shown to change in response to stimuli, such as thrombin stimulation (Morris et al. 2000), histamine treatment (Roberts et al. 2005), insulin secretion (Sbrissa et al. 2004; Sarkes and Rameh 2010), oxidative stress (Wilcox and Hinchliffe 2008; Sarkes and Rameh 2010; Jones et al. 2013), and specific oncogenes expression (Dupuis-Coronas et al. 2011).

1.1.4 PI(3,4)P2

PI(3,4)P2 localizes mostly to the plasma membrane, however PI(3,4)P2 can be produced by phosphoinositide 3-kinase (PI3K) at the nuclear surface (Yokogawa et al. 2000). PI(3,4)P2 is part of PI3K/AKT signalling pathway. PI(3,4)P2 is bound by pleckstrin homology (PH) domain of protein kinase B (AKT) and this interaction mediates AKT plasma membrane localization and its activation (Yuan and Cantley, 2008). On the other hand, decreasing level of PI(3,4)P2 attenuates AKT activation and also exerts antiproliferative effect (Ivetac et al. 2009). PI(3,4)P2 at plasma membrane contributes to regulation of endocytosis (Posor et al. 2013; Boucrot et al. 2015).

PI(3,4)P2 localized to focal adhesion influences dynamics in MDA-MB-231 basal breast cancer cells. Fukumoto et al. (2017) found that knockdown of SHIP-2 decreased PI(3,4)P2 levels, which in turn induced development of focal adhesions and suppression of invasion. Therefore inhibition of PI(3,4)P2 generation and/or downstream signaling can be used as a tool for the inhibition of breast cancer metastasis (Fukumoto et al. 2017).

1.1.5 PI(3,5)P2

PI(3,5)P2 constitutes only 0.05~0.1% of total cellular PIs. It is mainly synthesized through PI(3)P phosphorylation pathway by type III PIP kinase (PIKfyve); (reviewed in McCartney et al. 2014). PI(3,5)P2 is localized at plasma membrane and late endosomes (at the multivesicular body). It is a key lipid regulator in endocytic and retrograde trafficking (Rutherford et al. 2006; Zhang et al. 2007; de Lartigue et al. 2009).

PI(3,5)P2 generation was found to control the activation and localization of the mammalian target of rapamycin complex 1 (mTORC1) complex via a direct association between Raptor and PI(3,5)P2 (Bridges et al. 2012). PI(3,5)P2 can be recognized for example by binding of the phox (PX) domain of SNX1 protein (Cozier et al. 2002).

1.1.6 PI(4,5)P2

The essential phospholipid PI(4,5)P2 is generated by a well conserved phosphatidylinositol-4-phosphate-5-kinase (PI4P5K). The majority of PI(4,5)P2 is present at the inner leaflet of plasma membrane where it is estimated to reach 5 mM concentration (which corresponds to 1-2 mol%);(Stephens et al. 1991). PI(4,5)P2 also localizes to membrane of Golgi apparatus, endosomes and endoplasmatic reticulum. PI(4,5)P2 can be bound by proteins containing its specific binding domains, such as PH, ENTH, FERM, Tubby and MARCKS.

A hundreds of PI(4,5)P2 effectors have been identified such as ion channels (Suh and Hille, 2005), vesicle exocytosis receptors (McLaughlin et al. 2005), Ras family small GTPases (Heo et al. 2006), actin regulatory proteins (Ling et al. 2006; Yin and Janmey, 2003), regulators of vesicular trafficking (Downes et al. 2005), IQGAP1 scaffolds (Choi et al. 2013) and nuclear proteins (Lewis et al. 2011). PI(4,5)P2 can act directly or serve as a substrate for generation of IP3 and DAG second messengers (Bertagnolo et al. 1995; Liu et al. 1996; Kim et al. 1996; Bertagnolo et al. 1997; Yamaga et al. 1999; Yoda et al. 2004; Larman et al. 2004; Klein et al. 2008; Cooney et al. 2010; Fiume et al. 2012).

1.1.7 PI(3,4,5)P3

PI(3,4,5)P3 is a low abundance phosphoinositide and together with PI(4,5)P2 represents less than 1% of membrane phospholipids. PI(3,4,5)P3 localizes mainly to the inner leaflet of the plasma membrane but it is also present at the Golgi apparatus and endosomes. PI(3,4,5)P3 as other PI3K products, controls many processes at the plasma membrane, including phagocytosis, pinocytosis, regulated exocytosis, and cytoskeletal organization (reviewed in Salamon and Backer 2013; Viaud et al. 2015). PI(3,4,5)P3 can be recognized by PH domain of GRP1-containing proteins, which have the affinity for PI(3,4,5)P3 two to three orders of magnitude greater than for PI(4,5)P2 (Kavran et al.1998).

Very recently, Lin et al. (2017) show that a long non-coding RNA named long intergenic non-coding RNA for kinase activation (LINK-A) directly and specifically interacts with AKT and PI(3,4,5)P3. The LINK-A–AKT–PIP3 interaction facilitates AKT recruitment and its subsequent activation. They have identified that single nucleotide mutation within 4 central nucleotides in the stem-loop of LINK-A is required for PIP3 and AKT binding. The association

between the PH domain of AKT and PIP3 may cause a conformational change of AKT which makes the phosphorylation sites accessible to its activating kinases. LINK-A-dependent AKT hyperphosphorylation and thus hyperactivation leads to tumorigenesis and resistance to AKT inhibitors.

1.2 Generation of PIs in the cell nucleus

PIs have very well established cytoplasmic roles and in the past decades, it becomes clear that PIs play important roles also in the cell nucleus (reviewed in Shah et al. 2013). However, it is still unclear whether PIs are transported from the cytoplasm to the nucleus or whether they are synthetized directly in the nucleus. Two isoforms of PI transfer proteins (PIPTs) are able to translocate to the nucleus (De Vries et al. 1996) and many PIs metabolizing enzymes are present in the nucleus (Divecha et al. 1993; Martelli et al. 1992; Vann et al. 1997). It is possible that PIs are translocated by PIPTs to the nucleus, where they are substrates for their metabolizing enzymes. However, early experimental data from Cocco et al. (1987) demonstrate that isolated intact nuclei from Murine erythroleukemia cells were still able to synthesize PIs *in vitro*. Moreover, they also showed that upon differentiation, there was a change in the phosphorylation of PIs present in the isolated intact nuclei. Therefore collectively, *in vitro* and *in vivo* studies confirmed the existence of nuclear phosphoinositide pathway, and that its regulation and metabolizing enzymes are independent of the cytoplasmic ones (Gonzales and Anderson 2006; Irvine and Divecha, 1992).

1.2.1 Metabolism of nuclear phosphoinositides

As mentioned above (chapter 1.2), it is clear that many enzymes of the PIs metabolism localize to the cell nucleus (Fig. 2). These include several isoforms of phosphatidylinositol-specific phospholipase C enzymes: β1 (Follo et al. 2006; Lukinovic-Skudar et al. 2005; Manzoli et al. 2005), δ1 (Crjlen et al. 2004; Stallings et al. 2005), and δ4 (Liu et al. 1996), two isoforms phosphatidylinositol 3-kinase type IIα (Didichenko and Thelen, 2001) and phosphatidylinositol 3-kinase type IIβ (Sindić et al. 2001), class I phosphatidylinositol 3-kinases PI3Kβ and PI3Kγ (Neri et al. 1994; Zini et al. 1996; Metjian et al. 1999; Bacqueville et al. 2001), both phosphatidylinositol 4-kinase α (Kakuk et al. 2006) and phosphatidylinositol 4-kinase β/Pik1 (de Graaf et al. 2002; Strahl et al. 2005), phosphatidylinositol 5-phosphate 4-kinase type IIα, phosphatidylinositol 5-phosphate 4-kinase type IIβ (Boronenkov et al. 1998; Richardson et al. 2007; Wang et al. 2010; Clarke and Irvine 2012) and phosphatidylinositol 5-phosphate 4-kinase

Iγ (Clarke et al. 2009; Clarke and Irvine, 2012), the phosphatidylinositol 4-phosphate 5-kinase type Iα, and phosphatidylinositol 4-phosphate 5-kinase type Iγ_i4 (Boronenkov et al. 1998; Mellman et al. 2008; Schill and Anderson, 2009) and Inositol polyphosphate multikinase (IPMK); (Nalaskowski et al. 2002; Resnick et al. 2005; Maag et al. 2011).

In addition to the phospholipases and kinases, inositidephosphatases are also present in the nucleus and were shown to shuttle between cytoplasm and cell nucleus. An increased nuclear shuttling of phosphatase and tensin homolog (PTEN) to the nucleus was shown as an oxidative stress response (Chang et al. 2008). Src-homology 2-containing inositol 5-phosphatase 1 (SHIP-1) and Src-homology 2-containing inositol 5-phosphatase 2 (SHIP-2) phosphatases (Déléris et al. 2003; Elong Edimo et al. 2011; Nalaskowski et al. 2012; Ehm et al. 2015) localize to the cell nucleus and 4-Ptase I translocates to the cell nucleus upon DNA damage (Zou et al. 2007).

1.2.1.1 Metabolism of nuclear PI(4,5)P2

PI(4,5)P2 is one of the most abundant nuclear phosphoinositides and its localization in the cell nucleus is very well described (Sobol et al. 2013; Yildirim et al. 2013; Mellman et al. 2008; Osborne et al. 2001). PI(4,5)P2 can be generated by phosphatidylinositol 4-phosphate 5-kinases or phosphatidylinositol 5-phosphate 4-kinases by utilizing different substrates, PI(4)P and PI(5)P, respectively (Rameh et al. 1997; Anderson et al. 1999; Halstead et al. 2005; Fiume et al. 2012). A metabolic radioisotope labelling in the rat liver nuclei revealed that the predominant way of PI(4,5)P2 production in the nucleus is by phosphorylating PI(4)P. This is also true for PI(4,5)P2 production in a whole cell as PI(4)P is more abundant than PI(5)P (Vann et al. 1997).

PI(4,5)P2 is also a substrate for phosphoinositides phosphatases. Both SHIP-1 and SHIP-2 can hydrolyse PI(4,5)P2 and PI(3,4,5)P3. After SHIP-2 phosphorylation at serine 132, SHIP-2 translocates to nuclear speckles and PI(4,5)P2 becomes its only substrate to generate PI(4)P (Déléris et al. 2003; Elong Edimo et al. 2011). A specific phosphatase is 4-Ptase I (PI(4,5)P2 4-Ptase 1) which dephosphorylates PI(4,5)P2 at position 4 and generates PI(5)P (Ungewickell et al. 2005).

Moreover, PI(4,5)P2 might be specifically cleaved by phospholipase C (PI-PLC) and generates second messengers - IP3 and DAG (Bertagnolo et al. 1995; Liu et al. 1996; Kim et al. 1996; Bertagnolo et al. 1997; Yamaga et al. 1999; Yoda et al. 2004; Larman et al. 2004; Klein et al. 2008; Cooney et al. 2010; Fiume et al. 2012).

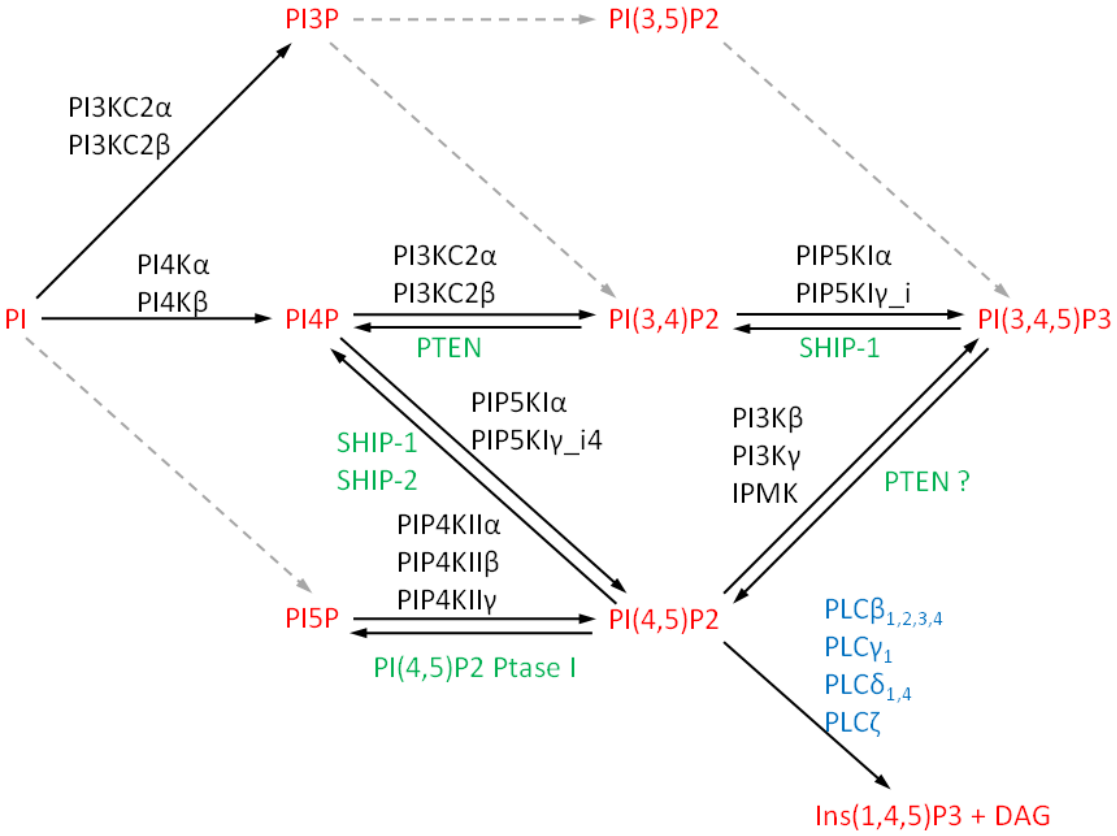

Fig. 2 PIs metabolism in the cell nucleus. PIs kinases (black), phosphatases (green), and phospholipases (blue) establish a metabolism that ensures a synthesis of seven PIs species (red) in the nucleus. Pathways catalysed by enzymes confirmed as present in the nucleus (solid black arrows) and possible pathways without known nuclear enzyme (dashed grey arrows) are depicted. A specific case is PTEN phosphatase, which localizes to the nucleus but has been shown to be unable to dephosphorylate nuclear PI(3,4,5)P3 (Lindsay et al. 2006).

1.3 Phosphoinositides in regulation of gene expression

In vitro studies have pointed out that nuclear phospholipids could be involved in DNA associated process (Rose and Frenster, 1965) for instance, addition of PIs to purified nuclei influences DNA replication and transcription (Capitani, 1986). Other studies showed that *in vitro* addition of positively charged lipids lead to chromosome condensation while negatively charged lipids caused decondensation (revieved in Kuvichkin, 2002). Undoubtedly, the accessibility of DNA is crucial for regulation of genes expression.

1.3.1 PI(5)P function

Most of the studies have been centered on the role of nuclear PI(4,5)P2 in gene expression but there are also examples of other phosphoinositides that interact with chromatin. However, to date, there is no evidence for a role of nuclear PI(3)P, PI(4)P or PI(3,4)P2 in the gene expression. On the other hand, the identification of PI(5)P binding proteins and their nuclear functions are have appeared over the last decade. A breakthrough came with a finding that ING2, which regulates p53 acetylation and function, binds to PI(5)P through its PHD (plant homeodomain) motif (Gozani et al. 2003; Bua et al. 2013). ING2 promotes acetylation of p53 and induces p53-mediated apoptosis in response to UV and etoposide. ING2 carrying point mutation, which causes loss of PI(5)P binding, was unable to induce apoptosis and p53 acetylation.

Jones et al. (2006) showed that PIP4Kβ becomes phosphorylated by p38 mitogen-activated protein kinase in response to genotoxic stress. This phosphorylation inhibits PIP4Kβ what results in accumulations of PI(5)P in the nucleus. This increase of the nuclear PI(5)P causes translocation of ING2 to the chromatin bound fraction, where it modulates p53 acetylation and function. The PHD motif of ING2 also binds trimethylated lysine 4 at histone H3 (H3K4me3) not only PI(5)P. After DNA damage, ING2 binds to H3K4me3, and this binding is essential for the ING2 activity (Shi a et al., 2006). ING2 forms a transcription-repressing complex with HDAC1 and Sin3A protein. After DNA damage, PI(5)P levels become elevated and recruit ING2 to specific promoters. At these promoters, ING2 binds to H3K4me3. This interaction stabilizes and activates ING2 in order to regulate its transcriptional activity.

Gelato et al. (2014) described regulation of ubiquitin-like with PHD and RING finger domains 1 (UHRF1) by PI(5)P. The tandem tudor domain (TTD) of UHFR1 binds trimethylated lysine 9 at histone H3 (H3K9me3), (Nady et al., 2011), while the PHD finger recognizes the unmodified N-terminus of histone H3 (Rajakumara et al. 2011). PI(5)P binds directly to the polybasic region (PBR) in the C-terminal part of UHRF1. This interaction controls access of the TTD and PHD domain to their substrates. Hence, PI5P allosterically regulates binding of UHRF1 to either unmodified histone H3 or H3K9me3. Allosteric regulation of UHRF1 through PI(5)P contributes to UHRF1 localization to heterochromatin and to its function.

Data obtained from plants suggest that PI(5)P might regulate the levels of H3K4me3 (Alvarez-Venegas et al. 2006). ATX1 (Arabidopsis homolog of trithorax) is a trimethyltransferase for H3K4 at the promoter regions of nucleosomes. Ndakong et al. (2010) showed not only that ATX1 binds PI(5)P through the PHD domain, but also that PI(5)P binding negatively affects ATX1 activity as a trimethyltransferase. PI(5)P binding causes that ATX1

disassociate from promoters and translocate from the nucleus to the cytoplasm. This is an opposite effect to PI(5)P as a positive regulator of ING2 activity. This suggests that the effect of PI(5)P binding to PHD domains has a different influence on binding partners activity. Thus PI(5)P function depends also on protein binding partner and not only on binding domain.

Interestingly, the PHD finger of ATP-dependent chromatin remodeling factor (ACF) strongly and specifically interacts with PI(5)P in a protein-lipid overlay assay (Gozani et al. 2003), suggesting that it could have potential for use as an in vivo probe for PI(5)P.

Moreover, PI(5)P can influence chromatin remodeling also through proteins that do not possess PHD fingers (Viiri et al. 2009). The Sin3A corepressor complex SAP30 and SAP30L bound to PIs, mostly to PI(5)P through a zinc finger motif that overlaps with SAP30 DNA binding site. Viiri et al. (2009) proposed that PI(5)P binding displaces DNA from the Sin3A corepressor complex by modulating SAP30 repressor activity and translocate them from the nucleus to the cytoplasm.

1.3.2 PI(3,5)P2 function

A study on *Saccharomyces cerevisiae* revealed PI(3,5)P2 chromatin architecture modulating function. Han and Emr (2011) have identified Tup1 and Cti6 as PI(3,5)P2 specific interacting partners. Tup1, in a complex with Cyc-8, acts as a transcriptional co-repressor and this complex interacts with HDAC (Malave and Dent, 2006). Additionally, it is known that Cti6 is a Cyc-8 binding protein. Cti6 co-activates Tup-1/Cyc-8 complex and links it with SAGA complex, which disrupts nucleosomes and promotes transcription (Papamichos-Chronakis et al. 2002). PI(3,5)P2-dependent chromatin architecture-modulating mechanism is to convert Tup1-driven repressed state to a SAGA-containing activated state, e.g. at the GAL1 promoter. Authors propose that during GAL induction, PI(3,5)P2 converts Cyc8–Tup1 co-repressor complex to a co-activator complex by recruiting Cti6. Moreover, PI(3,5)P2 mediates the assembly of Cti6–Cyc8–Tup1, a transcriptional co-activator complex. Results suggest that cytoplasmic PI(3,5)P2 lipid signalling is closely linked with nuclear regulatory events in modulation of the chromatin architecture and epigenetic status of a gene (Han and Emr, 2011).

1.3.3 PI(4,5)P2 function

There are data establishing an important role of PI(4,5)P2 in the regulation of DNA topological change and chromatin remodelling, since it interacts with proteins involved in these

processes (Lewis et al. 2011; Rando et al. 2002; Toska et al. 2012; Yu et al. 1998; Zhao et al. 1998). Very well-known process influencing the state of chromatin is histone acetylation. Acetylation of histones reduces the positive charge of histones and relaxes their association with negatively charged DNA, thus DNA is more accessible for transcription factors (Lee et al. 1993; Garcia-Ramirez et al. 1995). A recent study showed that chromatin acetylation is repressed by a myristoylation of transcriptional co-repressor brain acid soluble protein 1 (BASP1) and its interaction with PI(4,5)P2. It was shown that nuclear PI(4,5)P2 interacts with BASP1 through this myristoylation and mediates BASP1 interaction with histone deacetylase 1 (HDAC1). BASP1-PI(4,5)P2-HDAC1 complex is then recruited to target genes promoters, where HDAC1 deacetylates histones and diminishes promoter accessibility for transcription factors (Toska et al. 2012).

Moreover, PI(4,5)P2 was shown to bind directly to the C-terminal tail of histones H1 and H3. Depletion of histone H1 causes decondensation of chromatin fibers and increases RNA polymerase II transcriptional activity, and therefore histone H1 acts as inhibitor of RNA pol II transcription. On the other hand, PI(4,5)P2 acts as a positive regulator of RNA polymerase II transcription because its binding to H1 releases H1 from DNA and therefore reverses H1 mediated inhibition (Yu et al. 1998). Furthermore, PI(4,5)P2 forms a complex with the active form of RNA pol II (Osborne et al. 2001; Toska et al. 2012), but there has been no evidence of a direct interaction between PI(4,5)P2 and RNA pol II yet.

It was also shown that depletion of PI(4,5)P2 from HeLa cells nuclear extract by anti-PI(4,5)P2 antibody causes an inhibition of pre-mRNA splicing *in vitro*. However, addition of exogenous PI(4,5)P2 into depleted nuclear extract does not restore splicing activity. This indicates that not only PI(4,5)P2 itself but also its binding partners are necessary for splicing (Osborne et al. 2001).

The PI(4,5)P2 regulation of RNA pol I transcription is described in more detail compared to RNA pol II transcription. The upstream binding factor (UBF) and the promoter selectivity factor 1 (SL1) form a complex, which is recruited to the rDNA promoter and facilitates the initiation of RNA pol I transcription (Bell et al. 1988). Previously, we have shown that PI(4,5)P2 binds to UBF and enhances the binding of UBF to the rDNA promoter. Moreover, depletion of PI(4,5)P2 by anti-PI(4,5)P2 antibody from HeLa cells nuclear extract decreases level of RNA pol I transcription *in vitro*; the decrease can be partially restored by addition of exogenous PI(4,5)P2 (Yildirim et al. 2013). These data suggest that PI(4,5)P2 interaction with UBF might be required for binding of the transcription initiation complex with rDNA and activation of RNA pol I transcription.

PI(4,5)P2 can also influence chromatin structure by the interaction with SWItch/Sucrose Non-Fermentable (SWI/SNF) -like chromatin remodeling complex called BAF (Brahma-related gene association factor) (Zhao et al. 1998). The mammalian BAF complex contains BAF53, actin and a central ATPase subunit called BRG-1 (Brahma-realted gene 1). Binding of actin to BRG-1 facilitates recruitment of BAF to chromatin. However, upon PI(4,5)P2 binding the association of actin and Brg1 is blocked. This leads to inefficient recruitment of BAF complex to chromatin and loss of its chromatin remodeling activity (Bourachot et al. 1999; Rando et al. 2002; Shen et al. 2003).

1.3.4 PI(3,4,5)P3 function

Recent findings show that both PI(4,5)P2 and PI(3,4,5)P3 can interact with steroidogenic factor 1 (SF-1);(Blind et al. 2012; Blind et al. 2014). SF-1 is a transcription factor which regulates transcription of genes involved a lipid and steroid metabolism, cytoskeleton dynamics, cell cycle, or apoptosis (reviewed in Lalli et al. 2013). PI(4,5)P2 or PI(3,4,5)P3 bind to binding pocket of SF-1 through acyl chains and stabilizes its tertiary structure. SF-1 in a complex with PI(3,4,5)P3 displays significantly higher affinity for a co-activator peptide than in a complex with PI(4,5)P2, and thus stimulates the transcription of SF-1 target genes (Blind et al. 2012; Blind et al. 2014).

The ErbB3 binding protein-1 (EBP1) belongs to a family of DNA/RNA binding proteins implicated in cell growth, apoptosis and differentiation (Zhang et al. 2005). Karlsson et al. (2016) identified EBP1 as a PI(3,4,5)P3-binding protein. PI(3,4,5)P3 binds to EBP1 trough C-terminal lysine rich PBR (polybasic) region and these two molecules partially co-localize in the nucleolus. Even though, authors propose that PI(3,4,5)P3 directly influences unknown EBP1-mediated nucleolar function the detailed molecular mechanism of these events are still missing (Karlsson et al. 2016).

2 AIMS

PIs can regulate various important cellular processes through interactions with proteins, e.g. chromatin modifying enzymes. We would like to contribute to the knowledge about essential nuclear functions of PIs and their binding partners (such as PHF8) in context of regulation of gene expression. Therefore, we asked these questions:

1. **Which PIs localize to the cell nucleus and to which nuclear subdomain?**
2. **Can PI(4,5)P2 interact with proteins involved in epigenetic regulation and thus contribute to the regulation of gene expression at the epigenetic level?**
3. **Is PI(4,5)P2 important for the regulation of gene expression in *C. elegans,* a complex model organism?**
4. **Which proteins can interact with nuclear F-actin, a PI(4,5)P2 binding partner?**

3 RESEARCH PAPERS

Tools for visualization of phosphoinositides in the cell nucleus

Kalasova I, Fáberová V, Kalendová A, Yildirim S, Uličná L, Venit T and Hozák P
Histochem Cell Biol. 2016. 145(4):485-96. doi: 10.1007/s00418-016-1409-8.
IF: 2.55 (2016)
L.U. performed experiments (indirect immunofluorescence, protein expression and purification)

PIP2 epigenetically represses rRNA genes transcription interacting with PHF8

Ulicna L., Kalendova A., Kalasova I., Vacik T. and Hozak P.

BBA-Molecular and Cell Biology of Lipids. 2017. 1863(3):226-275 doi: 10.1016/j.bbalip.2017.12.008

IF: 5.547 (2016/2017)

L.U. designed and performed almost all experiments (DNA cloning, DNA mutagenesis, protein expression and purification, pull-down assays, immunoprecipitations, indirect immunofluorescence and fluorescence microscopy, demethylation assays, qPCR, ChIP) and wrote the paper.

PIP2 functions at the intersection of chromatin structure, transcription, DNA damage in meiosis I progression in *C. elegans*

Ulicna L., Rohozkova J. and Hozak P.

manuscript

L.U. designed and performed most of the experiments (DNA cloning, RNAi interference experiments, indirect immunofluorescence and fluorescence microscopy, *C. elegans* handling) and wrote the manuscript.

Nuclear actin filaments recruit cofilin and Arp3 and their formation is connected with a mitotic block

Kalendová A, Kalasová I, Yamazaki S, Uličná L, Harata M and Hozák P
Histochem Cell Biol. 2014. Aug;142(2):139-52. doi: 10.1007/s00418-014-1243-9.
IF: 3.054 (2014)
L.U. performed experiments (indirect immunofluorescence)

3.1 Tools for visualization of phosphoinositides in the cell nucleus

Kalasova I, Fáberová V, Kalendová A, Yildirim S, Uličná L, Venit T and Hozák P

Histochem Cell Biol. 2016. 145(4):485-96. doi: 10.1007/s00418-016-1409-8.

IF: 2.55 (2016)

L.U. performed experiments (indirect immunofluorescence, protein expression and purification)

Histochem Cell Biol (2016) 145:485–496
DOI 10.1007/s00418-016-1409-8

ORIGINAL PAPER

Tools for visualization of phosphoinositides in the cell nucleus

Ilona Kalasova[1,2] · Veronika Fáberová[1] · Alžběta Kalendová[1] · Sukriye Yildirim[1] · Lívia Uličná[1] · Tomáš Venit[1] · Pavel Hozák[1]

Accepted: 14 January 2016 / Published online: 4 February 2016

Abstract Phosphoinositides (PIs) are glycerol-based phospholipids containing hydrophilic inositol ring. The inositol ring is mono-, bis-, or tris-phosphorylated yielding seven PIs members. Ample evidence shows that PIs localize both to the cytoplasm and to the nucleus. However, tools for direct visualization of nuclear PIs are limited and many studies thus employ indirect approaches, such as staining of their metabolic enzymes. Since localization and mobility of PIs differ from their metabolic enzymes, these approaches may result in incomplete data. In this paper, we tested commercially available PIs antibodies by light microscopy on fixed cells, tested their specificity using protein–lipid overlay assay and blocking assay, and compared their staining patterns. Additionally, we prepared recombinant PIs-binding domains and tested them on both fixed and live cells by light microscopy. The results provide a useful overview of usability of the tools tested and stress that the selection of adequate tools is critical. Knowing the localization of individual PIs in various functional compartments should enable us to better understand the roles of PIs in the cell nucleus.

Keywords Nucleus · Phosphoinositides · PI(4,5)P2 · PI(4)P

✉ Pavel Hozák
hozak@img.cas.cz

[1] Department of Biology of the Cell Nucleus, Institute of Molecular Genetics of the Academy of Sciences of the Czech Republic, v.v.i., Vídeňská 1083, 142 20 Prague, Czech Republic

[2] Faculty of Science, Charles University in Prague, Albertov 6, 128 43 Prague, Czech Republic

Introduction

Phosphoinositides (PIs) are glycerol-based phospholipids. As amphipathic molecules, they consist of hydrophobic tail and hydrophilic head. Their head is formed by the inositol ring that can be phosphorylated at three different positions yielding seven mono-, bis-, or tris-phosphorylated PIs species. PIs are important signalling molecules involved in membrane and cytoskeletal dynamics, modulation of ion channels and transporters, or generation of second messengers (reviewed in Balla 2013; Tan et al. 2015). These functions are related to PIs present in the cytoplasm and the plasma membrane. Approximately 15 % of cellular PIs are nuclear (York and Majerus 1994). It is, however, not well understood whether nuclear PIs originate in the cytoplasm or whether they are synthesized in the nucleus de novo. Many PIs metabolizing enzymes—kinases, phosphatases, and phospholipases (reviewed in Keune et al. 2011; Martelli et al. 2011; Shah et al. 2013)—as well as phosphatidylinositol (PI) transfer proteins (De Vries et al. 1996) localize to the nucleus. Besides, several in vitro studies reported intranuclear synthesis of PIs (Smith and Wells 1983; Cocco et al. 1987; Yildirim et al. 2013). These data suggest that PIs are in the nucleus metabolized independently of the cytoplasm and do not require the presence of membranes. However, spatiotemporal visualization of such events in the nucleus is still missing. Since a large fraction of PIs does not associate with nuclear membrane (Vann et al. 1997), it is currently unclear where the synthesis and metabolism of nuclear PIs occur. Several studies suggested that PIs are retained in the nucleus in the form of protein–lipid complexes, where proteins shield the hydrophobic tails of PIs (Blind et al. 2014; Sablin et al. 2015) and thus could prevent their extraction by detergents. Using various approaches, more than 300 nuclear PIs-interacting

Table 1 Summary of PIs-binding domains used for overexpression in U2OS cells

Domain	Specificity	Protein	Size (kDa)	Mutant
EEA1-FYVE	PI(3)P	Early endosome antigen 1	~18	RRHH126-129AANN
OSH1-PH	PI(4)P	Oxysterol-binding protein homolog 1	~15	KR37,39EE
Akt-PH	PI(3,4)P2, PI(3,4,5)P3	Protein kinase B	~21	KR14,15AA
Tubby	PI(4,5)P2	Tubby-like protein	~31	KR300,302AA
PLCδ1-PH	PI(4,5)P2	Phosphoinositide phospholipase C δ1	~20	R40A
Grp1-PH	PI(3,4,5)P3	General receptor for phosphoinositides 1	~15	K273A

Domains were mutated according to Yagisawa et al. (1998), Levine and Munro (2001), Santagata et al. (2001), Lee et al. (2005), Guillou et al. (2007), Jo et al. (2012)

proteins were identified. These proteins are involved in essential nuclear processes, and therefore, nuclear PIs are probably important regulators of these events (Lewis et al. 2011; Jungmichel et al. 2014). And indeed, nuclear phosphatidylinositol 4,5-bisphosphate (PI(4,5)P2) modulates protein functions and thus plays a role in chromatin remodelling (Zhao et al. 1998), transcription by RNA polymerase I and II (Osborne et al. 2001; Toska et al. 2012; Yildirim et al. 2013), or pre-mRNA processing (Osborne et al. 2001; Mellman et al. 2008). Nuclear phosphatidylinositol 3,4,5-trisphosphate (PI(3,4,5)P3) was linked to mRNA export (Okada et al. 2008; Wickramasinghe et al. 2013) and anti-apoptotic signalling (Ahn et al. 2004, 2005), while nuclear phosphatidylinositol 5-phosphate (PI(5)P) is implicated in DNA damage response (Gozani et al. 2003; Jones et al. 2006; Zou et al. 2007). Despite the fact that there are no data on functions of other nuclear PIs, their presence in the nucleus has been confirmed (Vann et al. 1997; Gillooly et al. 2000; Yokogawa et al. 2000; Clarke et al. 2001; Višnjić et al. 2003; Watt et al. 2004).

To better understand functions of individuals PIs, it is important to have information about their localization within the nucleus. So far, two fundamental approaches of PIs visualization have been employed. First, commercially available antibodies against PI(4,5)P2 (Mazzotti et al. 1995; Boronenkov et al. 1998; Osborne et al. 2001) and phosphatidylinositol 3,4-bisphosphate (PI(3,4)P2; Yokogawa et al. 2000) have been used. Second, PIs-binding domains from PLCδ1 (Watt et al. 2002; Hammond et al. 2009; Yildirim et al. 2013), Tapp1 (Watt et al. 2004), Hrs (Gillooly et al. 2000), and Grp1 (Lindsay et al. 2006) proteins specifically recognizing PI(4,5)P2, PI(3,4)P2, phosphatidylinositol 3-phosphate (PI(3)P), and PI(3,4,5)P3, respectively, were generated. The use of anti-PI(4,5)P2 and PLCδ1-PH domain provided similar results and made it possible to address functions of PI(4,5)P2 as well as its localization in the nucleus, nuclear speckles, and heterochromatin regions (Mazzotti et al. 1995; Boronenkov et al. 1998; Osborne et al. 2001; Watt et al. 2002; Hammond et al. 2009; Yildirim et al. 2013). Similarly, both antibodies and domains demonstrated localization of PI(3,4)P2 in the nuclear membrane. FYVE domain of tyrosine kinase Hrs detected PI(3)P signal in nucleoli of BHK cells (Gillooly et al. 2000). PH domain of Grp1 showed an increased level of nuclear PI(3,4,5)P3 after stimulation of Swiss 3T3 cells with PDGF (Lindsay et al. 2006).

In this paper, we explored localization of nuclear PI(4,5)P2, PI(3,4)P2, and phosphatidylinositol 4-phosphate (PI(4)P) in greater detail. First, we tested commercial antibodies against PI(4,5)P2, PI(3,4)P2, and PI(4)P. Since tools for visualization of nuclear PIs in live cells are missing, we next inspected nuclear patterns of different PIs-binding protein domains (Table 1) after overexpression in U2OS cells. Given that most domains did not specifically label nuclear PIs in live cells, we purified eGFP-fused PLCδ1-PH, OSH1-PH, and Tubby domains and used them in analogy to antibodies for labelling in fixed cells. Using these approaches, we identified anti-PI4P antibody, OSH1-PH, EEA1-FYVE, and PLCδ1-PH, and Tubby domains as a potential tools for visualization of PI(4)P, PI(3)P, and PI(4,5)P2 in live or fixed cells.

Materials and methods

Cell cultures and transfections

U2OS were cultured in D-MEM supplemented with 10 % FBS in 5 % CO_2/air, 37 °C, and humidified atmosphere. Cells were transfected with Lipofectamine (Life Technologies) according to manufacturer's instructions.

Constructs used in this study

For overexpression in U2OS cells, PLCδ1-PH, EEA1-FYVE, Grp1-PH, OSH1-PH, Akt-PH, and Tubby domains in pEGFP (Clontech, kind gifts from Dr Tamas Balla, National Institutes of Health, Bethesda, MD) were used. PLCδ1-PH with nuclear localization signal (NLS) was

prepared by insertion of SV40 NLS into PLCδ1-PH pEGFP-N1 by BsrGI and AFlII restriction sites. Mutant domains (PLCδ1-PH R40A, EEA1-FYVE RRHH123-129AANN, Grp1-PH K273A, OSH1-PH KR37,39EE, Akt-PH KR14,15AA, Tubby domain KR330,332AA) were prepared by site-directed mutagenesis by Q5® Site-Directed Mutagenesis Kit (New England Biolabs, E0552S) according to the manufacturer's instructions. For expression in *E. Coli*, eGFP fusions of wild-type as well as mutant forms of PLCδ1-PH, OSH1-PH domains were amplified by PCR and ligated to pET-15b (Merck Millipore). Tubby domain in pET-23a (Merck Millipore, a kind gift from Dr Tamas Balla, National Institutes of Health, Bethesda, MD) was used, and mutant Tubby domain was prepared as described above.

Antibodies

Following primary antibodies were used: anti-PI(4)P (Echelon, Z-P004; 10 μg/ml), anti-PI(3,4)P2 (Echelon, Z-P034b; 20 μg/ml), anti-PI(4,5)P2 (Echelon, Z-A045; 4.9 μg/ml).

For immunofluorescence, secondary antibodies were used: goat anti-mouse IgG conjugated with Alexa Fluor 555 and goat anti-mouse IgM conjugated with Alexa Fluor 555 all purchased from Life Sciences. For protein–lipid overlay assay, the following secondary antibodies were used: donkey anti-mouse IgG IRDye®680RD and goat anti-mouse IgM IRDye®680RD (LI-COR Biosciences).

Expression and purification of recombinant proteins

Recombinant PLCδ1-PH, OSH1-PH, and Tubby domains were expressed in *E. coli* BL21-Gold(DE3). Bacteria transformed with PLCδ1-PH and Tubby domains were grown up to OD(600) = 0.6. The expression of PLCδ1-PH was induced with 0.6 mM IPTG for 4 h at 37 °C. The expression of Tubby domain was induced with 0.3 mM IPTG for 8 h at 18 °C. Bacteria transformed with OSH1-PH domain were grown up to OD(600) = 0.4. The expression of OSH1-PH was induced with 0.1 mM IPTG for 16 h at 25 °C. Cells were lysed in lysis buffer (10 mM Tris, pH 7.4, 150 mM NaCl, 0.5 % Triton X-100, AEBSF) and sonicated. The purification was carried on HIS-Select Nickel Affinity Gel (Sigma, P6611). The beads were equilibrated with lysis buffer and incubated with protein lysates for 1 h at 4 °C. Then the beads were washed three times (10 m M Tris, pH 7.4, 150 mM NaCl, AEBSF). Bound proteins were eluted (10 mM Tris, pH 8, 150 mM NaCl, 250 mM imidazole, pH 8, 20 % glycerol, AEBSF). Subsequently, imidazole was removed by dialysis (10 mM Tris, pH 8, 150 mM NaCl, 20 % glycerol, AEBSF). Purified PIs-binding domains were used for immunofluorescence (1 μg/μl).

Indirect immunofluorescence and confocal fluorescence microscopy

Cells seeded on glass coverslips were washed with PBS, fixed with 3 % paraformaldehyde in PBS, and permeabilized with 0.1 % Triton X-100 in PBS for 20 min. Coverslips were blocked with 5 % normal goat serum (Invitrogen) in PBS for 30 min. Coverslips were incubated with primary antibodies diluted in PBS for 1 h at room temperature (RT) and then washed with PBS or with purified domains diluted in PBS with 0.05 % Tween 20 (PBS-T) for 1 h at RT and then washed with PBS-T. In case of antibodies, coverslips were incubated with corresponding secondary antibodies diluted in PBS-T for 1 h at RT. After final washes in PBS-T, coverslips were mounted in ProLong Gold anti-fade reagent with DAPI (Life Technologies). Images were acquired using confocal microscope Leica TCS SP8 with 63× (NA 1.4) immersion oil objective lens with 405 and 561 laser excitations, Leica advanced fluorescence software (LAS AF).

Antibody blocking assay

Antibodies were incubated with phosphatidylinositol diC8 (P-0008), PI(3)P diC8 (P-3008), PI(4)P diC8 (P-4008), PI(5)P diC8 (P-5008), PI(3,4)P2 diC8 (P-3408), phosphatidylinositol 3,5-bisphosphate diC8 (P-3508), PI(4,5)P2 diC8 (P-4508), PI(3,4,5)P3 diC8 (P-3908), all purchased from Echelon Biosciences Inc. Antibodies were incubated with PIs in molar ratio 1:1000. Concentrations of antibodies were as described above. Concentrations of PIs were 5, 10, and 130 nM to block anti-PI(4,5)P2, anti-PI(4)P, and anti-PI(3,4)P2 antibody, respectively. Incubations were performed in 1 % BSA, PBS for 30 min. Pre-blocked antibodies were used for immunostaining.

Protein–lipid overlay assay

PIP Strips (P-6001, Echelon Biosciences Inc.) were blocked with 3 % BSA in PBS-T for 1 h at RT and then incubated with antibodies (1 ug/ml) in 3 % BSA, PBS-T for 1 h at RT. Membranes were washed three times with PBS-T for 1 h at RT. Membranes were incubated with goat/donkey anti-mouse IgG or anti-mouse IgM secondary antibodies conjugated to IRDye. The signal was detected by Odyssey Infrared Imaging System (LI-COR Biosciences).

Results

Antibodies show nuclear localization of PI(4,5)P2, PI(3,4)P2, and PI(4)P

To describe the localization of particular nuclear PIs, we used antibodies against PI(4,5)P2, PI(3,4)P2, and PI(4)P, which are all commercially available (Echelon).

As it has been reported before, the antibody against PI(4,5)P2 detects nuclear PI(4,5)P2 in nuclear speckles and nucleoplasmic foci. Moreover, weak nucleolar PI(4,5)P2 pool can be also detected (Osborne et al. 2001; Yildirim et al. 2013; Fig. 1a, inset). To test the specificity of PI(4,5)P2 antibody, we used protein–lipid overlay assay, where the antibody is incubated with different phospholipids spotted on a nitrocellulose membrane. Protein–lipid overlay assay shows that PI(4,5)P2 antibody detects not only PI(4,5)P2 but also PI(3,4,5)P3 (Fig. 2a). Therefore, we used lipid blocking assay to further investigate the antibody specificity. In this approach, the antibody was preincubated with an excess amount of each PI (1:1000) and then used for immunofluorescence (Fig. 2b). Although preincubation with PI(3,4,5)P3 decreased the detected signal to 15 % of the original value, preincubation with PI(4,5)P2 abolished the signal completely (Fig. 2c). The results of protein–lipid overlay assay suggest that PI(4,5)P2 antibody has higher affinity to PI(3,4,5)P3 (Fig. 2a). However, the lipid blocking assay shows that PI(4,5)P2 antibody detects mostly PI(4,5)P2 in fixed cells, as shown in Fig. 2c. As the total amount of cellular PI(3,4,5)P3 is more than 20-fold lower than the amount of cellular PI(4,5)P2 (Stephens et al. 1993; Nasuhoglu et al. 2002), we believe that the antibody predominantly but not exclusively recognizes PI(4,5)P2 in the cells.

The antibody against PI(3,4)P2 shows nuclear pattern similar to PI(4,5)P2 with nuclear speckles and smaller nucleoplasmic foci (Fig. 1b). The antibody recognizes mainly PI(3,4)P2 on protein–lipid overlay assay, but binds also to PI(4,5)P2 and PI(3,4,5)P3 (Fig. 2d). Lipid blocking assay shows that the fluorescence signal is not abolished after preincubation of anti-PI(3,4)P2 antibody with PI(3,4)P2; however, the signal decreases after preincubations with PI(3)P, PI(4)P, PI(5)P, PI(3,4)P2, PI(3,5)P2, and PI(3,4,5)P3 (Fig. 2e). Our results therefore suggest that although the PI(3,4)P2 antibody can be used to detect PI(3,4)P2 spotted on a membrane, it is not suitable for immunofluorescence studies under experimental conditions we tested.

The antibody against PI(4)P detects nuclear PI(4)P signal, which resembles the signal of PI(4,5)P2 in nuclear speckles and small foci in nucleoplasm and nucleoli (Fig. 1c). The antibody detects specifically PI(4)P on protein–lipid overlay assay with a weak signal coming from PI(4,5)P2 and PI(3)P (Fig. 2f). Moreover, the lipid blocking assay shows that the fluorescence signal diminishes only after preincubation with PI(4)P (Fig. 2g). Therefore, we concluded that the PI(4)P antibody can be used for PI(4)P detection by immunofluorescence in fixed cells.

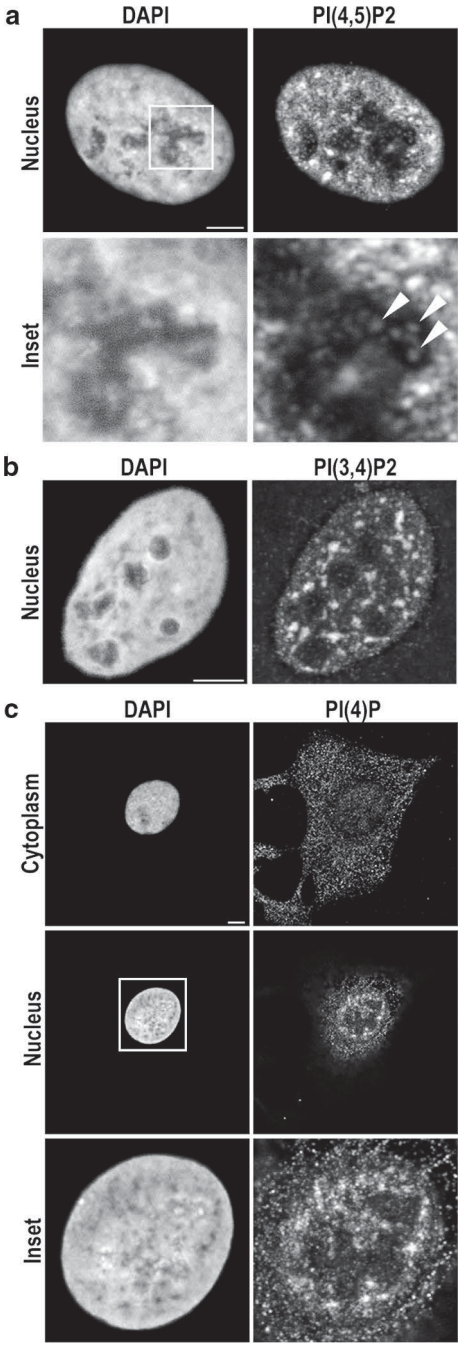

Fig. 1 Antibodies detect nuclear PI(4,5)P2, PI(3,4)P2, and PI(4)P. Anti-PI(4,5)P2 detects PI(4,5)P2 in the nucleoplasm and nuclear speckles (**a**) and weak foci in nucleoli (*inset*, *arrowheads*). Anti-PI(3,4)P2 antibody detects nuclear pattern similar to anti-PI(4,5)P2 antibody (**b**) Anti-PI(4)P antibody detects both cytoplasmic and nuclear signal (**c**, optical sections focused on the cytoplasm and on the nucleus). In the nucleus, anti-PI(4)P antibody gives similar pattern to anti-PI(4,5)P2 antibody (*inset*). *Scale bars* 5 μm

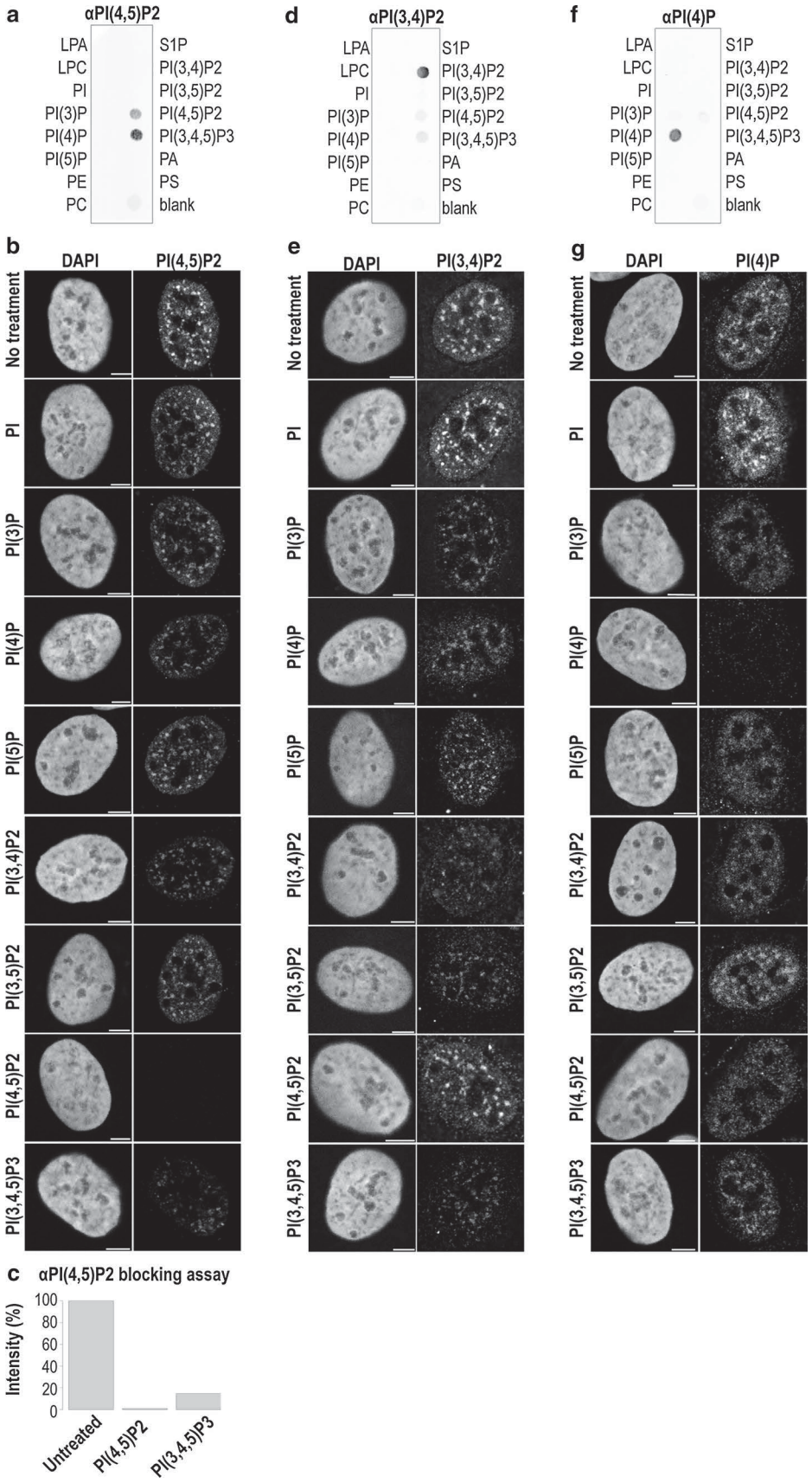

Fig. 2 Antibody against PI(4,5)P2 binds to PI(4,5)P2 and PI(3,4,5)P3 on protein–lipid overlay assay (**a**). On immunofluorescence, the antibody is blocked by preincubation with PI(4,5)P2 and PI(3,4,5)P3 (**b**). The *graph* shows signal intensities from images of the cell without treatment and after pre-blocking with PI(4,5)P2 and PI(3,4,5)P3. The blocking is only partial (up to 85 %) after preincubation with PI(3,4,5)P3, while preincubation with PI(4,5)P2 blocks signal completely (**c**). The antibody against PI(3,4)P2 detects mostly PI(3,4)P2 and weakly also PI(4,5)P2 and PI(3,4,5)P3 on protein–lipid overlay (**d**). The immunofluorescence signal from anti-PI(3,4)P2 antibody is decreased after preincubation of the antibody with PI(3)P, PI(4)P, PI(5)P, PI(3,4)P2, PI(3,5)P2, and PI(3,4,5)P3 (**e**). Anti-PI(4)P antibody detects PI(4)P and very weakly binds to PI(3)P and PI(4,5)P2 on protein–lipid overlay assay (**f**). Immunofluorescence signal of anti-PI(4)P antibody is completely abolished after preincubation with PI(4)P only (**g**). LPA, lysophosphatidic acid, LPC, lysophosphocholine, PtdIns, phosphatidylinositol, PE, phosphatidylethanolamine, S1P, sphingosine-1-phosphate, PA, phosphatidic acid, PS, phosphatidylserine, *Scale bars* 5 μm

Overexpressed PIs-binding domains show nuclear staining in U2OS cells

In addition to commercially available antibodies, we tested several PIs-binding domains (Table 1). These protein modules have been used before for PIs detection in cellular membranes (reviewed in Balla and Várnai 2009). We transfected PLCδ1-PH, EEA1-FYVE, Akt-PH, Grp1-PH, OSH1-PH, and Tubby domains coupled to eGFP into U2OS cells and inspected their nuclear patterns. As a control, we prepared mutant form of each domain, which prevents binding of the domain to the respective PIs. As published before, PLCδ1-PH binds PI(4,5)P2 in the plasma membrane (Stauffer et al. 1998; Varnai and Balla 1998; Kavran et al. 1998). Indeed, overexpressed PLCδ1-PH localizes mainly to the plasma membrane and is diffused throughout the cytoplasm (Fig. 3a), while mutant PLCδ1-PH loses the plasma membrane localization (Fig. 3b). Both wild-type and mutant PLCδ1-PH show diffused nuclear signal. The nuclear signal is enriched in mutant probably due to relocalization of the domain from the plasma membrane. To target PLCδ1-PH to the nucleus, we cloned NLS sequence downstream of GFP. Even though this construct was efficiently imported into the nucleus, we did not observe any difference between localization patterns of wild-type and mutant domains (Fig. 3c, d). Since the overexpressed PLCδ1-PH does not seem to be a suitable tool for nuclear PI(4,5)P2 detection, we tested also another PI(4,5)P2 binding domain, a Tubby domain (Santagata et al. 2001; Quinn et al. 2008; Szentpetery et al. 2009). Similarly to PLCδ1-PH, wild-type Tubby domain localizes to the plasma membrane (Fig. 3e). Moreover, we detected signal in the nucleus and small foci in nucleoli. Mutant Tubby domain loses the plasma membrane localization and relocalizes to the nucleus, where the pattern resembles the signal of wild-type Tubby domain (Fig. 3f). In conclusion, both PLCδ1-PH and Tubby fail to specifically recognize nuclear PI(4,5)P2.

EEA1-FYVE has been previously used for visualization of PI(3)P in endosomes (Burd and Emr 1998; Gaullier et al. 1998). We observed the same pattern, which is lost after mutation in EEA1-FYVE confirming its specificity (Fig. 3g, h). Both wild-type and mutant EEA1-FYVE enter nucleus, where they show the same diffused nuclear signal. In addition, wild-type also recognizes foci in nucleoli, which are absent in mutant (Fig. 3h, inset). This suggests that EEA1-FYVE domain recognizes nucleolar specific pool of PI(3)P.

Akt-PH binds PI(3,4,5)P3 and PI(3,4)P2 (Kavran et al. 1998; Watton and Downward 1999; Rowland et al. 2012). After overexpression, Akt-PH localizes to the plasma membrane and intracellular membranes (Fig. 3i), while mutant Akt-PH is diffused throughout the cytoplasm (Fig. 3j). Both wild-type and mutant Akt-PH localize to the nucleus, where they display a similar pattern suggesting their inability to recognize nuclear PI(3,4,5)P3 or PI(3,4)P2. An alternative tool for visualization of PI(3,4,5)P3 is Grp1-PH domain (Venkateswarlu et al. 1998; Kavran et al. 1998; Gray et al. 1999; Manna et al. 2007). Using Grp1-PH, we detected only a weak signal in the cytoplasm (Fig. 3k, l). It is therefore possible that Akt-PH detects mostly PI(3,4)P2 in the plasma membrane. Both, wild-type and mutant Grp1-PH domains localized mostly to the nucleus, where they display a similar pattern suggesting the inability of Grp1 to detect nuclear PI(3,4,5)P3 specifically (Fig. 3k, l).

It has been reported that overexpressed OSH1-PH binds to PI(4)P present in the plasma membrane and Golgi apparatus (Roy and Levine 2004; Yu et al. 2004; Balla et al. 2008). In agreement with this, we show OSH1-PH localization to the plasma membrane and other cellular membranes (Fig. 3m), while mutant OSH1-PH is diffused throughout the cytoplasm (Fig. 3n). Both wild-type and mutant OSH1-PH localize to the nucleus, where they display a similar pattern.

Taken together, our results are consistent with previously published data and show that overexpressed PIs-binding domains localize to the nucleus. Careful comparison with mutant domains, however, revealed that in the nucleus, these domains do not specifically interact with PIs. Among

Fig. 3 Comparison of PIs-binding domains after overexpression in U2OS cells. Images are taken at optical sections focused on the plasma membrane (*Cytopl.*) and on the nucleus (*Nucleus*). Wild-type PLCδ1-PH (**a**) but not mutant PLCδ1-PH (**b**) is accumulated at the plasma membrane. Both domains are diffused throughout the cytoplasm and the nucleus (**a**, **b** *inset*). With NLS, both wild-type PLCδ1-PH (**c**) and mutant PLCδ1-PH (**d**) are accumulated in the nucleus and display the same nuclear pattern (**c**, **d** *inset*). Wild-type Tubby domain localizes to the plasma membrane and weakly also to the nucleus (**e**), where it forms small foci in the nucleoli (*inset, arrowheads*). Mutant Tubby domain is absent from the plasma membrane and accumulates in the nucleus (**f**), where it displays pattern similar to the wild-type domain (*inset, arrowheads*). Wild-type EEA1-FYVE localizes to endosomes and also to the nucleus (**g**), where it localizes to the nucleoplasm and forms foci in the nucleoli (*inset, arrowheads*). Mutant EEA1-FYVE is diffused throughout the cytoplasm and the nucleus (**h**), whereas nucleoli foci are absent (*inset*). Wild-type Akt-PH localizes to the plasma membrane and other cellular membranes (**i**) and to the nucleus (*inset*). While mutant Akt-PH is absent from the membranes (**j**), it displays similar nuclear pattern as the wild-type domain (*inset*). Both wild-type Grp1-PH (**k**) and mutant Grp1-PH (**l**) are almost absent from the cytoplasm and are accumulated in the nucleus, where they display similar pattern (**k**, **l** *inset*). Wild-type OSH1-PH localizes to the plasma membrane and other cellular membranes, probably Golgi apparatus (**m**), while the mutant OSH1-PH is diffused throughout the cytoplasm (**n**). Both wild-type and mutant OSH1-PH domains localize to the nucleus (**m**, **n** *inset*). *Scale bars* 5 μm

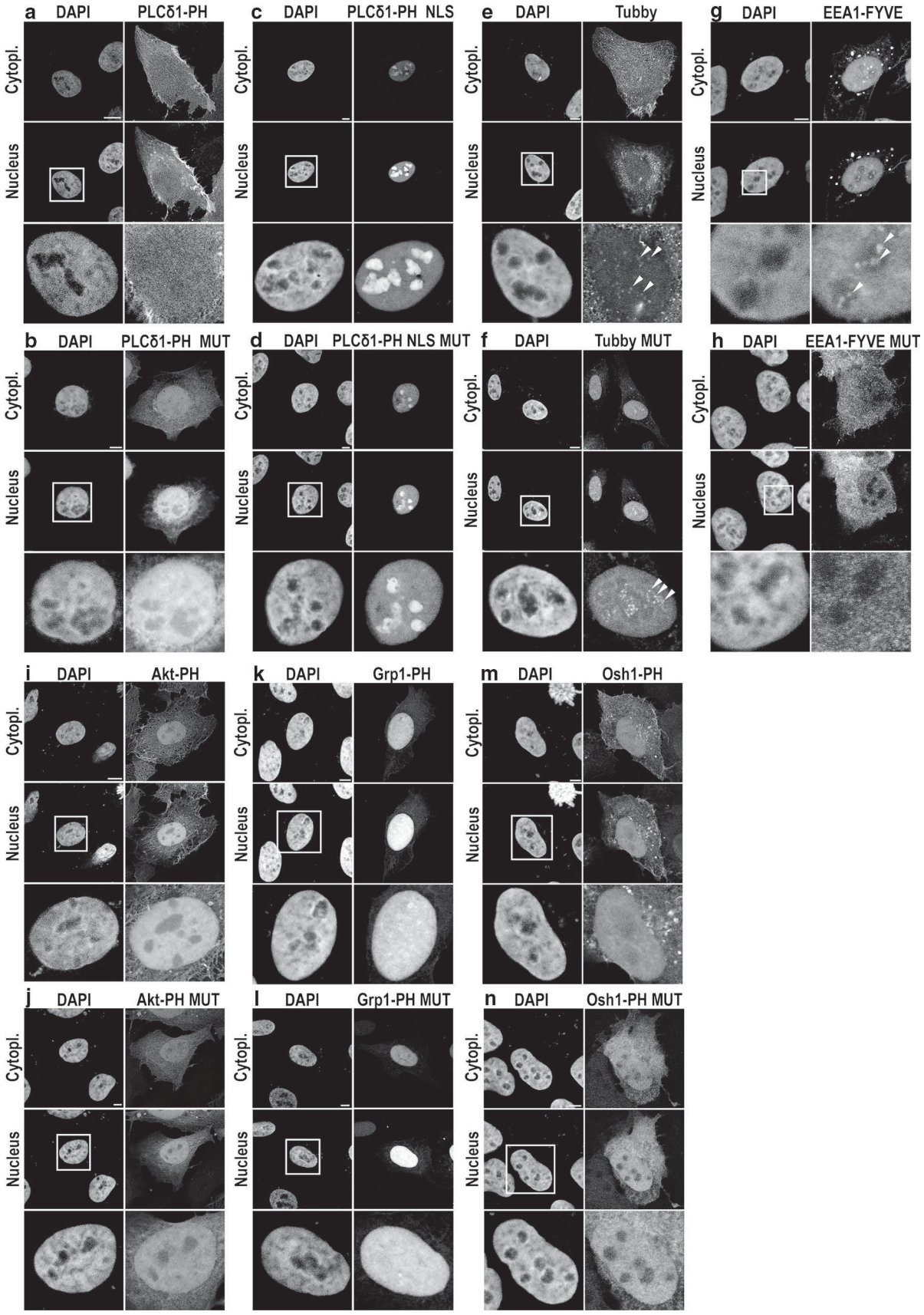
a DAPI PLCδ1-PH
c DAPI PLCδ1-PH NLS
e DAPI Tubby
g DAPI EEA1-FYVE
b DAPI PLCδ1-PH MUT
d DAPI PLCδ1-PH NLS MUT
f DAPI Tubby MUT
h DAPI EEA1-FYVE MUT
i DAPI Akt-PH
k DAPI Grp1-PH
m DAPI Osh1-PH
j DAPI Akt-PH MUT
l DAPI Grp1-PH MUT
n DAPI Osh1-PH MUT
Cytopl.
Nucleus

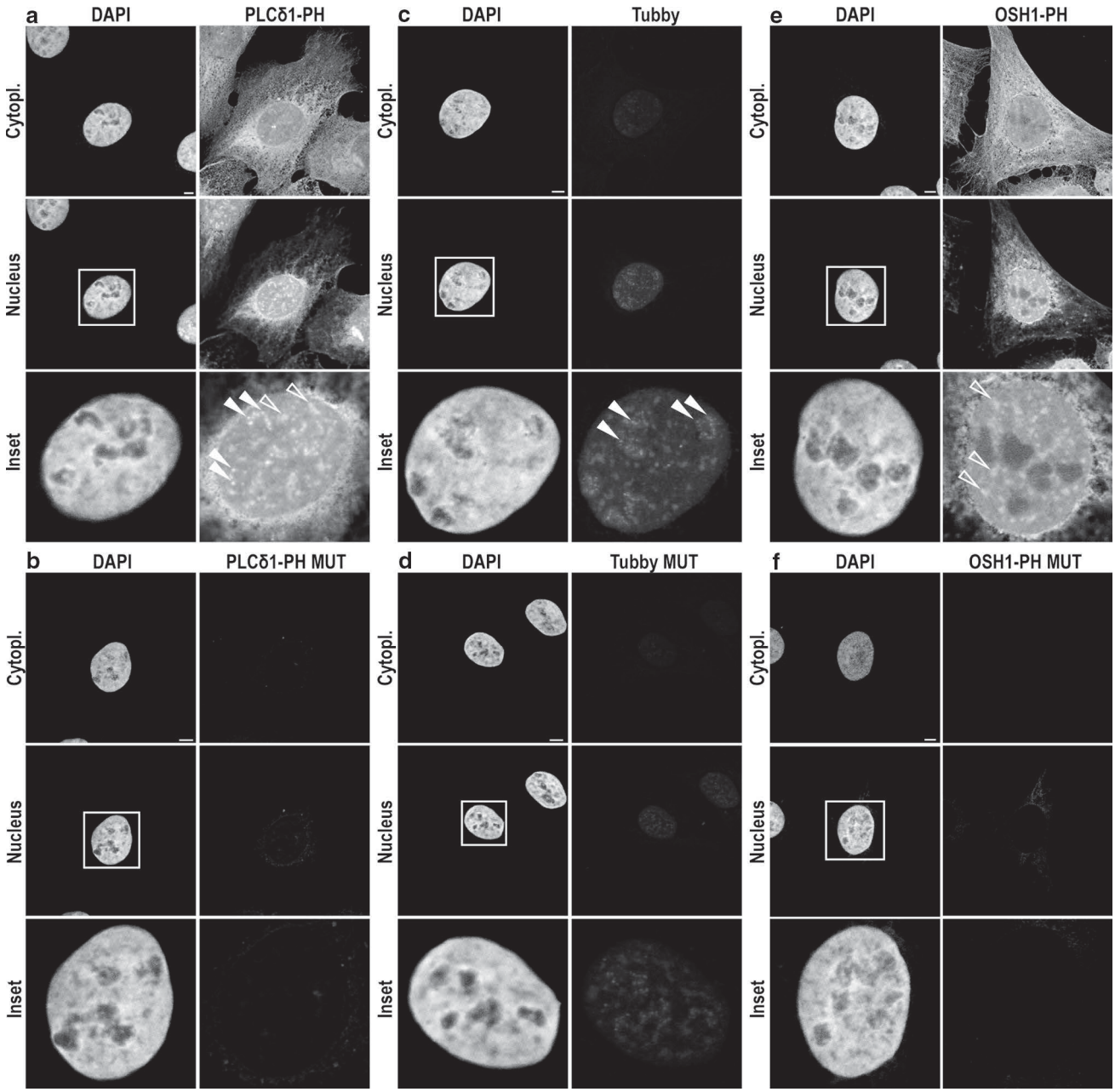

Fig. 4 Purified PLCδ1-PH, Tubby, and OSH1-PH domains recognize nuclear PIs. The images are taken at optical sections focused on the plasma membrane (*Cytopl.*) and on the nucleus (*Nucleus*). Purified PLCδ1-PH detects PI(4,5)P2 in intracellular membranes and in a lesser extent also in the plasma membrane (**a**). Moreover, wild-type PLCδ1-PH detects nuclear PI(4,5)P2 in the nucleus (**a** *inset*), where it accumulates in nucleoli (*arrowheads*) and nuclear speckles (*empty arrowheads*). The signal is completely abolished when mutant PLCδ1-PH is used (**b**). Wild-type Tubby domain detects PI(4,5)P2 only in the nucleus (**c**), where it localizes to nucleolar foci (*inset, arrowheads*). Mutant Tubby shows very weak nuclear signal (**d**). Wild-type OSH1-PH detects PI(4)P in the plasma membrane and other cellular membranes (**e**). Moreover, it has strong nuclear signal with larger bright foci, probably nuclear speckles (*inset, empty arrowheads*). Mutant OSH1-PH detects very weak cytoplasmic signal (**f**), while nuclear signal is completely abolished (*inset*). *Scale bars* 5 μm

the domains tested, the only exception was the EEA1-FYVE. It displays nucleolar localization, which is lost after mutation of PIs-binding site. Therefore, we believe that overexpressed EEA1-FYVE can be used for imaging of PI(3)P in nucleoli.

Purified PIs-binding domains conjugated with eGFP show nuclear pattern

Since overexpressed PIs-binding domains do not follow PIs to the nucleus, we looked for an alternative approach.

Fused with GST, PIs-binding domains have been successfully used for imaging of nuclear PIs in fixed cells (Gilloloy et al. 2000; Watt et al. 2002, 2004; Lindsay et al. 2006; Yildirim et al. 2013). In this system, the purified domain was incubated with fixed and permeabilized cells and subsequently detected by anti-GST antibody. To omit the use of an additional antibody, we fused PLCd1-PH, OSH1-PH, and Tubby domains with eGFP, cloned them into bacterial expression vector, and purified them from bacteria. The purified domains were tested for specificity in protein–lipid overlay assay and then used in an analogy to antibodies for immunofluorescence staining (Fig. 4). Mutant domains which are not able to bind PIs were used as negative controls.

It has been reported that GST tagged PLCδ1-PH recognizes PI(4,5)P2 in nuclear speckles and nucleoli (Watt et al. 2002; Hammond et al. 2009; Yildirim et al. 2013). Therefore, we selected PI(4,5)P2 binding domains—PLCδ1-PH and Tubby—to test their eGFP fusions on immunofluorescence. In addition, we purified eGFP tagged OSH1-PH that recognizes PI(4)P, whose nuclear signal is unknown. Since antibodies against both PI(4,5)P2 and PI(4)P are available and specific, we were able to compare results obtained by immunofluorescence.

Purified PLCδ1-PH detects PI(4,5)P2 foci in nucleoli and nuclear speckles (Fig. 4a). The signal is diminished in mutant PLCδ1-PH (Fig. 4b). In comparison with overexpressed wild-type PLCδ1-PH (Fig. 3a), purified PLCδ1-PH stains the plasma membrane to a lesser extent but detects signal from other cellular membranes. On the other hand, the nuclear pattern of purified PLCδ1-PH resembles PI(4,5)P2 labelling obtained by anti-PI(4,5)P2 antibody. In contrast, purified Tubby domain shows PI(4,5)P2 signal only in nucleoli of U2OS cells (Fig. 4c). We still detected a weak signal from mutant Tubby domain (Fig. 4d); however, the signal from wild-type domain was stronger, and therefore, we believe that it is specific. Similarly to PLCδ1-PH, Tubby is also absent from the plasma membrane. These results suggest that purified PLCδ1-PH is specific and detects similar pool of PI(4,5)P2 as anti-PI(4,5)P2 antibody. Tubby domain probably specifically recognizes nucleolar PI(4,5)P2 only.

Purified wild-type OSH1-PH detects PI(4)P in the plasma membrane and other cellular membranes, in the nucleoplasm and larger nuclear foci, and probably in nuclear speckles (Fig. 4e). The signal is lost when the cells are incubated with mutant OSH1-PH (Fig. 4f). The nuclear pattern of purified OSH1-PH resembles anti-PI(4)P labelling. We conclude that purified OSH1-PH can be used for visualization of PI(4)P in the nucleus. Importantly, we noted that nuclear patterns of all domains used for staining on fixed cells are similar to antibody-based labelling; however, they differ significantly from the patterns of overexpressed domains.

Table 2 Summary and specificity of tools used for PIs detection in the cytoplasm and in the nucleus

Tools	Target	Suitable for detection in	
		Cytoplasm	Nucleus
Antibodies			
αPI(4,5)P2	PI(4,5)P2	−	+++
αPI(3,4)P2	PI(3,4)P2	−	−
αPI(4)P	PI(4)P	−	+++
Overexpressed domains			
EEA1-FYVE	PI(3)P	+++	+ (nucleoli)
OSH1-PH	PI(4)P	+++	−
Akt-PH	PI(3,4)P2, PI(3,4,5)P3	+++	−
Tubby	PI(4,5)P2	+++	−
PLCδ1-PH	PI(4,5)P2	+++	−
PLCδ1-PH NLS	PI(4,5)P2	−	−
Grp1-PH	PI(3,4,5)P3	−	−
Purified domains			
Tubby	PI(4,5)P2	−	+ (nucleoli)
PLCδ1-PH	PI(4,5)P2	+	+++
OSH1-PH	PI(4)P	+	+++

Based on our results, antibodies and domains were rated as unsuitable (−), good (+), or very good (+++)

Discussion

Nuclear PIs have been identified as important regulators of various nuclear functions (reviewed in Shah et al. 2013). To better understand their role in the nucleus, tools for nuclear PIs visualization both in vivo and in vitro are needed. Here we performed a screen in which we aimed to identify an approach to track nuclear PIs in space and time. We compared labelling patterns of antibodies and protein domains that can be used for detection of nuclear PIs (summarized in Table 2). We showed that PI(4,5)P2 antibody recognizes PI(4,5)P2 and PI(3,4,5)P3 on protein–lipid overlay. However, according to the results of the blocking assay, the antibody is blocked by PI(3,4,5)P3 only partially while the incubation with PI(4,5)P2 abolishes the antibody signal completely (Fig. 2a–c). Because the cellular level of PI(3,4,5)P3 is more than 20-fold smaller in comparison with PI(4,5)P2 (Stephens et al. 1993; Nasuhoglu et al. 2002), we believe that the signal detected by anti-PI(4,5)P2 antibody comes from the nuclear PI(4,5)P2. Although antibody against PI(3,4)P2, the second antibody we tested, is specific on protein–lipid overlay assay, we show that it is not suitable for immunofluorescence

under our experimental conditions since it can be partially blocked by preincubation with most PIs tested (Fig. 2a, b). We suspect that these discrepancies are caused by high concentration of PIs spotted on the membrane, which do not resemble well enough the physiological conditions. On the other hand, the antibody against PI(4)P, the third antibody we tested, recognizes mainly PI(4)P as shown on both protein–lipid overlay and blocking assay (Fig. 2a, b). Using this antibody, we demonstrated for the first time that PI(4)P can be detected in the cell nucleus and that its pattern resembles the localization of PI(4,5)P2 in nuclear speckles. This antibody also detects small foci in the nucleoplasm and nucleoli (Fig. 1c). These results are in agreement with published data, which repeatedly reported localization of PI(4)P metabolizing enzymes in nuclear speckles (Boronenkov et al. 1998; Szivak et al. 2006; Mellman et al. 2008; Schill and Anderson 2009; Elong Edimo et al. 2011) and nucleoli (Kakuk et al. 2008). Regarding the nucleolar PI(4)P signal, we have shown previously that nucleolar PI(4,5)P2 forms foci in fibrillar centres and in the dense fibrillar component where it regulates rDNA synthesis and processing (Sobol et al. 2013; Yildirim et al. 2013). It is possible that the nucleolar PI(4)P serves as a precursor for PI(4,5)P2 in these compartments.

To track PIs in live cells, we overexpressed PIs-binding domains fused with eGFP in U2OS cells (Table 1; Fig. 3). We confirm that these domains are suitable for PIs monitoring in the plasma membrane and other cellular membranes. The localization of overexpressed PIs-binding domains in the nucleus has been described earlier, and it was considered as a consequence of overexpression. Since the domains are relatively small, they could diffuse passively through the nuclear pore (reviewed in Hammond and Balla 2015). We decided to inspect carefully the nuclear signal of several overexpressed domains. Mostly, we observed similar nuclear patter of wild-type and mutant domains. However, we show that wild-type but not mutant EEA1-FYVE domain localizes to foci in nucleoli. Therefore, the overexpressed EEA-1 FYVE domain can be used for visualization of PI(3)P in nucleoli.

Since most of the overexpressed PIs-binding domains were not suitable for PIs detection in the nucleus, we prepared purified PLCδ1-PH, Tubby, and OSH1-PH domains fused with eGFP. In contrast to the results obtained after overexpression, purified PLCδ1-PH and Tubby domains specifically detect PI(4,5)P2 in nucleoli. Moreover, PLCδ1-PH shows PI(4,5)P2 localization also in nuclear speckles. OSH1-PH detects nuclear PI(4)P in the nucleoplasm and concentrated in bigger nucleoplasmic foci, probably nuclear speckles. It is known that the concentration and type of detergent used for permeabilization affect the detection of PIs in the cell (Mazzotti et al. 1995; Hammond et al. 2009). Therefore, we think that different conditions used for PIs detection are the reason for diversities between overexpressed and purified domains staining. After overexpression, PIs-binding domains are targeted to the site of their ligand, where they are fixed, and therefore, stronger signal from cellular membranes can be detected. In case of purified PIs-binding domains and antibodies, cell membranes are first permeabilized, and then, PIs detection tools are applied. We believe that these differences in sample preparation result in reduction in the PIs signal from cellular membranes while the signal from the nucleus, where PIs form complexes with nuclear proteins, is more prominent. Therefore, purified domains are more suitable tools for nuclear PIs detection.

We also report differences in the nuclear signal detected by purified domains and antibodies in fixed cells. We show that anti-PI(4,5)P2 detects signal mostly in nuclear speckles and the nucleoplasm while purified PLCδ1-PH detects strong signal also in nucleolar foci. Tubby domain detects PI(4,5)P2 predominantly in nucleoli (Figs. 1a, 4). We believe that domains and antibodies recognize different pools of nuclear PIs with different affinities. It might be caused by different mechanism of PIs recognition. Moreover, anti-PI(4,5)P2 is IgM isotype and is therefore more than tenfold larger than both purified domains. Therefore, the antibody might not be able to access the nucleolar pool of PI(4,5)P2.

Here we identified some useful tools for PIs detection in the nucleus (Table 2). Unfortunately, the tools which would enable the visualization of nuclear PIs in vivo are still missing. One possibility is the use of labelled PIs. However, their use is problematic since they can be modified or cleaved in the cell. The future goal is thus to engineer such modifications of PIs which would enable their delivery to the nucleus and subsequently study their involvement in endogenous pathways, while preventing their cleavage.

Acknowledgments P. H., I. K., V. F., and L. U. were supported by the Grant agency of the Czech Republic (15-08738S, P305/11/2232, 16-03403S), P. H. and L. U. were supported by Human Frontier Science Program (RGP0017/2013), I. K., A. K., and L. U. were supported by the Grant Agency of the Charles University (606112), and I. K., V. F., A. K., and L. U. were supported by the Charles University in Prague. This publication is supported by the project "BIOCEV—Biotechnology and Biomedicine Centre of the Academy of Sciences and Charles University" (CZ.1.05/1.1.00/02.0109), from the European Regional Development Fund. This research was performed with support of the Institute of Molecular Genetics, Academy of Sciences of the Czech Republic (RVO: 68378050). We are very grateful to Dr. Tamas Balla (National Institutes of Health, Bethesda) for providing us the PLCδ1-PH, EEA1-FYVE, Grp1-PH, OSH1-PH, Akt-PH, and Tubby domains constructs. We would like to thank Iva Jelínková and Pavel Kříž for excellent technical assistance.

Compliance with ethical standards

Conflict of interest The authors have no conflict of interest to declare.

References

Ahn J-Y, Rong R, Liu X, Ye K (2004) PIKE/nuclear PI 3-kinase signaling mediates the antiapoptotic actions of NGF in the nucleus. EMBO J 23:3995–4006. doi:10.1038/sj.emboj.7600392

Ahn JY, Liu X, Cheng D et al (2005) Nucleophosmin/B23, a nuclear PI(3,4,5)P3 receptor, mediates the antiapoptotic actions of NGF by inhibiting CAD. Mol Cell 18:435–445. doi:10.1016/j.molcel.2005.04.010

Balla T (2013) Phosphoinositides: tiny lipids with giant impact on cell regulation. Physiol Rev 93:1019–1137. doi:10.1152/physrev.00028.2012

Balla T, Várnai P (2009) Visualization of cellular phosphoinositide pools with GFP-fused protein-domains. Curr Protoc Cell Biol 24(4). doi: 10.1002/0471143030.cb2404s42

Balla A, Kim YJ, Varnai P et al (2008) Maintenance of hormone-sensitive phosphoinositide pools in the plasma membrane requires phosphatidylinositol 4-kinase IIIalpha. Mol Biol Cell 19:711–721. doi:10.1091/mbc.E07-07-0713

Blind RD, Sablin EP, Kuchenbecker KM et al (2014) The signaling phospholipid PIP3 creates a new interaction surface on the nuclear receptor SF-1. Proc Natl Acad Sci USA 111:15054–15059. doi:10.1073/pnas.1416740111

Boronenkov IV, Loijens JC, Umeda M, Anderson RA (1998) Phosphoinositide signaling pathways in nuclei are associated with nuclear speckles containing pre-mRNA processing factors. Mol Biol Cell 9:3547–3560

Burd CG, Emr SD (1998) Phosphatidylinositol(3)-phosphate signaling mediated by specific binding to RING FYVE domains. Mol Cell 2:157–162. doi:10.1016/S1097-2765(00)80125-2

Clarke JH, Letcher AJ, D'santos CS et al (2001) Inositol lipids are regulated during cell cycle progression in the nuclei of murine erythroleukaemia cells. Biochem J 357:905–910. doi:10.1042/0264-6021:3570905

Cocco L, Gilmour RS, Ognibene A et al (1987) Synthesis of polyphosphoinositides in nuclei of friend cells. Evidence for polyphosphoinositide metabolism inside the nucleus which changes with cell differentiation. Biochem J 248:765–770

De Vries KJ, Westerman J, Bastiaens PI et al (1996) Fluorescently labeled phosphatidylinositol transfer protein isoforms (alpha and beta), microinjected into fetal bovine heart endothelial cells, are targeted to distinct intracellular sites. Exp Cell Res 227:33–39. doi:10.1006/excr.1996.0246

Elong Edimo W, Derua R, Janssens V et al (2011) Evidence of SHIP2 Ser132 phosphorylation, its nuclear localization and stability. Biochem J 439:391–401. doi:10.1042/BJ20110173

Gaullier JM, Simonsen A, D'Arrigo A et al (1998) FYVE fingers bind PtdIns(3)P. Nature 394:432–433. doi:10.1038/28767

Gillooly DJ, Morrow IC, Lindsay M et al (2000) Localization of phosphatidylinositol 3-phosphate in yeast and mammalian cells. EMBO J 19:4577–4588. doi:10.1093/emboj/19.17.4577

Gozani O, Karuman P, Jones DR et al (2003) The PHD finger of the chromatin-associated protein ING2 functions as a nuclear phosphoinositide receptor. Cell 114:99–111. doi:10.1016/S0092-8674(03)00480-X

Gray A, Van Der Kaay J, Downes CP (1999) The pleckstrin homology domains of protein kinase B and GRP1 (general receptor for phosphoinositides-1) are sensitive and selective probes for the cellular detection of phosphatidylinositol 3,4-bisphosphate and/or phosphatidylinositol 3,4,5-trisphosphate. Biochem J 344(Pt 3):929–936

Guillou H, Lécureuil C, Anderson KE et al (2007) Use of the GRP1 PH domain as a tool to measure the relative levels of PtdIns(3,4,5)P3 through a protein-lipid overlay approach. J Lipid Res 48:726–732. doi:10.1194/jlr.D600038-JLR200

Hammond GRV, Schiavo G, Irvine RF (2009) Immunocytochemical techniques reveal multiple, distinct cellular pools of PtdIns4*P* and PtdIns(4,5) P_2. Biochem J 422:23–35. doi:10.1042/BJ20090428

Hammond GRV, Balla T (2015) Polyphosphoinositide binding domains: key to inositol lipid biology. Biochim Biophys Acta 1851:746–758. doi:10.1016/j.bbalip.2015.02.013

Jo H, Mondal S, Tan D et al (2012) Small molecule-induced cytosolic activation of protein kinase Akt rescues ischemia-elicited neuronal death. Proc Natl Acad Sci USA 109:10581–10586. doi:10.1073/pnas.1202810109

Jones DR, Bultsma Y, Keune W-J et al (2006) Nuclear PtdIns5P as a transducer of stress signaling: an in vivo role for PIP4Kbeta. Mol Cell 23:685–695. doi:10.1016/j.molcel.2006.07.014

Jungmichel S, Sylvestersen KB, Choudhary C et al (2014) Specificity and commonality of the phosphoinositide-binding proteome analyzed by quantitative mass spectrometry. Cell Rep 6:578–591. doi:10.1016/j.celrep.2013.12.038

Kakuk A, Friedländer E, Vereb G et al (2008) Nuclear and nucleolar localization signals and their targeting function in phosphatidylinositol 4-kinase PI4K230. Exp Cell Res 314:2376–2388. doi:10.1016/j.yexcr.2008.05.006

Kavran JM, Klein DE, Lee A et al (1998) Specificity and promiscuity in phosphoinositide binding by pleckstrin homology domains. J Biol Chem 273:30497–30508. doi:10.1074/jbc.273.46.30497

Keune Wj, Bultsma Y Y, Sommer L et al (2011) Phosphoinositide signalling in the nucleus. Adv Enzyme Regul 51:91–99. doi:10.1016/j.advenzreg.2010.09.009

Lee SA, Eyeson R, Cheever ML et al (2005) Targeting of the FYVE domain to endosomal membranes is regulated by a histidine switch. Proc Natl Acad Sci USA 102:13052–13057. doi:10.1073/pnas.0503900102

Levine TP, Munro S (2001) Dual targeting of Osh1p, a yeast homologue of oxysterol-binding protein, to both the Golgi and the nucleus-vacuole junction. Mol Biol Cell 12:1633–1644

Lewis AE, Sommer L, Arntzen MO et al (2011) Identification of nuclear phosphatidylinositol 4,5-bisphosphate-interacting proteins by neomycin extraction. Mol Cell Proteomics 10:M110.003376. doi:10.1074/mcp.M110.003376

Lindsay Y, McCoull D, Davidson L et al (2006) Localization of agonist-sensitive PtdIns(3,4,5)P3 reveals a nuclear pool that is insensitive to PTEN expression. J Cell Sci 119:5160–5168. doi:10.1242/jcs.000133

Manna D, Albanese A, Park WS, Cho W (2007) Mechanistic basis of differential cellular responses of phosphatidylinositol 3,4-bisphosphate- and phosphatidylinositol 3,4,5-trisphosphate-binding pleckstrin homology domains. J Biol Chem 282:32093–32105. doi:10.1074/jbc.M703517200

Martelli AM, Ognibene A, Buontempo F et al (2011) Nuclear phosphoinositides and their roles in cell biology and disease. Crit Rev Biochem Mol Biol 46:436–457. doi:10.3109/10409238.2011.609530

Mazzotti G, Zini N, Rizzi E et al (1995) Immunocytochemical detection of phosphatidylinositol 4,5-bisphosphate localization sites within the nucleus. J Histochem Cytochem 43:181–191. doi:10.1177/43.2.7822774

Mellman DL, Gonzales ML, Song C et al (2008) A PtdIns4,5P2-regulated nuclear poly(A) polymerase controls expression of select mRNAs. Nature 451:1013–1017. doi:10.1038/nature06666

Nasuhoglu C, Feng S, Mao J et al (2002) Nonradioactive analysis of phosphatidylinositides and other anionic phospholipids by anion-exchange high-performance liquid chromatography with suppressed conductivity detection. Anal Biochem 301:243–254. doi:10.1006/abio.2001.5489

Okada M, Jang S-W, Ye K (2008) Akt phosphorylation and nuclear phosphoinositide association mediate mRNA export and

cell proliferation activities by ALY. Proc Natl Acad Sci USA 105:8649–8654. doi:10.1073/pnas.0802533105

Osborne SL, Thomas CL, Gschmeissner S, Schiavo G (2001) Nuclear PtdIns(4,5)P2 assembles in a mitotically regulated particle involved in pre-mRNA splicing. J Cell Sci 114:2501–2511

Quinn KV, Behe P, Tinker A (2008) Monitoring changes in membrane phosphatidylinositol 4,5-bisphosphate in living cells using a domain from the transcription factor tubby. J Physiol 586:2855–2871. doi:10.1113/jphysiol.2008.153791

Rowland MM, Gong D, Bostic HE et al (2012) Microarray analysis of Akt PH domain binding employing synthetic biotinylated analogs of all seven phosphoinositide headgroup isomers. Chem Phys Lipids 165:207–215. doi:10.1016/j.chemphyslip.2011.12.001

Roy A, Levine TP (2004) Multiple pools of phosphatidylinositol 4-phosphate detected using the pleckstrin homology domain of Osh2p. J Biol Chem 279:44683–44689. doi:10.1074/jbc.M401583200

Sablin EP, Blind RD, Uthayaruban R et al (2015) Structure of liver receptor homolog-1 (NR5A2) with PIP3 hormone bound in the ligand binding pocket. J Struct Biol 192:342–348. doi:10.1016/j.jsb.2015.09.012

Santagata S, Boggon TJ, Baird CL et al (2001) G-protein signaling through tubby proteins. Science 292:2041–2050. doi:10.1126/science.1061233

Schill NJ, Anderson RA (2009) Two novel phosphatidylinositol-4-phosphate 5-kinase type Igamma splice variants expressed in human cells display distinctive cellular targeting. Biochem J 422:473–482. doi:10.1042/BJ20090638

Shah ZH, Jones DR, Sommer L et al (2013) Nuclear phosphoinositides and their impact on nuclear functions. FEBS J 280:6295–6310. doi:10.1111/febs.12543

Smith CD, Wells WW (1983) Phosphorylation of rat liver nuclear envelopes. I. Characterization of in vitro protein phosphorylation. J Biol Chem 258:9360–9367

Sobol M, Yildirim S, Philimonenko VV et al (2013) UBF complexes with phosphatidylinositol 4,5-bisphosphate in nucleolar organizer regions regardless of ongoing RNA polymerase I activity. Nucleus 4:478–486. doi:10.4161/nucl.27154

Stauffer TP, Ahn S, Meyer T (1998) Receptor-induced transient reduction in plasma membrane PtdIns(4,5)P2 concentration monitored in living cells. Curr Biol 8:343–346. doi:10.1016/S0960-9822(98)70135-6

Stephens LR, Jackson TR, Hawkins PT (1993) Agonist-stimulated synthesis of phosphatidylinositol(3,4,5)-trisphosphate. Biochim Biophys Acta Mol Cell Res 1179:27–75. doi:10.1016/0167-4889(93)90072-W

Szentpetery Z, Balla A, Kim YJ et al (2009) Live cell imaging with protein domains capable of recognizing phosphatidylinositol 4,5-bisphosphate; a comparative study. BMC Cell Biol 10:67. doi:10.1186/1471-2121-10-67

Szivak I, Lamb N, Heilmeyer LMG (2006) Subcellular localization and structural function of endogenous phosphorylated phosphatidylinositol 4-kinase (PI4K92). J Biol Chem 281:16740–16749. doi:10.1074/jbc.M511645200

Tan X, Thapa N, Choi S, Anderson RA (2015) Emerging roles of PtdIns(4,5)P2 - beyond the plasma membrane. J Cell Sci 128:4047–4056. doi:10.1242/jcs.175208

Toska E, Campbell HA, Shandilya J et al (2012) Repression of transcription by WT1-BASP1 requires the myristoylation of BASP1 and the PIP2-dependent recruitment of histone deacetylase. Cell Rep 2:462–469. doi:10.1016/j.celrep.2012.08.005

Vann LR, Wooding FB, Irvine RF, Divecha N (1997) Metabolism and possible compartmentalization of inositol lipids in isolated rat-liver nuclei. Biochem J 327(Pt 2):569–576

Varnai P, Balla T (1998) Visualization of phosphoinositides that bind Pleckstrin homology domains: calcium- and agonist-induced dynamic changes and relationship to myo-[3H]inositol-labeled phosphoinositide pools. J Cell Biol 143:501–510. doi:10.1083/jcb.143.2.501

Venkateswarlu K, Gunn-Moore F, Oatey PB et al (1998) Nerve growth factor- and epidermal growth factor-stimulated translocation of the ADP-ribosylation factor-exchange factor GRP1 to the plasma membrane of PC12 cells requires activation of phosphatidylinositol 3-kinase and the GRP1 pleckstrin homology domain. Biochem J 335(Pt 1):139–146

Višnjić D, Ćurić J, Crljen V et al (2003) Nuclear phosphoinositide 3-kinase C2β activation during G2/M phase of the cell cycle in HL-60 cells. Biochim Biophys Acta Mol Cell Biol Lipids 1631:61–71. doi:10.1016/S1388-1981(02)00356-6

Watt SA, Kular G, Fleming IN et al (2002) Subcellular localization of phosphatidylinositol 4,5-bisphosphate using the pleckstrin homology domain of phospholipase C delta1. Biochem J 363:657–666. doi:10.1074/jbc.M301418200

Watt SA, Kimber WA, Fleming IN et al (2004) Detection of novel intracellular agonist responsive pools of phosphatidylinositol 3,4-bisphosphate using the TAPP1 pleckstrin homology domain in immunoelectron microscopy. Biochem J 377:653–663. doi:10.1042/BJ20031397

Watton SJ, Downward J (1999) Akt/PKB localisation and 3′ phosphoinositide generation at sites of epithelial cell–matrix and cell–cell interaction. Curr Biol 9:433–436. doi:10.1016/S0960-9822(99)80192-4

Wickramasinghe V, Savill J, Chavali S et al (2013) Human inositol polyphosphate multikinase regulates transcript-selective nuclear mRNA export to preserve genome integrity. Mol Cell 51:737–750. doi:10.1016/j.molcel.2013.08.031

Yagisawa H, Sakuma K, Paterson HF et al (1998) Replacements of single basic amino acids in the pleckstrin homology domain of phospholipase C-δ1 alter the ligand binding, phospholipase activity, and interaction with the plasma membrane. J Biol Chem 273:417–424. doi:10.1074/jbc.273.1.417

Yildirim S, Castano E, Sobol M et al (2013) Involvement of phosphatidylinositol 4,5-bisphosphate in RNA polymerase I transcription. J Cell Sci 126:2730–2739. doi:10.1242/jcs.123661

Yokogawa T, Nagata S, Nishio Y et al (2000) Evidence that 3′-phosphorylated polyphosphoinositides are generated at the nuclear surface: use of immunostaining technique with monoclonal antibodies specific for PI 3,4-P2. FEBS Lett 473:222–226. doi:10.1016/S0014-5793(00)01535-0

York JD, Majerus PW (1994) Nuclear phosphatidylinositols decrease during S-phase of the cell cycle in HeLa cells [published erratum appears in J Biol Chem 1994 Dec 9;269(49):31322]. J Biol Chem 269:7847–7850

Yu JW, Mendrola JM, Audhya A et al (2004) Genome-wide analysis of membrane targeting by *S. cerevisiae* pleckstrin homology domains. Mol Cell 13:677–688. doi:10.1016/S1097-2765(04)00083-8

Zhao K, Wang W, Rando OJ et al (1998) Rapid and phosphoinositol-dependent binding of the SWI/SNF-like BAF complex to chromatin after T lymphocyte receptor signaling. Cell 95:625–636. doi:10.1016/S0092-8674(00)81633-5

Zou J, Marjanovic J, Kisseleva MV et al (2007) Type I phosphatidylinositol-4,5-bisphosphate 4-phosphatase regulates stress-induced apoptosis. Proc Natl Acad Sci USA 104:16834–16839. doi:10.1073/pnas.0708189104

3.2 PIP2 epigenetically represses rRNA genes transcription interacting with PHF8

Ulicna L., Rohozkova J., Kalendova A., Kalasova I., Vacik T. and Hozak P.

BBA-Molecular and Cell Biology of Lipids. 2017. 1863(3):226-275 doi: 10.1016/j.bbalip.2017.12.008

IF: 5.547 (2016/2017)

L.U. designed, performed and evaluated almost all experiments (DNA cloning, DNA mutagenesis, protein expression and purification, pull-down assays, immunoprecipitations, indirect immunofluorescence and fluorescence microscopy, demethylation assays, qPCR, ChIP) and wrote the paper.

BBA - Molecular and Cell Biology of Lipids 1863 (2018) 266–275

Contents lists available at ScienceDirect

BBA - Molecular and Cell Biology of Lipids

journal homepage: www.elsevier.com/locate/bbalip

PIP2 epigenetically represses rRNA genes transcription interacting with PHF8

Livia Ulicna[a], Alzbeta Kalendova[a], Ilona Kalasova[a], Tomas Vacik[a], Pavel Hozák[a,b,c,*]

[a] Department of Biology of the Cell Nucleus, Institute of Molecular Genetics of the Academy of Sciences of the Czech Republic, v.v.i., 142 20 Prague, Czech Republic
[b] Department of Epigenetics of the Cell Nucleus, Institute of Molecular Genetics of the Academy of Sciences of the Czech Republic, v.v.i., division BIOCEV, 25250 Vestec, Czech Republic
[c] Microscopy Center the Institute of Molecular Genetics of the Academy of Sciences of the Czech Republic, v.v.i., 142 20 Prague, Czech Republic

ARTICLE INFO

Keywords:
PIP2
PHF8
rDNA transcription
H3K9me2
Nucleus

ABSTRACT

Phosphoinositides are present in the plasma membrane, cytoplasm and inside the cell nucleus. Here we identify phosphatidylinositol-4,5-bisphosphate (PIP2) as a regulator of rRNA genes transcription at the epigenetic level. We show that PIP2 directly interacts with histone lysine demethylase PHF8 (PHD finger protein 8) and represses demethylation of H3K9me2 through this interaction. We identify the C-terminal K/R-rich motif as PIP2-binding site within PHF8, and address the function of this PIP2-PHF8 complex. PIP2-binding mutant of PHF8 has increased the activity of rDNA promoter (20%) and expression of pre-rRNA genes (47S-100%; 45S-66%). Furthermore, trypsin digestion reveals a potential conformational change of PHF8 upon PIP2 binding. These observations identify the function of nuclear PIP2, and suggest that PIP2 contributes to the fine-tuning of rDNA transcription.

1. Introduction

Phosphoinositides (PIs) are phosphorylated derivatives of phosphatidylinositol, a glycerol-based lipid. Phosphorylation of *myo*-inositol head group at every permutation of the 3-,4-,5-position yields seven isomers with independent biological functions. Phosphoinositides are known to act as signaling molecules involved in the regulation of membrane dynamics, cell architecture and motility, cell differentiation, proliferation and cell cycle progression, modulation of ion channels and transporters, or generation of second messengers [1,2]. PIs, as signaling molecules, are connected with direct dynamic regulation of nuclear receptors through which many of transcriptional effects can be mediated [3]. Not only PIs but also PIs-metabolizing enzymes such as Inositol polyphosphate multikinase (IMPK) also possess multiple functions. IMPK is able to act in transcription and epigenetic regulation through (i) interactions with steroidogenic factor 1 (SF1, nuclear receptor), (ii) generation of Ins(1,4,5,6)P4 thus increasing histone deacetylase activity, or (iii) interactions with transcription factors such as serum response factor (SRF), CREB-binding protein (CBP) and p53 [4]. Additionally, publications targeting the nuclear phosphoinositide-specific phospholipase C beta1 (PI-PLCbeta1), are showing its importance in processes such as myogenic, osteogenic or hematopoietic differentiation [5].

In the cell nucleus, the presence of almost all PIs, except PI(3,5)P2, has been documented [6–13]. To address PIs nuclear function, two high-throughput screens have been recently performed aiming to identify molecular interactions of PIs. More than 300 nuclear proteins were found and many of them contain lysine/arginine (K/R)-rich motif which mediates their interactions with the negatively charged phosphorylated *myo*-inositol head group of PIs [14,15]. These proteins are involved in processes such as cell division, cell signaling, and transcription, which indicate previously uncharacterized roles of nuclear PIs.

The most studied nuclear phosphoinositide is phosphatidylinositol-4,5-bisphosphate (PIP2) which localizes to nuclear speckles, small foci in the nucleoplasm, and to the nucleolus [6,7,11,16]. Nuclear PIP2 acts as a transcription activator interacting with the catalytic complex of both RNA polymerases I and II [11,16]. PIP2 regulates RNA polymerase II transcription probably by the direct interaction with histone H1 and histone H3 [17]. This interaction shields H1/H3 positive charges and thus interferes with their DNA binding ability, which leads to an altered chromatin structure. In addition, PIP2 negatively regulates RNA polymerase II transcription by binding to the myristoylated transcriptional co-repressor BASP1 [18]. It was shown that BASP1 requires PIP2 in order to recruit HDAC1. The presence of HDAC1 at chromatin leads to histone deacetylation which decreases promoter accessibility for

* Corresponding author at: Department of Biology of the Cell Nucleus, Institute of Molecular Genetics of the Academy of Sciences of the Czech Republic, v.v.i., 142 20 Prague, Czech Republic.
E-mail address: hozak@img.cas.cz (P. Hozák).

https://doi.org/10.1016/j.bbalip.2017.12.008
Received 20 October 2017; Received in revised form 5 December 2017; Accepted 9 December 2017
Available online 12 December 2017
1388-1981/

transcription [18].

We have previously shown that PIP2 is in a complex with RNA polymerase I, and it binds directly to the upstream binding factor (UBF) and fibrillarin [19,16]. PIP2 binding provokes a conformational change of UBF and fibrillarin, and increases their affinities for DNA and for RNA. In addition, a PIP2 depletion by anti-PIP2 antibody from HeLa cells nuclear extract results in a decrease of transcription. The transcription activity can be restored by addition of exogenous PIP2 [16]. In conclusion, PIP2 increases the binding affinity of UBF and fibrillarin and thus facilitates not only RNA polymerase I transcription, but also subsequent rRNA processing.

Among proteins from the high-throughput screens, PHD finger protein 8 (PHF8) a histone lysine demethylase has been identified as a possible interacting partner of nuclear PIP2 [14,15]. The PHF8 demethylates mono- and dimethylated lysine 9 of histone H3 [20–22], dimethylated lysine 27 of histone H3 [22], and monomethylated lysine 20 of histone H4 [23]. As all these modifications are epigenetic repressive marks [24–26], PHF8 acts as a transcription activator. Possessing this ability, PHF8 is involved in the regulation of numerous physiological processes, such as craniofacial and brain development of zebrafish [23]. In contrast, the absence of PHF8 or its loss of function caused by mutation in the catalytic domain results in X-linked mental retardation and cleft lip/palate [27,28].

Besides RNA polymerase II transcription, PHF8 also facilitates rDNA transcription, which is executed by RNA polymerase I and its associated factors in the nucleolus. PHF8 regulates rDNA transcription *via* binding to H3K4me3 and subsequently demethylating H3K9me1/2. Moreover, PHF8 associates with the RNA polymerase I catalytic subunit as well as with the upstream binding factor (UBF) [21,22].

Current data suggest that PHF8 and PIP2 act at different stages of RNA polymerase I transcription however, there is no description of PIP2 as an epigenetic regulator. To find whether PIP2 indeed affects such events, we studied the role of the complex formed by PIP2 and PHF8. Here we demonstrate a direct interaction between PIP2 and PHF8, which affects the conformation of PHF8 and subsequently its ability to activate transcription of rRNA genes.

2. Materials and methods

2.1. Cell cultures and transfections

Human cervical carcinoma (HELA), osteosarcoma (U2OS), and human embryonic kidney 293 (HEK 293) cells were grown in D-MEM supplemented with 10% fetal bovine serum (FBS) at 37 °C in 5% CO_2 humidified atmosphere. Suspension HELA cells were kept in S-MEM supplemented with 5% FBS at 37 °C in 5% CO_2 humidified atmosphere. Transfections were carried out using Lipofectamine 2000 (Invitrogen) according to the manufacturer's protocol. Stable cell lines were prepared by Lipofectamine 2000 transfection and selected in D-MEM with 10% FBS with addition of geneticin (G418) in final concentration 0.5 mg/ml.

2.2. Constructs

PHF8 was cloned from human cDNA into pET-42(a)$^+$ (Novagen) and used for protein purification. For mammalian expression, PHF8 was inserted into pCMV-Tag4B (Strategene). Truncated forms of PHF8 as followed 1-360 AA, 361-674 AA, 675-1024 AA were inserted into pET-42(a)$^+$ and used for protein purification. PIP2 binding mutant of PHF8 with mutated 282-836 AA (KSRPKKKK motif mutated to ASRPAGAA) was prepared by Q5 site direct mutagenesis kit (New England Biolabs) in pET-42(a)$^+$ (Novagen) and pCMV-Tag4B (Strategene). Human rDNA promoter for luciferase assay was prepared as described previously [29] and cloned into pGL4.10 (Promega). The primers used in this study are summarized in Sup. Table 1.

2.3. Antibodies

Following primary antibodies were used in this study: anti-PIP2 mouse monoclonal IgM antibody (Echelon Biosciences Inc., clone 2C11, Z-A045), anti-PHF8 rabbit polyclonal (Abcam, ab36068 and kind gift from Ingrid Grummt, GCRC Heidelberg, Germany); anti-H3 goat polyclonal IgG (Abcam, ab12079), anti-H3K9me2 rabbit polyclonal IgG antibody (Abcam, ab32521); anti-H3K9me1 rabbit polyclonal IgG antibody (Abcam, ab9045), anti-H3K27me2 rabbit polyclonal IgG (Abcam, ab24684), anti-H3K36me2 rabbit polyclonal (Abcam, ab9049), anti-H3K9 acetyl rabbit polyclonal (Abcam, ab10812), anti-H4K20me1 rabbit polyclonal (Abcam, ab9051), anti-Flag mouse monoclonal IgG (Stratagene, clone M2, 200471), anti-GST mouse monoclonal (Abcam, ab92), anti-GAPDH mouse monoclonal (Acris, clone 6G5), anti-RPA194 (Santa Cruz, sc-28714), control mouse anti-IgG (Abcam, ab81032), control mouse anti-IgM (Abcam, ab18401), control rabbit anti-IgG (Abcam, ab46540).

Following secondary antibodies were used in this study: goat anti-mouse IgM (μ-chain specific) antibody conjugated with Alexa Fluor 555 (Invitrogen, A21426), goat anti-rabbit IgG (H + L) antibody conjugated with Alexa Fluor 488 (Invitrogen, A11034), IRDye 680 donkey anti-mouse IgG (H + L) antibody (LI-COR Biosciences, 926-68072), IRDye 800 donkey anti-mouse IgG (H + L) antibody (LI-COR Biosciences, 926-32212), IRDye 800 donkey anti-rabbit IgG (H + L) antibody (LI-COR Biosciences, 925-32213), IRDye 680 donkey anti-rabbit IgG (H + L) antibody (LI-COR, Biosciences, 926-68073), IRDye 800 Goat anti-Mouse IgM (μ chain specific) antibody (LI-COR Biosciences 926-32280), IRDye 800 donkey-anti Goat IgG (H + L) antibody (LI-COR Biosciences, 926-32214), IRDye 680 donkey-anti Goat IgG (H + L) antibody (LI-COR Biosciences, 926-68074).

2.4. Expression and purification of recombinant proteins

Construct of truncated forms of PHF8-GST and PIP2 binding mutant of PHF8-GST in pET-42(a)$^+$ plasmid vector (Novagen) were transformed and expressed in *E. coli* BL21(DE3). Transformed cells were incubated for approximately 4 h at 37 °C until OD = 0.6. Expression was then induced by 0.5 mM IPTG for 2 h at 30 °C. Samples were lysed by sonication in buffer (50 mM Tris (pH 7.5), 150 mM NaCl, 1% Triton-X, complete protease inhibitors (Roche)) and purified using GST-agarose beads according to manufacturer's protocol (Sigma). SDS-PAGE electrophoresis was used to check expression and purity.

2.5. Indirect immunofluorescence for super-resolution fluorescence microscopy

U2OS cells seeded on glass coverslips (18 × 18 mm) were fixed and permeabilized with 90% ice-cold methanol in MeS buffer (100 mM 2-(*N*-morpholino)ethanesulfonic acid pH 6.9, 1 mM EGTA, 1 mM $MgCl_2$) for 5 min at 4 °C. Coverslips were further blocked with 4% BSA in PBS for 20 min at room temperature. After three washes with PBS, coverslips were incubated with the particular primary antibody diluted in PBS overnight at 4 °C in a wet chamber. After incubation with primary antibody, coverslips were washed with PBS-T (PBS supplemented with 0.05% Tween20). Subsequently, coverslips were incubated with corresponding secondary antibody for 1 h at room temperature in a wet chamber. After three washes in PBS-T, coverslips were mounted in Vectashield antifade medium with DAPI (Vector laboratories). Images were acquired using microscope ECLIPSE Ti-E equipped with Andor iXon3 897 EMCCD camera and objective CFI SR Apochromat TIRF 100 ×/1.49 oil (Nikon). Software NIS-Elements AR 4.20.01 and NIS Elements AR 4.30 was used for capturing and analysis of the images. Pearson's correlation coefficient was measured from 10 region of interest of five cells nuclei as is expressed as mean ± standard deviation.

2.6. Pull-down assay and co-immunoprecipitation

Nuclei were isolated from suspension HeLa cells as described previously [30]. Pure nuclei were extracted using RIPA buffer (50 mM Tris pH 7.5, 150 mM NaCl, 0.5% deoxycholate, 1% NP-40, complete protease inhibitors (Roche)), sonicated and spun at 16000 g for 15 min. Whole cell lysate was prepared by scrapping cells in lysis buffer (150 mM NaCl, 50 mM Tris-HCl (pH 7.5), 5 mM EDTA, NP-40 (0,5% vol/vol), Triton-X (1% vol/vol)), sonication and subsequent centrifugation. Clear lysate (1.5 mg/ml) was incubated with RIPA buffer pre-equilibrated PIP2 or other phosphoinositides coated on agarose beads (50 µl of slurry per sample; Echelon Biosciences) for 3–4 h at 4 °C. Beads were then washed three times with RIPA. Bound proteins were eluted by boiling in Laemmli buffer, separated by 10–15% SDS-PAGE, and detected by subsequent immunoblotting. For co-immunoprecipitation RIPA buffer pre-equilibrated protein L or protein A beads were incubated with primary antibody (2 µg) for 2 h at 4 °C and subsequently incubated with clear lysate (0.7 mg/ml) overnight at 4 °C. After three washes with RIPA buffer, bound proteins were processed as described for pull-down. For a direct interaction between PHF8 and phosphoinositides coated agarose beads was used 5 µg of recombinant Flag-PHF8 (Active Motif) per sample.

2.7. RNA isolation and Q-PCR

Total RNA was isolated using TRIzol reagent (Thermo Fisher Scientific) according to manufacturer's protocol. Concentration of RNA was measured on a spectrophotometer and integrity checked on a 1% standard agarose gel. A total of 100 ng of RNA was reverse-transcribed with random hexamer primers using SuperScript III First-Strand Synthesis System kit (Invitrogen, Life technologies). Real-time PCR was performed on ABI Prism 7300 instrument using SYBR Green PCR Master Mix (Applied Biosystems, Life Technologies) with appropriate primers. Data were evaluated with ΔΔCt method and transcript levels normalized to GAPDH gene. The experiment was performed in triplicates and repeated at least three times. Primers were previously published [31–33] and are summarized in Sup. Table 1.

2.8. Chromatin immunoprecipitation (ChIP)

ChIP was performed according to [34]. 5×10^6 HEK293 cells were crosslinked with 1% formaldehyde and quenched with 125 mM glycine. Subsequently, DNA was sheared with 30 sonication cycles (30 s ON, 30 s OFF; intensity HIGH) using Bioruptor Next Gen sonicator (Diagenode). Used lysis/IP buffer contained: 150 mM NaCl, 50 mM Tris-HCl (pH 7.5), 5 mM EDTA, NP-40 (0.5% vol/vol), Triton X-100 (1.0% vol/vol). 2 µg of antibodies against PHF8, Flag, H3K9me2, control rabbit anti-IgG, control mouse anti-IgG or 4 µg of anti-PIP2 antibody and control mouse anti-IgM were used. Input and immunoprecipitated DNA was quantified by Q-PCR. Primers for rDNA promoter detection were used as described previously [29]. Enrichment was calculated as IP over chromatin input. The experiment was performed at least in three biological replicates.

2.9. Luciferase reporter assay

The firefly luciferase reporter pGL4.10 vector with inserted human rDNA promoter (spanning −410 to +314 bp; accession number K01105) or empty pGL4.10 vector were co-transfected with renilla luciferase reporter vector pGL4.74 into HEK293 cells stably overexpressing PHF8 WT or PIP2 binding mutant of PHF8 by Lipofectamine 2000 (Invitrogen, Life technologies). After 24 h cells were lysed and luciferase activity was measured according to Dual-Glo®Luciferase Assay System protocol (Promega), using ModulusTM II Microplate Multimode Reader (Turner Biosystems). Luminescence signal from empty vectors was set as threshold for background signal. Data were normalized to renilla luciferase activity and assay was performed in triplicate and repeated at least three times.

2.10. Limited protease digestion assay

Limited protease digestion assay was performed as described previously [16] with following modifications. Recombinant PHF8-Flag (800 ng, Active Motif) was incubated with PIP2 and PIP3 (1 µg) in BC100 buffer (20 mM Tris pH 8, 20% glycerol, 100 mM NaCl) for 30 min at room temperature. After this period, trypsin (0.5 ng) was added to the mixtures, and further incubated for 1 min at room temperature. The digestion was stopped by adding Laemmli buffer and the samples were denatured at 100 °C for 5 min. Then samples were separated by 15% SDS-PAGE and changes in digestion pattern were detected by subsequent immunoblotting.

2.11. Demethylation assay

The demethylation assay was performed as described previously [35]. 3 µg of bulk histones (Sigma), 5 µg of PHF8-Flag (Active Motif) and PIP2 (100 µM or 200 µM in Fig. 5b) or PIP2 and PIP3 (100 µM in Fig. 5c) were incubated in reaction buffer (20 mM Tris-HCl (pH 7,5), 15 mM NaCl, 50 µM $(NH_4)_2Fe(SO_4)_2 + 6(H_2O)$, 1 mM α-ketoglutarate, 2 mM ascorbic acid) for 3 h at 37 °C. The reaction was stopped by Laemmli buffer, samples were separated by 15% SDS-PAGE and immunoblotting detection was performed.

3. Results

3.1. PIP2 is in complex with PHF8

Among proteins identified in high-throughput screens as a possible phosphoinositides-interacting protein [14,15], we selected to focus on PHF8 histone lysine demethylase. To assess whether PIP2 and PHF8 are in a complex, we performed pull-down of interacting proteins from nuclear extract using PIP2, PI(3,4)P2 and PIP3-coated agarose beads. Our results show that PHF8 was pulled-down only with PIP2, but not with PI(3,4)P2, PIP3 beads or empty agarose beads (Fig. 1A). Additionally, anti-PIP2 antibody co-immunoprecipitates PHF8 (Fig. 1B). These data show that PHF8 forms a complex with PIP2 specifically. *Vice versa*, we co-immunoprecipitated PIP2 together with PHF8 from HeLa cells nuclear extract using anti-PHF8 antibody, thus confirming that PIP2 is in complex with PHF8 (Fig. 1C).

The majority of PHF8 localize to the nucleolus [21,22] while a majority of PIP2 localize to nuclear speckles and only a minority localize to the nucleolus [7,11,16,19,36]. In agreement with published data and our observations, PIP2 and PHF8 co-localize in the cell nucleus when visualized by indirect immunofluorescence. We observed a significant co-localization (Pearson's correlation coefficient = 0.72 ± 0.125) of these two molecules within the nucleus using a fluorescent confocal microscopy (Fig. S1A) and a super-resolution structured illumination microscopy (N-SIM, Nikon) method (Fig. 1D).

3.2. PIP2 interacts with PHF8 directly through a lysine/arginine-rich motif

The evidence about PIP2/PHF8 binding and their obvious co-localization in the cell nucleus led us to the next aim - to decipher the mechanism of their interaction. To investigate whether PIP2 and PHF8 interact directly, we performed *in vitro* pull-down, where the PI(4)P, PI(5)P, PIP2 or PIP3-coated agarose beads were incubated with recombinant Flag-tagged PHF8 (Flag-PHF8). Since we pulled-down Flag-PHF8 by PIP2 beads only, we conclude that PIP2 and PHF8 are not only in complex, but they interact directly (Fig. 1E).

To identify the specific PIP2-binding site at the PHF8 molecule, we took advantage of bioinformatic analysis performed in Lewis et al. [11]. This parsing revealed three potential phosphoinositide-binding sites

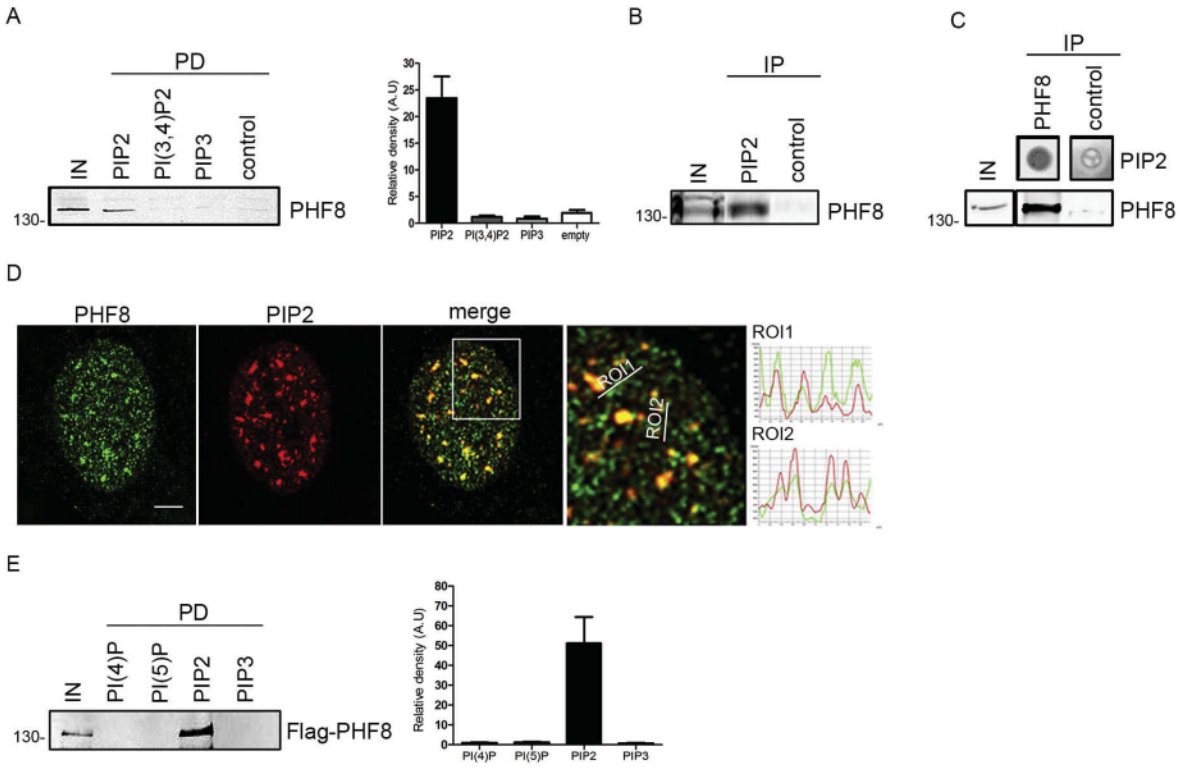

Fig. 1. PIP2 and PHF8 interact directly. (A) *In vitro* pull-down of PHF8 from HeLa nuclear extract by PIP2, PI(3,4)P2, PIP3-coated agarose beads and empty control agarose beads. Graph depicts measurement of PHF8 interaction with PIs or empty agarose beads by relative density from 3 biological replicates. (B) Co-immunoprecipitation of PHF8 by anti-PIP2 and control mouse anti-IgM antibody from HeLa cells nuclear extract. (C) Co-immunoprecipitation of PIP2 by anti-PHF8 and control rabbit anti-IgG antibody from HeLa cells nuclear extract. PIP2 was visualized by dot-blotting using anti-PIP2 antibody. Anti-PHF8 antibody immunoprecipitates PHF8. (D) Indirect immunofluorescence of PHF8 and PIP2 in U2OS cell. Images were acquired by N-SIM super-resolution microscopy. Graphs show signal intensities along the linear regions of interests (ROI). Scale bar is 5 μm. (E) *In vitro* binding assay. Recombinant Flag-PHF8 was incubated with PI(4)P, PI(5)P, PIP2 or PIP3-coated agarose beads. Flag-PHF8 was detected by anti-Flag antibody. Graph depicts measurement of PHF8 interaction with PIs beads by relative density from 3 biological replicates.

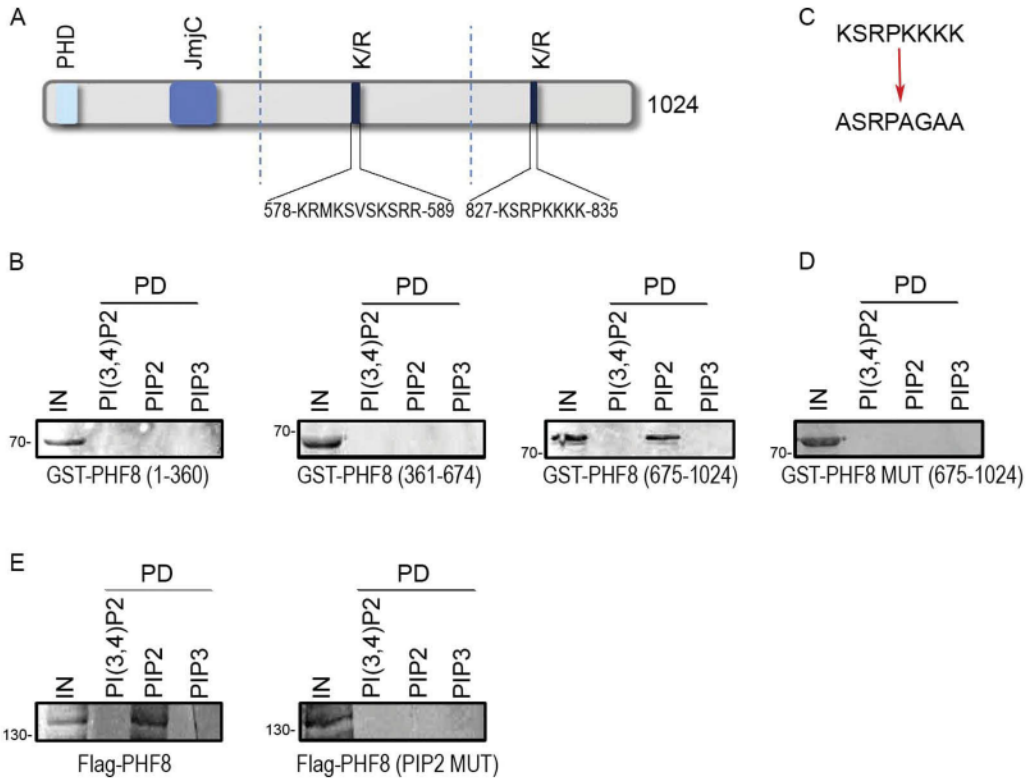

Fig. 2. C-terminal K/R-rich motif is the PIP2 binding site. (A) A scheme of PHF8 with putative phosphoinositides binding sites marked: PHD finger (light blue) and two lysine/arginine-rich motifs (K/R, dark blue). Position and composition of amino acid residues in K/R rich motifs is depicted. (B) *In vitro* binding assay. Recombinant GST-PHF8 truncated forms were incubated with PI(3,4)P2, PIP2 or PIP3-coated agarose beads and detected by anti-GST antibody. Truncated forms of PHF8 contain one putative phosphoinositide binding site: GST-PHF8 (1-360)/PHD finger, GST-PHF8 (361-674)/K/R-rich motif, GST-PHF8 (675-2014)/C-terminal K/R-rich motif. (C) A scheme of site-directed mutagenesis of PIP2 binding site. (D) *In vitro* binding assay. Pull-down of mutated truncated form of PHF8 (675-2014) with PI(3,4)P2, PIP2 or PIP3-coated agarose beads and detected by anti-GST antibody. (E) Pull-down of Flag-PHF8 or Flag-PHF8 (PIP2 MUT) overexpressed in HEK293 cells by PI(3,4)P2, PIP2 or PIP3-coated agarose beads. Anti-Flag antibody was used for detection.

within PHF8: two lysine/arginine (K/R)-rich motifs and one plant homeodomain finger (PHD; Fig. 2A). To specify which part of PHF8 containing predicted lipid binding motifs is the exact PIP2-binding site, we prepared three truncated forms of PHF8, where each truncation contains just one putative PIs binding site. By pulling-down PI(3,4)P2, PIP2 or PIP3-coated agarose beads incubated with purified truncated forms of PHF8, we observed that only the C-terminal K/R-rich motif, but neither PHD finger nor N-terminal K/R-rich motif interacted directly with PIP2 (Fig. 2B). To diminish the positive charge of the K/R-rich motif and thus to avoid binding of negatively charged head of PIP2, we mutated the basic stretches of lysines and arginines to neutral glycines or alanines by site-directed mutagenesis (Fig. 2C). After using this mutated truncated form of PHF8 PHF8 (PIP2 MUT) in an *in vitro* pull-down, the binding was not observed (Fig. 2D). Binding of Flag-PHF8 and Flag-PHF8 (PIP2 MUT) overexpressed in HEK293 cells to PI(3,4)P2, PIP2 or PIP3 (Fig. 2E) confirmed that mutation of C-terminal K/R rich motif is enough to diminish PIP2 binding to PHF8. This experiment confirms that C-terminal K/R-rich region is a PIP2-binding site within the PHF8.

Altogether, we can conclude that PIP2 and PHF8 are not only present within the same molecular complex in the cell nucleus, but they interact directly through the K/R-rich motif present at the C-terminus of PHF8.

3.3. PIP2 represses PHF8 function at the rDNA promoter

It has been previously shown that PIP2 anchors splicing factors in the nuclear speckles [36,7]. To investigate if PIP2 possesses the anchoring function in complex with PHF8 in the nucleolus, we prepared HEK293 stable cell lines expressing either wild type (WT) or PIP2-binding mutant (PIP2 MUT) of PHF8. We observed by indirect immunofluorescence that PHF8 with mutated C-terminal K/R rich motif (PIP2 MUT) is still present in the nucleolus (Fig. S1B) and that levels of PIP2 where not changed (Fig. S1C). This observation indicates that PIP2 does not anchor PHF8 in the nucleolus in a similar manner as it anchors splicing factors in nuclear speckles. We thus hypothesized that PIP2 rather influences PHF8 enzymatic function and focused then on specific changes in histone post-translational modifications in PHF8 and PHF8 (PIP2 MUT) cell lines. Although, PHF8 is able to demethylate H3K9me1, H3K9me2, H3K27me2 and H4K20me1 [20–23], we observed a significant decrease of H3K9me2 level upon mutation only, while the other histone levels remained unchanged (Fig. 3). Consistently, after siRNA-mediated knockdown of PHF8 a decrease of H3K9me2 level was diminished in PHF8 (WT) or PHF8 (PIP2 MUT) (Fig. 3E and S2A-B). As there is an interplay between histone post-translational modifications [37], we looked for changes in non-substrate histone marks for PHF8 including H3K4me3, H3K9me3, H3K36me2 and H3K9ac (Fig. S2C-F). We observed no significant changes in these histone modifications either. To rule out the possibility that the effect is caused by an unequal PHF8 overexpression or endogenous PHF8 in these two cell lines, we measured the level of over-expressed and endogenous PHF8 in HEK293 stable cell lines on western blot (Fig. S3). The quantification confirms that there is an identical amount of both PHF8 and PHF8 (PIP2 MUT) over-expressed in cell lines. To conclude, we can claim that PIP2 negatively influences PHF8 activity as a H3K9me2 histone demethylase.

It was shown that PHF8 activates rRNA genes transcription by demethylating H3K9me1/2 directly at the rDNA promoter [21,22]. This suggests that PHF8-PIP2 complex might have a function in rRNA genes transcription. To test this hypothesis, we performed chromatin immunoprecipitation (ChIP) and confirmed that both PIP2 and PHF8 associate with the rDNA promoter (Fig. 4A). Moreover, ChIP further revealed that PHF8 (PIP2 MUT) is still bound to the rDNA promoter, again providing the evidence that PIP2 does not anchor PHF8 to the chromatin (Fig. 4B). To study the effect of PHF8 mutation on the rDNA expression, we inserted rDNA promoter upstream of the firefly luciferase gene and measured luciferase expression. When we over-expressed this array in PHF8 (PIP2 MUT) cell line, the promoter activity was significantly increased by approx. 20% in comparison with PHF8 (WT) stable cell line (Fig. 4C). No difference in the promoter activity was observed, when only empty vector with luciferase gene was over-expressed in these cell lines. This led us to conclude that the PHF8-PIP2 complex affects rRNA genes transcription in a negative manner. To further confirm this result, we isolated RNA from HEK293 cell line stably over-expressing PHF8 (WT) or PHF8 (PIP2 MUT) or empty Flag plasmid as control, and performed RT-qPCR to detect rRNA genes transcription. We measured the expression of 47S pre-rRNA (primary rRNA transcript) and 45S pre-rRNA (processed primary transcript) genes and observed that the mutation in the PIP2-binding site caused a significant increase in 47S and 45S pre-rRNA expression by approximately 57% and 30%, resp. (Fig. 4D) compared to PHF8 (WT) or approximately by 100% and 66%, resp. compared to endogenous PHF8. We confirmed these results for increased 47S pre-rRNA transcription (~80%) also by metabolic labeling of nascent RNA (Fig. S4A). Next, we investigated RNA polymerase I association with rDNA promoter in from HEK293 cell line stably over-expressing PHF8 (WT) or PHF8 (PIP2 MUT) or empty Flag plasmid as control. We observed increased presence in PHF8 (PIP2 MUT) compared to PHF8 (WT) and HEK293-Flag (Fig. 4E) and this result is coherent with increased pre-rRNA genes expression. To rule out the possibility that observed increased RNA polymerase I transcription is a secondary or unrelated effect of increased cell proliferation we measured cell proliferation in PHF8 (PIP2 MUT) upon siRNA treatment (Fig. S4B.) and we did not observe any difference. These data are consistent with the increase in reporter activity upon PHF8 (PIP2 MUT) over-expression. Altogether, these data show that the capability of PHF8 to associate with PIP2 diminishes its H3K9me2 demethylation activity leading to an efficient repression of rDNA transcription.

3.4. PIP2 binding probably changes conformation of PHF8 and represses H3K9me2 demethylation at the rDNA promoter

Here we show that PIP2 and PHF8 form a functional complex, which influences histone demethylation and rDNA transcription. We performed ChIP of H3K9me2 from PHF8 (WT) and PHF8 (PIP2 MUT) or control Flag HEK293 cell lines, and we found approximately 20% decrease in the H3K9me2 level at the rDNA promoter in PHF8 (PIP2 MUT) cell line (Fig. 5A). We further tested whether PIP2 is able to affect directly the PHF8 demethylation activity, and performed *in vitro* histone demethylation assay with recombinant PHF8 on bulk histones. PHF8 itself was active, as we observed a decrease in H3K9me2 down to 50% of the input. When PHF8 was pre-incubated with PIP2 (100 μM and 200 μM), we did not observe any changes in H3K9me2 level from the input level (Fig. 5B), thus PIP2 represses PHF8 activity. Furthermore, when we pre-incubated PHF8 with PIP3 (100 μM), we observed a H3K9me2 decrease as with the PHF8 itself (Fig. 5C). We also tested PIP2 influence on demethylation of H4K20me1 by PHF8 but we did not observe any change in PHF8 activity upon PIP2 or PIP3 addition (Fig. S2G). Therefore, we conclude that PIP2 represses H3K9me2 demethylation activity of PHF8 directly and this repression is PIP2 specific. Taking these data together, we claim that PIP2 directly represses PHF8 function as an H3K9me2 demethylase and subsequently represses its function as a transcription activator of rRNA genes.

The abovementioned results identify the specific motif of PIP2 interaction to PHF8, and the functional changes after PIP2 binding to the demethylase. In order to investigate the molecular mechanism by which PIP2 binding to PHF8 influences rRNA genes transcription, we performed limited protease digestion assay. The recombinant Flag-PHF8 was incubated with synthetic PIP2 or synthetic PIP3, and subsequently digested by trypsin. We observed that PHF8 trypsin digestion profile was significantly changed upon incubation with PIP2 but not with PIP3 (Fig. 5D). This result suggests that a potential conformational change of

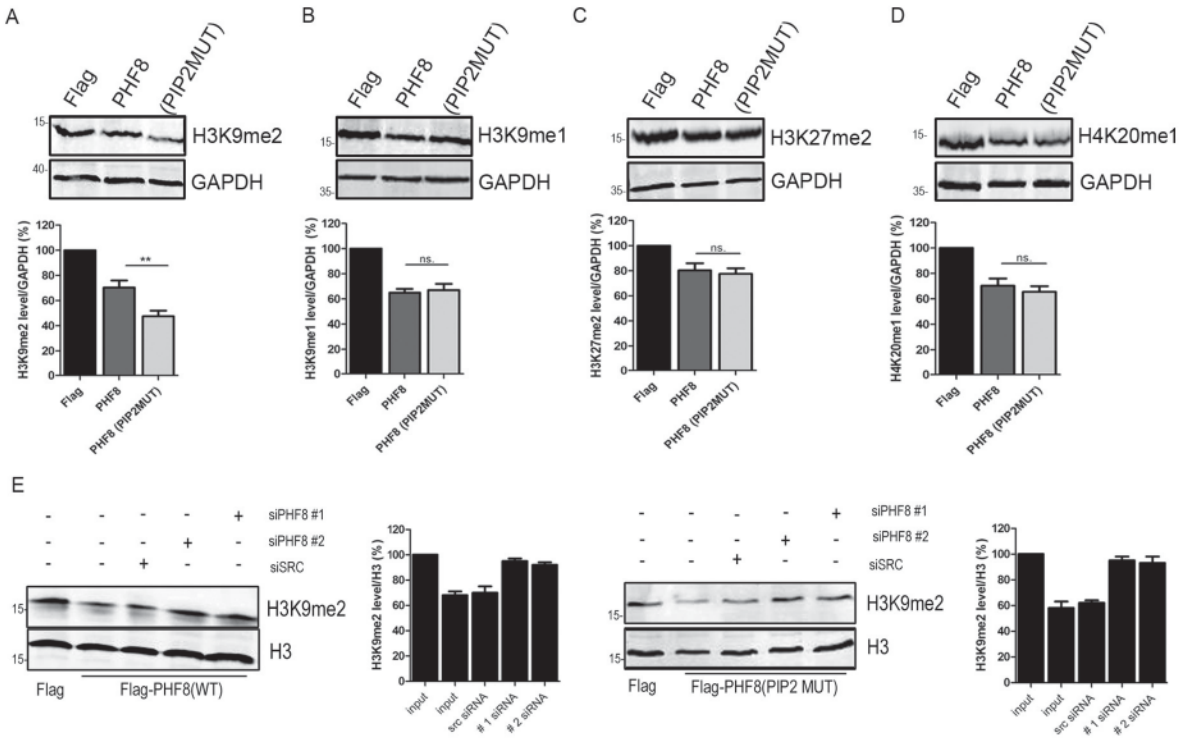

Fig. 3. PIP2 binding to PHF8 influences H3K9me2 level. Quantification of change in histone modifications in whole cell lysate from HEK 293 cells overexpressing Flag-PHF8 or Flag-PHF8 (PIP2 MUT) or empty Flag-plasmid. (A) H3K9me2 level, (B) H3K9me1 level, (C) H3K27me2 level, and (D) H4K20me1 level. Graphs show signal intensity of particular histone modification normalized to GAPDH from at least three biological replicates. (E) Quantification of change in H3K9me2 levels after control siRNA or PHF8 siRNA. Graphs show signal intensity of particular histone modification normalized to H3 from at least three biological replicates. n.s.; *p < 0.05, **p < 0.01, ***p < 0.001.

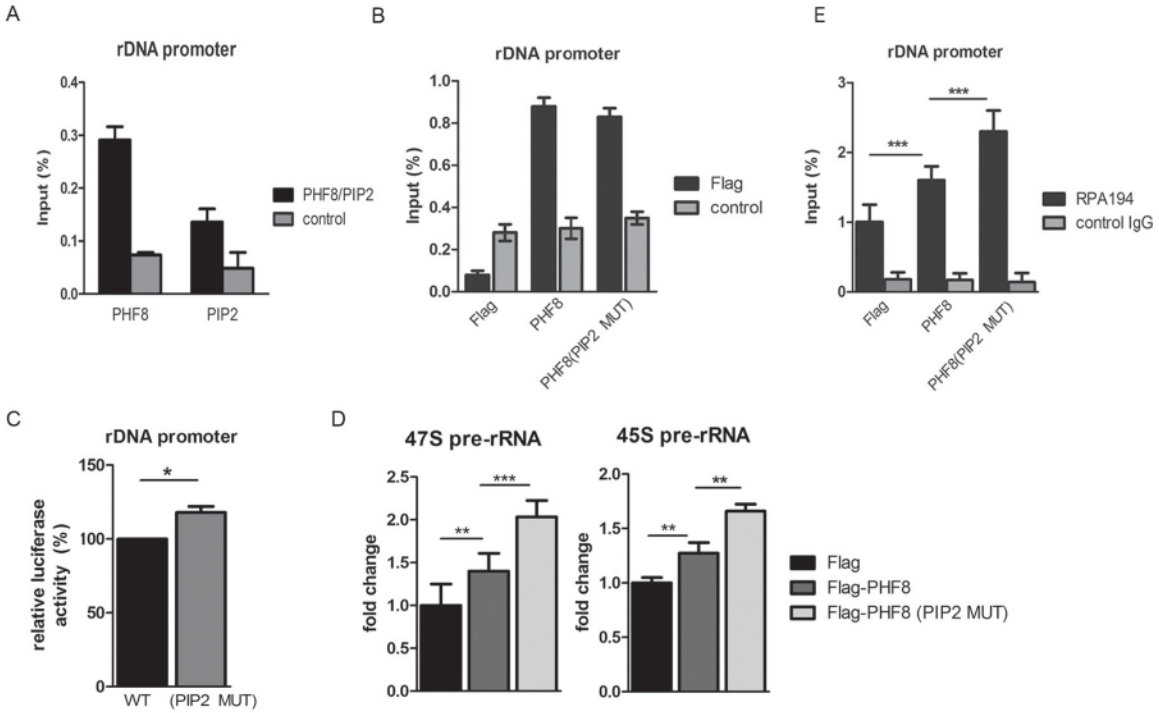

Fig. 4. PIP2 binding to PHF8 increases rDNA promoter activity and pre-rRNA genes expression. (A) ChIP by anti-PHF8, PIP2 and control antibody with subsequent detection of rDNA promoter from HEK293 cells with endogenous level of PHF8. The association is expressed as % of input. (B) ChIP by anti-Flag antibody from HEK 293 cell overexpressing PHF8 (WT) or PHF8 (PIP2 MUT) or overexpressing empty Flag-plasmid. (C) Measuring of rDNA promoter activity by luciferase assay. Expression of firefly luciferase under control of rDNA promoter was co-transfected with renilla luciferase to HEK293 cell line overexpressing PHF8 (WT) or PHF8 (PIP2 MUT). For normalization, renilla luciferase and firefly luciferase without promoter was co-transfected together to HEK293 PHF8 (WT) or PHF8 (PIP2 MUT). The luminescence was evaluated from three biological replicates at least. (D) pre-rRNA genes expression measured by RT-qPCR. Experiments were evaluated from three biological replicates at least. (E) ChIP by anti-RPA194 and anti-IgG antibody from HEK 293 cell overexpressing PHF8 (WT) or PHF8 (PIP2 MUT) or overexpressing empty Flag-plasmid. n.s.; *p < 0.05, **p < 0.01, ***p < 0.001.

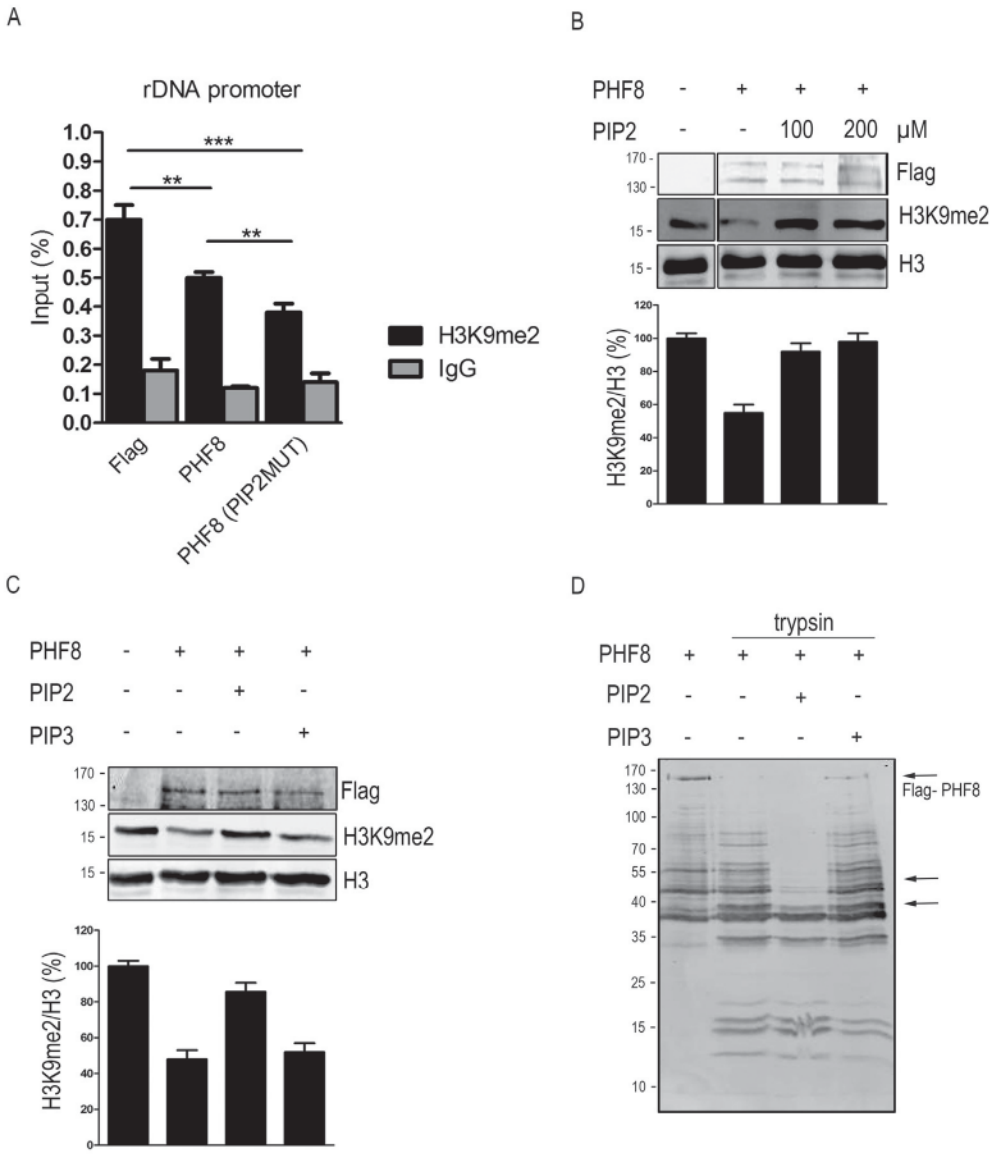

Fig. 5. PIP2 probably causes a conformational change in PHF8 which influences H3K9me2 demethylation activity of PHF8. (A) ChIP by anti-H3K9me2 antibody from HEK 293 cell over-expressing PHF8 or PHF8 (PIP2 MUT) or empty Flag plasmid. (B) *In vitro* demethylation assay. Bulk histones were incubated with Flag-PHF8 and increasing amount of PIP2 (100 or 200 μM). Below western blot is quantification of H3K9me2 signal normalized to H3 signal. Experiments were evaluated from three biological replicates at least. (C) *In vitro* demethylation assay. Bulk histones were incubated with Flag-PHF8 and PIP2 or PIP3 (100 μM). Below western blot is quantification of H3K9me2 signal normalized to H3 signal. Experiments were evaluated from three biological replicates at least. (D) Trypsin digestion of PHF8. Flag-PHF8 was incubated with PIP2 or PIP3 and subsequently digested by trypsin. Arrows show a change in digestion pattern after addition of PIP2. Experiments were evaluated from three biological replicates at least. n.s.; *p < 0.05, **p < 0.01, ***p < 0.001.

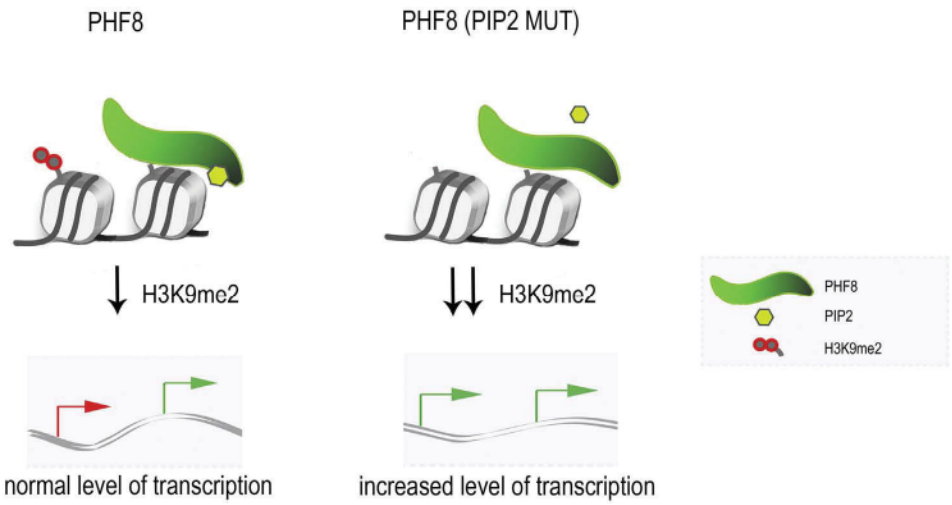

Fig. 6. PIP2 regulates rRNA genes expression by interaction with PHF8. Schematic representation of rRNA genes expression by Polymerase I in case of PIP2 binding to PHF8 or PIP2 binding mutant of PHF8 (PHF8 (PIP2 MUT)). In case of PIP2 binding to PHF8, PIP2 probably triggers a conformational change of PHF8 and represses its activity (normal level of transcription). In case of PHF8 (PIP2 MUT), PIP2 does not bind to PHF8 and therefore there is no repression of PHF8 (increased level of transcription). PHF8 (PIP2 MUT) is more active than PHF8 in complex with PIP2 what might lead to misregulation of rRNA genes expression.

PHF8 occurs upon PIP2 binding.

In conclusion, our results indicate that PIP2 binding to PHF8 negatively regulates PHF8 demethylase activity which leads to higher H3K9me2 levels at the rDNA promoter, and negatively regulates expression of pre-rRNA genes (Fig. 6). We propose that the mechanism behind this fine-tuning of rRNA genes transcription regulated by PIP2-PHF8 complex is PIP2-triggered conformational change of PHF8.

4. Discussion

Here we demonstrate a novel function of PIP2 as a regulator of rRNA genes transcription at the epigenetic level. PIP2 directly interacts with PHF8 and this binding most probably causes PHF8 conformational change. PIP2 binding negatively regulates PHF8 function as H3K9me2 histone lysine demethylase and thus negatively regulates pre-rRNA genes expression. Here we propose that PIP2 is an important player in fine-tuning of the regulation of rRNA genes transcription (Fig. 6).

In this study, we present data that PHF8 is in a complex with PIP2 and not with other phosphoinositides (PIs), and PIP2 binds to PHF8 directly. Our results complement the set of unique PIs interacting nuclear proteins and thus clarify the PIs involvement in the nuclear processes. Gozani et al. described the ING2 protein, involved in regulation of the p53 acetylation, as a specific interaction partner of PI(5)P [38]. Direct binding of phosphoinositide to a chromatin-associated protein was also described by Gelato et al. [39]. They showed a preferential binding of PI5P to UHRF1, a DNA methylation maintenance factor. Several phosphoinositides can directly bind to Pf1 through its polybasic region (PBR, enriched in lysine and arginine) C-terminally of the PHD domain [40]. Also, Viiri et al. identified the PBR region of SAP30 and SAP30L as a PIs binding site and the interaction of monophosphoinositides with SAP30L regulates its subcellular localization, chromatin association, and activity [41]. PI binding sites were identified in EBP1 as K/Rrich motifs and EBP1 associates with PIP3 in the nucleolus [42]. This is in conformity with our identification of PIP2-binding motif in PHF8. Another protein, the scaffold protein IQ motif containing GTPase activating protein 1 (IQGAP1), was shown to bind directly to PIs and multiple kinases. Based on known data a speculation about two possible roles of IQGAP1 raised. One possible role for IQGAP1 is though interaction with kinases as a PI(5)P controller and regulator. The second one is through direct interaction with PI(5)P where IQGAP1 serve as a PI(5)P reservoir in the cell nucleus [43]. Obviously, PIs are involved in various unknown nuclear processes through interactions with PIs binding proteins however, new innovative approaches are needed to fully understand PIs importance.

Not only PIP2 binds to PHF8, but we demonstrate a direct interaction and moreover, the influence of PIP2 on PHF8 activity. So far, it has been reported only an indirect effect of inositol pyrophosphate on histone demethylase [44]. Burton et al. have shown that chromatin association of JMJD2C histone demethylase is regulated by IP_6K1 (inositol hexakisphosphate kinase 1) and its 5PP-IP5, a isomer of IP7 (inositol pyrophosphate), production. Moreover, they observed a specific influence of IP_6K1 on H3K9me3 levels but not on H3K36me3 levels, although both trimethylations are substrates for JMJD2C activity. Their data are in agreement with our results. We claim that PIP2 influences specifically H3K9me2 levels, but not the level of other PHF8 substrates. The proposed mechanism for the specific influence of H3K9me2 level is caused by the possible PIP2-triggered conformational change of PHF8. Previously, Gelato et al. showed an allosteric conformational change of UHRF1 upon PI(5)P binding [39]. In agreement, the conformational change of UBF and fibrillarin upon PIP2 binding was observed by Yildirim et al. [16]. This might be a universal mechanism of PIs binding partners regulation. Based on this, we hypothesized that repression of PHF8 activity upon PIP2 binding might be caused by a conformational change in JmjC catalytic domain or in PHD finger, which is responsible for H3K4me3 recognition and binding.

The demethylation of H3K9me2 by PHF8 is connected with rRNA genes transcription [21,22]. Based on our data, we conclude that PIP2 binding to PHF8 represses rRNA genes transcription. Chakrabarti et al. observed a similar effect on rRNA (45S pre-rRNA and 18S rRNA) genes silencing caused by PI5PK, an enzyme that catalyzes phosphorylation of PI4P at 5 position, and its association with H3K9me3 and HP1-α. Based on our observations we are inclined to agree with authors' speculation about a direct role of the nucleolar PIP5K *per se* in modulating the biosynthesis of rRNA in the paper discussion [45]. Together our data suggest that PIP2 influences rRNA genes transcription by different pathways and interacting proteins than its kinase. On the other hand, it cannot be unquestionably excluded that PI5PK regulation observed by Chakrabarti et al. is caused by the production of PIP2 or downstream signaling molecules.

As rDNA transcription is an undoubtedly important cellular process, it needs to be regulated at multiple levels and by multiple pathways. Previously, we have published that PIP2 binds directly to UBF and fibrillarin, and interacts with RNA polymerase I machinery [16]. There we speculated that PIP2 mediates a connection between rRNA genes transcription, and early maturation processes as PIP2 directly binds to UBF and fibrillarin, proteins involved in these processes. This suggests that by interaction with specific protein partners, PIP2 can be involved in regulation of rRNA transcription at multiple levels, at the initiation of transcription, rRNA processing, and also at the epigenetic level. Similarly, the dual function of PIP2 has been observed for its involvement in the regulation of RNA polymerase II transcription. PIP2 promotes RNA polymerase II transcription by direct interaction with histone H1 [17] but on the other hand, PIP2 represses by RNA pol II transcription by interaction with BASP1 and subsequently mediated interaction with HDAC1 [18]. Moreover, the decrease of H3K9me2 levels in PHF8 (PIP2 MUT) was observed in whole cell lysate, where we cannot exclude the effect on RNA polymerase II transcription. Thus according to published and our data, we expect that PHF8-PIP2 complex influences not only RNA polymerase I but influences RNA polymerase II transcription as well.

In summary, we proposed a mechanism of PIP2 epigenetic function on rRNA genes expression in the mammalian cell line. Obviously, further investigation about PHF8 conformational change and interaction with other histone modifying enzymes is necessary. Nevertheless, the regulation of rRNA genes expression is undoubtedly a critical step of which misregulation may impair essential processes as cell growth, proliferation, and survival [46]. Since PIP2 is involved in this regulation at multiple levels, the results document its importance in the cell nucleus and reflect the need for further research on nuclear PIs functions.

Transparency document

The http://dx.doi.org/10.1016/j.bbalip.2017.12.008 associated with this article can be found, in the online version.

Acknowledgements

The authors would like to thank Iva Jelínková and Pavel Kříž for their excellent technical assistance. We are grateful to Ingrid Grummt (GCRC, Heidelberg, Germany) for sharing the anti-PHF8 antibody. We acknowledge the Microscopy Centre - Light/Electron CF, IMG AS CR supported by the Czech-BioImaging large RI project (LM2015062 funded by MEYS CR) for their support with obtaining scientific data presented in this paper.

Funding

This work was supported by the Human Frontier Science Program [grant number RGP0017/2013]; the Grant Agency of the Czech Republic [grant number 15-08738S]; and the Institutional Research Concept of the Institute of Molecular biology [grant number RVO:

68378050]. This work was supported by the project "BIOCEV – Biotechnology and Biomedicine Centre of the Academy of Sciences and Charles University" (CZ.1.05/1.1.00/02.0109), from the European Regional Development Fund. This work was supported by the Microscopy Centre; Light/Electron CF, IMG AS CR supported by the MEYS CR (LM2015062 Czech; BioImaging).

Competing interests

The authors declare no competing or financial interests.

Appendix A. Supplementary data

Supplementary data to this article can be found online at https://doi.org/10.1016/j.bbalip.2017.12.008.

References

[1] J.D. York, Regulation of nuclear processes by inositol polyphosphates, Biochim. Biophys. Acta 1761 (5-6) (2006) 552–559, http://dx.doi.org/10.1016/j.bbalip.2006.04.014.
[2] S.R. Ratti, G. Ramazzotti, I. Faenza, R. Fiume, S. Mongiorgi, A.M. Billi, J.A. McCubrey, P.G. Suh, L. Manzoli, L. Cocco, M.Y. Follo, Nuclear inositide signaling and cell cycle, Adv. Biol. Regul. S2212-4926 (17) (2017) 30173.
[3] M. Crowder, C.D. Seacrist, R.D. Blind, Phospholipid regulation of the nuclear receptor superfamily, Adv. Biol. Regul. 63 (2017) 6–14, http://dx.doi.org/10.1016/j.jbior.2016.10.006.
[4] E. Kim, J. Beon, S. Lee, J. Park, S. Kim, IPMK: a versatile regulator of nuclear signaling events, Adv. Biol. Regul. 61 (2016) 25–32, http://dx.doi.org/10.1016/j.jbior.2015.11.005.
[5] L. Cocco, L. Manzoli, I. Faenza, G. Ramazzotti, Y.R. Yang, J.A. McCubrey, P.G. Suh, M.Y. Follo, Modulation of nuclear PI-PLCbeta1 during cell differentiation, Adv. Biol. Regul. 60 (2016) 1–5, http://dx.doi.org/10.1016/j.jbior.2015.10.008.
[6] G. Mazzotti, N. Zini, E. Rizzi, R. Rizzoli, A. Galanzi, A. Ognibene, S. Santi, A. Matteucci, A.M. Martelli, N.M. Maraldi, Immunocytochemical detection of phosphatidylinositol 4,5-bisphosphate localization sites within the nucleus, J. Histochem. Cytochem. 43 (2) (1995) 181–191.
[7] I.V. Boronenkov, J.C. Loijens, M. Umeda, R.A. Anderson, Phosphoinositide signaling pathways in nuclei are associated with nuclear speckles containing pre-mRNA processing factors, Mol. Biol. Cell 9 (12) (1998) 3547–3560.
[8] V. Bertagnolo, L.M. Neri, M. Marchisio, C. Mischiati, S. Capitani, Phosphoinositide 3-kinase activity is essential for all-trans-retinoic acid-induced granulocytic differentiation of HL-60 cells, Cancer Res. 59 (1999) 542–546.
[9] D.J. Gillooly, I.C. Morrow, M. Lindsay, R. Gould, N.J. Bryant, J.M. Gaullier, R.G. Parton, H. Stenmark, Localization of phosphatidylinositol 3-phosphate in yeast and mammalian cells, EMBO J. 19 (2000) 4577–4588.
[10] T.S. Yokogawa, Y. Nagata, T. Nishio, S. Tsutsumi, R. Ihara, K. Shirai, M. Morita, Y. Umeda, N. Shirai, Fukui Y. Saitoh, Evidence that 3′-phosphorylated polyphosphoinositides are generated at the nuclear surface: use of immunostaining technique with monoclonal antibodies specific for PI 3,4-P(2), FEBS Lett. 473 (2000) 222–226.
[11] S.L. Osborne, C.L. Thomas, S. Gschmeissner, G. Schiavo, Nuclear PtdIns(4,5)P2 assembles in a mitotically regulated particle involved in pre-mRNA splicing, J. Cell Sci. 114 (Pt 13) (2001) 2501–2511.
[12] J.Y. Ahn, X. Liu, D. Cheng, J. Peng, P.K. Chan, P.A. Wade, K. Ye, Nucleophosmin/B23, a nuclear PI(3,4,5)P(3) receptor, mediates the antiapoptotic actions of NGF by inhibiting CAD, Mol. Cell 18 (2005) 435–445.
[13] I. Kalasova, V. Fáberová, A. Kalendová, S. Yildirim, L. Uličná, T. Venit, P. Hozák, Tools for visualization of phosphoinositides in the cell nucleus, Histochem. Cell Biol. 144 (2016) 1–12.
[14] S. Jungmichel, K.B. Sylvestersen, C. Choudhary, S. Nguyen, M. Mann, M.L. Nielsen, Specificity and commonality of the phosphoinositide-binding proteome analyzed by quantitative mass spectrometry, Cell Rep. 6 (3) (2014) 578–591, http://dx.doi.org/10.1016/j.celrep.2013.12.038.
[15] A.E. Lewis, L. Sommer, M. Arntzen, Y. Strahm, N.A. Morrice, N. Divecha, C.S. D'Santos, Identification of nuclear phosphatidylinositol 4,5-bisphosphate-interacting proteins by neomycin extraction, Mol. Cell. Proteomics 10 (2) (2011) M110.003376, , http://dx.doi.org/10.1074/mcp.M110.003376.
[16] S. Yildirim, E. Castano, M. Sobol, V.V. Philimonenko, R. Dzijak, T. Venit, P. Hozák, Involvement of phosphatidylinositol 4,5-bisphosphate in RNA polymerase I transcription, J. Cell Sci. 126 (Pt 12) (2013) 2730–2739, http://dx.doi.org/10.1242/jcs.123661.
[17] Yu HY, K. Fukami, Y. Watanabe, C. Ozaki, T. Takenawa, Phosphatidylinositol 4,5-bisphosphate reverses the inhibition of RNA transcription caused by histone H1, Eur. J. Biochem. 251 (1–2) (1998) 281–287, http://dx.doi.org/10.1046/j.1432-1327.1998.2510281.x.
[18] E. Toska, H.A. Campbell, J. Shandilya, S.J. Goodfellow, P. Shore, K.F. Medler, S.G.E. Roberts, Repression of transcription by WT1-BASP1 requires the myristoylation of BASP1 and the PIP2-dependent recruitment of histone deacetylase, Cell Rep. 2 (3) (2012) 462–469, http://dx.doi.org/10.1016/j.celrep.2012.08.005.
[19] M. Sobol, S. Yildirim, V.V. Philimonenko, P. Marášek, E. Castaño, P. Hozák, UBF complexes with phosphatidylinositol 4,5-bisphosphate in nucleolar organizer regions regardless of ongoing RNA polymerase I activity, Nucleus 4 (6) (2013) 478–486, http://dx.doi.org/10.4161/nucl.27154.
[20] W. Liu, B. Tanasa, O.V. Tyurina, T.Y. Zhou, R. Gassmann, W.T. Liu, K.A. Ohgi, C. Benner, I. Garcia-Bassets, A.K. Aggarwal, A. Desai, P.C. Dorrestein, C.K. Glass, M.G. Rosenfeld, PHF8 mediates histone H4 lysine 20 demethylation events involved in cell cycle progression, Nature 466 (7305) (2010) 508–512, http://dx.doi.org/10.1038/nature09272.
[21] W. Feng, M. Yonezawa, J. Ye, T. Jenuwein, I. Grummt, PHF8 activates transcription of rRNA genes through H3K4me3 binding and H3K9me1/2 demethylation, Nat. Struct. Mol. Biol. 17 (4) (2010) 445–450, http://dx.doi.org/10.1038/nsmb.1778.
[22] Z. Zhu, Y. Wang, X. Li, L. Xu, X. Wang, T. Sun, X. Dong, L. Chen, H. Mao, Y. Yu, J. Li, P.A. Chen, C.D. Chen, PHF8 is a histone H3K9me2 demethylase regulating rRNA synthesis, Cell Res. 20 (7) (2010) 794–801, http://dx.doi.org/10.1038/cr.2010.75.
[23] H.H. Qi, M. Sarkissian, Hu GQ, Z. Wang, A. Bhattacharjee, D.B. Gordon, M. Gonzales, F. Lan, P.P. Ongusaha, M. Huarte, N.K. Yaghi, H. Lim, B.A. Garcia, L. Brizuela, K. Zhao, T.M. Roberts, Y. Shi, Histone H4K20/H3K9 demethylase PHF8 regulates zebrafish brain and craniofacial development, Nature 466 (7305) (2010) 503–507, http://dx.doi.org/10.1038/nature09261.
[24] E. Bártová, J. Krejcí, A. Harnicarová, G. Galiová, S. Kozubek, Histone modifications and nuclear architecture: a review, J. Histochem. Cytochem. 56 (8) (2008) 711–721, http://dx.doi.org/10.1369/jhc.2008.951251.
[25] T. Kouzarides, Chromatin modifications and their function, Cell 128 (4) (2007) 693–705.
[26] A. Bannister, T. Kouzarides, Regulation of chromatin by histone modifications, Cell Res. 21 (2011) 381–395.
[27] F. Laumonnier, S. Holbert, N. Ronce, F. Faravelli, S. Lenzner, C.E. Schwartz, J. Lespinasse, H. Van Esch, D. Lacombe, C. Goizet, F. Phan-Dinh Tuy, H. van Bokhoven, J.P. Fryns, J. Chelly, H.H. Ropers, C. Moraine, B.C. Hamel, S. Briault, Mutations in PHF8 are associated with X linked mental retardation and cleft lip/cleft palate, J. Med. Genet. 42 (10) (2005) 780–786, http://dx.doi.org/10.1136/jmg.2004.029439.
[28] C. Loenarz, W. Ge, M.L. Coleman, N.R. Rose, C.D. Cooper, R.J. Klose, P.J. Ratcliffe, C.J. Schofield, PHF8, a gene associated with cleft lip/palate and mental retardation, encodes for an Nepsilon-dimethyl lysine demethylase, Hum. Mol. Genet. 19 (2) (2010) 217–222, http://dx.doi.org/10.1093/hmg/ddp480.
[29] K. Ghoshal, S. Majumder, J. Datta, T. Motiwala, S. Bai, S. Sharma, W. Frankel, S. Jacob, Role of human ribosomal RNA (rRNA) promoter methylation and of methyl-CpG-binding protein MBD2 in the suppression of rRNA gene expression, J. Biol. Chem. 279 (2004) 6783–6793.
[30] L. Trinkle-Mulcahy, S. Boulon, Y.W. Lam, R. Urcia, F.M. Boisvert, F. Vandermoere, N.A. Morrice, S. Swift, U. Rothbauer, H. Leonhardt, A. Lamond, Identifying specific protein interaction partners using quantitative mass spectrometry and bead proteomes, J. Cell Biol. 183 (2) (2008) 223–239, http://dx.doi.org/10.1083/jcb.200805092.
[31] S. Majumder, K. Ghoshal, J. Datta, D. Smith, S. Bai, S. Jacob, Role of DNA methyltransferases in regulation of human ribosomal RNA gene transcription, J. Biol. Chem. 281 (31) (2006) 22062–22072.
[32] M. Uemura, Q. Zheng, C. Koh, W. Nelson, S. Yegnasubramanian, A. De Marzo, Overexpression of ribosomal RNA in prostate cancer is common but not linked to rDNA promoter hypomethylation, Oncogene 31 (10) (2012) 1254–1263.
[33] T. Venit, R. Dzijak, A. Kalendová, M. Kahle, J. Rohožková, V. Schmidt, T. Rülicke, B. Rathkolb, W. Hans, A. Bohla, O. Eickelberg, T. Stoeger, E. Wolf, A. Yildirim, V. Gailus-Durner, H. Fuchs, M. de Angelis, P. Hozák, Mouse nuclear myosin I knockout shows interchangeability and redundancy of myosin isoforms in the cell nucleus, PLoS One 8 (4) (2013) 1–11, http://dx.doi.org/10.1371/journal.pone.0061406.
[34] J. Nelson, O.K.B. Denisenko, Protocol for the fast chromatin immunoprecipitation (ChIP) method, Nat. Protoc. 1 (1) (2006) 179–185.
[35] C. Huang, Y. Xiang, Y. Wang, X. Li, L. Xu, Z. Zhu, T. Zhang, Q. Zhu, K. Zhang, N. Jing, C.D. Chen, Dual-specificity histone demethylase KIAA1718 (KDM7A) regulates neural differentiation through FGF4, Cell Res. 20 (2) (2010) 154–165, http://dx.doi.org/10.1038/cr.2010.5.
[36] E. Mortier, G. Wuytens, I. Leenaerts, F. Hannes, M.Y. Heung, G. Degeest, G. David, P. Zimmermann, Nuclear speckles and nucleoli targeting by PIP2–PDZ domain interactions, EMBO J. 24 (14) (2005) 2556–2565.
[37] Y. Zhang, D. Reinberg, Transcription regulation by histone methylation: interplay between different covalent modifications of the core histone tails, Genes Dev. 15 (2001) 2343–2360.
[38] O. Gozani, P. Karuman, D. Jones, D. Ivanov, J. Cha, A. Lugovskoy, C. Baird, H. Zhu, S. Field, S. Lessnick, J. Villasenor, B. Mehrotra, J. Chen, V. Rao, J. Brugge, C. Ferguson, B. Payrastre, D. Myszka, L. Cantley, G. Wagner, N. Divecha, G. Prestwich, J. Y, The PHD finger of the chromatin-associated protein ING2 functions as a nuclear phosphoinositide receptor, Cell 114 (1) (2003) 99–111.
[39] K. Gelato, M. Tauber, M.S. Ong, S. Winter, K. Hiragami-Hamada, J. Sindlinger, A. Lemak, Y. Bultsma, S. Houliston, D. Schwarzer, N. Divecha, C.H. Arrowsmith, W. F, Accessibility of different histone H3-binding domains of UHRF1 is allosterically regulated by phosphatidylinositol 5-phosphate, Mol. Cell 54 (6) (2014) 905–919.
[40] M. Kaadige, D. Ayer, The polybasic region that follows the plant homeodomain zinc finger 1 of Pf1 is necessary and sufficient for specific phosphoinositide binding, J. Biol. Chem. 281 (39) (2006).
[41] K. Viiri, J. Jänis, T. Siggers, T. Heinonen, J. Valjakka, L. Bulyk, M. Maki, O. Lohi, DNA-binding and -bending activities of SAP30L and SAP30 are mediated by a zinc-dependent module and monophosphoinositides, Mol. Cell. Biol. 29 (2) (2009) 342–356.

[42] T. Karlsson, A. Altankhuyag, O. Dobrovolska, D. Turcu, A. Lewis, A polybasic motif in ErbB3-binding protein 1 (EBP1) has key functions in nucleolar localization and polyphosphoinositide interaction, Biochem. J. 473 (14) (2016) 2033–2047.
[43] S. Choi, N. Thapa, A. Hedman, Z. Li, D. Sacks, R. Anderson, IQGAP1 is a novel phosphatidylinositol 4,5 bisphosphate effector in regulation of directional cell migration, EMBO J. 32 (19) (2013) 2617–2630.
[44] A. Burton, C. Azevedo, C. Andreassi, A. Riccio, A. Saiardi, Inositol pyrophosphates regulate JMJD2C-dependent histone demethylation, 110 (47) (2013) 18970–18975.
[45] R. Chakrabarti, S. Sanyal, A. Ghosh, K. Bhar, C. Das, A. Siddhanta, Phosphatidylinositol-4-phosphate 5-kinase 1α modulates ribosomal RNA gene silencing through its interaction with histone H3 lysine 9 trimethylation and heterochromatin protein HP1-α, 290 (34) (2015) 20893–20903.
[46] D. Drygin, W.G. Rice, I. Grummt, The RNA polymerase I transcription machinery: an emerging target for the treatment of cancer, Annu. Rev. Pharmacol. Toxicol. 50 (2010) 131–156.

3.3 PIP2 functions at the intersection of chromatin structure, transcription, DNA damage in meiosis I progression in *C. elegans*

Ulicna L., Rohozkova J. and Hozak P.

Manuscript

L.U. designed, performed and evaluated almost all experiments (DNA cloning, RNAi interference experiments, indirect immunofluorescence and fluorescence microscopy, immunoprecipitation, *C. elegans* handling) and wrote the manuscript.

PIP2 functions at the intersection of chromatin structure, transcription, DNA damage in meiosis I progression in *C. elegans*

Ulicna Livia[1], Rohozkova Jana[2] and Hozák Pavel[1,2,3] *

[1] Department of Biology of the Cell Nucleus, Institute of Molecular Genetics of the Academy of Sciences of the Czech Republic, v.v.i., 142 20, Prague, Czech Republic.

[2] Department of Epigenetics of the Cell Nucleus, Institute of Molecular Genetics of the Academy of Sciences of the Czech Republic, v.v.i., division BIOCEV, 25250, Vestec, Czech Republic

[3] Microscopy Center the Institute of Molecular Genetics of the Academy of Sciences of the Czech Republic, v.v.i.,142 20, Prague, Czech Republic

* corresponding author: hozak@img.cas.cz

Abstract

One of the most studied phosphoinositides is phosphatidylinositol-4,5-bisphosphate (PIP2) which localizes to plasma membrane, nuclear speckles, small foci in the nucleoplasm, and to the nucleolus in mammalian cells. Here we discovered that PIP2 localizes to the nucleus in prophase I, during gametogenesis of *C. elegans* hermaphrodite. The depletion of PIP2, by PPK-1 kinase RNA interference, results in the altered chromatin and leads to various defects during meiotic progression. We observed decreased brood size and aneuploidy in progeny, defects in synapsis and crossover formation. Most probably, the presence of altered chromatin structure reflects in the increased transcription rate- a tightly regulated process in prophase I. To elucidate involvement of PIP2 in processes during *C. elegans* development, we have identified PIP2-binding partners (such as LRR-1, PBS-4), pointing to its involvement in the ubiquitin-proteasome pathway.

Key words: nucleus, phosphatidylinositol-4,5-bisphosphate, PPK-1, *C. elegans*

Introduction

Meiotic division is a specific process of gametogenesis, where DNA from maternal cell replicates and consequently divides in two turns of cell division, into new haploid germ cells. In *Caenorhabditis elegans*, this includes pairing of homologous chromosomes, which occurs during the leptotene and zygotene stages of prophase I (transition zone of the germ line). During this highly dynamic process, the two homologous copies of each chromosome find each other within the nucleus through an active search process that enables chromosomes to distinguish "self versus non-self" and assume a side-by-side alignment [1]. The process of pairing is coupled with synaptonemal complex assembly between homologs and crossovers (COs) formation which provide sufficient tension to align chromosomes on the spindle. As chromosome pairing, a prerequisite for CO formation, is complete by exit from the transition zone, the failure of COs formation results in randomly segregated chromosomes during the first meiotic division and subsequent aneuploidy [2,3].

Processes connected with meiotic progression are complexed and involve several regulation steps, which are influenced by the chromatin state. Modifications of DNA are modulating accessibility of the nucleosomal DNA, which is critical for transcription, replication, recombination and DNA damage repair [4]. DNA transcription in germ cells is tightly regulated and represents ~ 21% from transcription of all genes [5], mostly expressing only proteins involved or regulating the meiotic progression.

Additionally, changes in the nuclear structure and in both DNA and RNA polymerases activities can be caused also by nuclear phospholipids [6-11]. Previously studies showed that *in vitro* addition of positively charged lipids lead to chromosome condensation while negatively charged lipids caused decondensation [12]. Phosphatidylinositol-4,5-bisphosphate (PIP2) is one of the most studied phosphoinositides. PIP2 localization to plasma membrane, nuclear speckles, small foci in the nucleoplasm, and to the nucleolus was described in mammalian cells [13-16]. It is known that nuclear PIP2 acts as a transcription activator or repressor interacting with the protein complexes of RNA polymerases I and II or with the histone demethylase [15-17]. PIP2 regulates RNA polymerase II transcription apparently by the

direct interaction with histone H1 and H3, shielding positive charges of histones and thus competing with their ability to bind DNA [18]. Additionally, PIP2 can play a role in RNA polymerase II transcription repression through binding to the myristoylated transcriptional co-repressor BASP1. Toska et al. showed that BASP1 requires PIP2 binding for recruitment of histone deacetylase 1 (HDAC1) to chromatin which led to histone deacetylation and thus decreased promoter accessibility for transcriptional machinery [19].

Phosphoinositides metabolism is very complex thus to overcome this, a simple organism *Caenorhabditis elegans* have been used to investigate roles of phosphoinositides and its kinases or phosphatases [20-29]. In *C. elegans,* some enzymes have a unique role such as Type I PIP kinase (PPK-1 kinase, homolog of PI5PK) thus we can manipulated specific phosphoinositide species. PPK-1 is a specific kinase so far known to be responsible for PIP2 synthesis only. PPK-1 kinase localizes to the plasma membrane and is strongly expressed in the neuronal system of *C. elegans* [30]. They showed that purified PPK-1 kinase is able to generate PIP2 *in vitro* and PPK-1 overexpression increases PIP2 level *in vivo*.

Another described role of PPK-1 is in *C. elegans* ovulation. PPK-1 localization was observed in somatic tissues such as neuronal cells [30,31] and also in gonad sheath and distal tip cells, spermatheca, uterine and vulva muscles [31]. The reduced PPK-1 expression results in the depletion of PIP2 which causes worms sterility, defective ovulation, reduced contractility of sheath cells and disorganization of myosin filament.

Here in this study we show PIP2 localization in nuclei in the distal gonad of *C. elegans* hermaphrodite, and in nuclei of early embryos. Thus, we focus on PIP2 functions connected with *C. elegans* chromatin organization and their physiological importance. Interestingly, we discovered that depletion of PIP2 results in the altered chromatin, impaired chromosome pairing with consequent defect in crossover formation. Strikingly, these defects were accompanied with increased levels of DNA transcription. As DNA transcription in germ cells is tightly regulated [5], increased detection of RNA polymerase I and II in germ cell nuclei and increased 5-FU incorporation are most probably signals for observed DNA-damage-driven apoptosis in *C. elegans* gonad. Moreover, we identify PIP2 interacting proteins in gonadal nuclei, pointing to its involvement in ubiquitin-proteasome pathway.

Results

PIP2 is present in *C. elegans* prophase I nuclei and embryos

To described PIP2 role in *C. elegans* we decided to investigate its localization in the germinal part of gonad (prophase I and diakinesis) and in embryos of the wild type N2 (Bristol) strain. Indirect immunofluorescence using anti-PIP2 antibody showed localization of PIP2 in *C. elegans* germ cells. PIP2 was apparent inside of the prophase I nuclei (transition zone and pachynema) excluded from chromatin, possessing the same intensity and pattern (Fig. 1a). It is known that PPK-1 is PIP2 synthesizing enzyme, thus the depletion of PIP2 is possible via knockdown of PPK-1 [30]. After 48 hours of RNA interference (RNAi), we observed a dramatic decrease of PIP2 signal (down to 90%, Fig. 1b). The decrease of PIP2 level after *ppk-1(RNAi)* was additionally confirmed by dot blot detection of PIP2 in a single worm (whole body) lysate (Fig. 1c). Next, we observed by indirect immunofluorescence that PIP2 is present in the cytoplasm but also in the nucleus from 1-cell stage embryo through embryogenesis to 2-fold stage larvae (Fig. 1d). The intensity of PIP2 signal decreases after the bean stage of *C. elegans* embryo. In addition, we observed PIP2 co-localization with NOP-1 (fibrillarin) in *C. elegans* gonad and embryo (Fig. 1e-f). Importantly, observed PIP2 nuclear localization differs from PPK-1 localization (Sup. Fig. 1a-b). The observed nuclear pattern of PIP2 in meiotic nuclei and embryonic cells recapitulate known pattern, observed in interphase cells [16,32-34].

Depletion of PIP2 decreases brood size and increases male incidence

To assess PIP2 importance in the regulation of *C. elegans* gametogenesis, we further scored the brood size, male incidence and viability of progeny after PIP2 RNAi depletion. To differ between somatic and germ line effect of PIP2, we used the rrf-1(pk1417) worm strain, which is sensitive to RNA interference in the germ line but resistant on the somatic level [35]. This revealed an original role of PIP2 in germ cells, additional to already described function in soma, or contractile part of the uterus resp. [30,31]. For depletion of PIP2 in rrf-1 strain, we applied RNAi feeding strategy to decrease levels of PPK-1 kinase (*ppk-1(RNAi)*). As a control strain, we used rrf-1(pk1417) *C. elegans* strain fed only with an empty L4440 RNAi vector

(wild-type). After 48 hours of RNAi via feeding, we observed a decreased brood size (around 60%; Fig. 1g) and a higher male incidence in the progeny (Fig. 1h) upon PIP2 depletion (*ppk-1 (RNAi)*) in comparison to mock fed control. In contrast, we did not notice any change in worms viability, all laid worms were hatched (Fig. 1h). All data together, suggest that PIP2 is involved in germ cells processes independently from its somatic function.

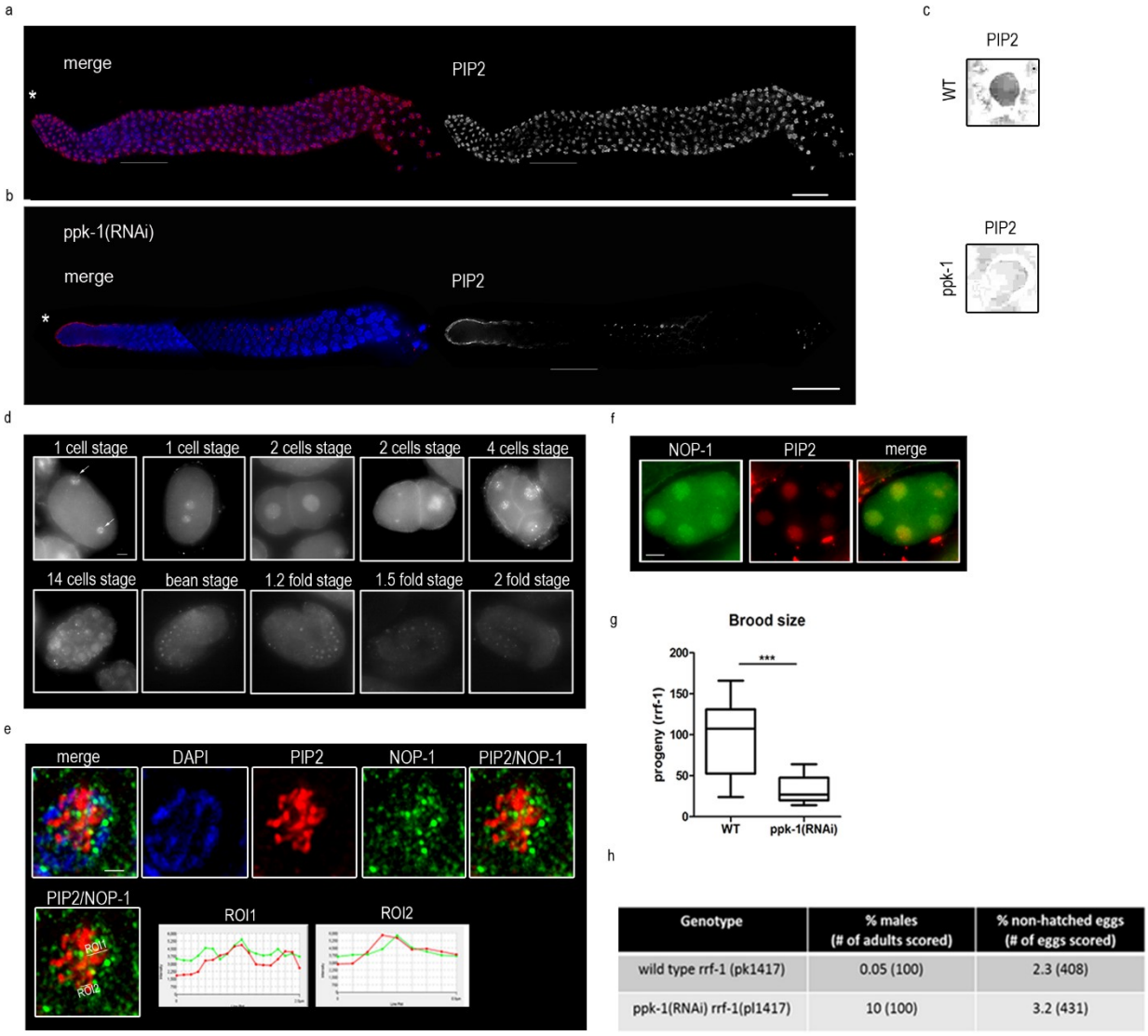

Genotype	% males (# of adults scored)	% non-hatched eggs (# of eggs scored)
wild type rrf-1 (pk1417)	0.05 (100)	2.3 (408)
ppk-1(RNAi) rrf-1(pl1417)	10 (100)	3.2 (431)

Figure 1. PIP2 in *C. elegans*. (a) Indirect immunoflourescence of PIP2 in disected N2 *C.elegans* gonad. Asterisks mark the distal tip. Transition zone is underlined. Scale bar represents 20µm. (b) Indirect immunoflourescence of PIP2 in germ cell nuclei in *ppk-1(RNAi)* background. Asterisks mark the distal tip. Transition zone is underlined. Scale bar represents 20µm. (c) Dot blot dection of anti-PIP2 upon single worm rrf-1(pk1417) whole body lysis in *ppk-1(RNAi)* or WT background. (d) Indirect immunoflourescence

of anti-PIP2 in embryogenesis of *C.elegans* N2 strain. Arrows point to pronuclei. Scale bar represents 5µm. (e) Co-localization of anti-PIP2 (red) and anti-NOP-1(green) in N2 strain germ cell nucleus. Scale bar represents 1µm. (f) Co-localization of anti-PIP2 (red) and anti-NOP-1(green) in N2 strain 5-cell stage embryo. Scale bar represents 10µm. (g) Quantification of brood size per rrf-1(pk1417) worm in *ppk-1(RNAi)* or L4440 (WT) background; (N (number of biological replicates) = 3, n (number of animals per replica) = 30). (h) Quantification of worms viability and male incidence of rrf-1(pk1417) strain in *ppk-1(RNAi)* or L4440 (WT) background. Statistical comparisons between genotypes were performed using Student t-test: n.s. non-significant; * $P \leq 0.05$; ** $P \leq 0.01$; *** $P \leq 0.001$

PIP2 depletion causes aneuploidy and altered chromatin structure in oocytes

In the next set of experiments, we focused on an explanation behind previously observed increase of males (X0) and a decrease of progeny after PIP2 depletion from the gonad by *ppk-1(RNAi)*. To address this question we focused on nuclei in the proximal part of *C. elegans* gonad and oocytes [36,37]. For experiments with *ppk-1(RNAi)* we again took advantage of rrf-1(pk1417) *C. elegans* strain which is RNAi somatic cells insensitive but germ cells sensitive [35]. After 48 hours of RNAi treatment we visualized DNA by DAPI (4',6-Diamidino-2-Phenylindole) in dissected gonads. We scored proximal oocyte nuclei that have entered diakinesis. The most proximal oocyte is designated as -1 before ovulation into the spermatheca, where fertilization occurs. We observed that oocytes in proximal part of gonad are dispositioned compare to WT (Fig. 2a) and moreover, that the chromatin structure was altered (Fig. 2a inset). We counted DAPI stained bodies and revealed a presence of univalents (Fig. 2a inset, Fig. 2b). According to statistical evaluation, approximately 20% of *ppk-1(RNAi)* nuclei have univalent DAPI stained bodies compare to approximately only 3% of univalents in nuclei of *C. elegans* WT oocytes (Fig. 2b).

These are serious phenotypes observed after PIP2 depletion by *ppk-1(RNAi)* specifically from the gonad. During the meiotic division, chromatin state is inevitable to allow proper chromosome pairing and segregation. Thus, our observation of the univalent DAPI stained bodies and the altered chromatin in oocytes led us to speculation that these might be the cause of previously observed increase of male incidence (X0) in the population and progeny reduction.

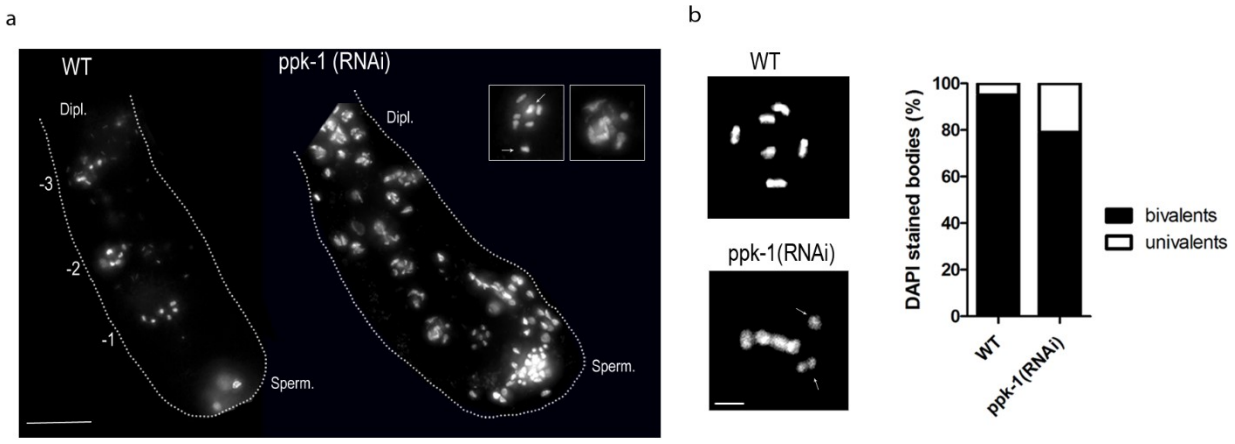

Figure 2. Increased number of DAPI stained bodies. (a) DAPI staining of oocytes DNA in the distal part of dissected rrf-1(pk1417) gonads in *ppk-1(RNAi)* or WT background. Numbers represents oocytes positions. In the inset arrows point to supernumerary DAPI stained bodies and altered chromatin. Scale bar represents 15µm. (b) Number of DAPI stained bodies in *ppk-1(RNAi)* or WT oocytes. Arrows point to supernumerary bodies. Graph represents quantification of ration between univalent and bivalent DAPI stained bodies in *ppk-1(RNAi)* or WT oocytes (N=3, n=20). Scale bar represent 2,5µm.

DNA transcription increases upon PIP2 depletion in germ cells nuclei

Germ cell nuclei in prophase I are highly condensed and the transcriptional activity is tightly regulated. After observed altered chromatin structure we hypothesized that this might lead to chromatin decondensation therefore, we decided to investigate changes in the transcriptional activity. In this experiment, we used again rrf-1(pk1417*) C. elegans* strain for specific depletion of PIP2 from gonad. We performed indirect immunofluorescence by anti- RNA polymerase II CTD subunit phosphorylated at serine 2 antibody (RNA pol II pCTD) and detected approximately 20% increase in RNA pol II pCTD signal upon *ppk-1(RNAi)* compare to WT gonads (Fig. 3a). Next, we performed the same set up of experiment but investigated RNA polymerase I localization by anti-RNA polymerase I (RPA116) antibody (Fig. 3b). Also, we evaluated that RPA116 has increased fluorescent signal by around 30% in *ppk-1(RNAi)* gonads compare to WT. Here we confirmed the increased presence of RNA polymerase I and II in germ cells nuclei after PIP2 depletion from *C. elegans* gonad.

To examine a change in the transcriptional activity we treated rrf-1(pk1417) worms with 8mM 5-Fluorouridine (5-FU) which incorporates into newly transcribed RNA. Then we performed indirect immunofluorescence to visualize RNA incorporated with 5-FU using anti-BrdU antibody which recognizes also 5-FU. We observed that in *ppk-1(RNAi)* worms, the nascent RNA incorporated with 5-FU, was detected after just 5 minutes' incubation. The 5-FU signal was still detected even after 10 and 15 minutes' incubation. On the other hand in WT control gonads, we detected the nascent RNA with incorporated 5-FU neither after 5 nor 10 minutes' incubation. The 5-FU signal was in WT gonads detected first after 15 minutes' incubation (Fig. 3c-d). Moreover, when we inhibited transcription by actinomycin D (AMD) in concentrations of 0.01, 0.05, 1 or 2 μg/ml, we detected any 5-FU incorporation after 5 minutes 5-FU treatment neither in WT nor *ppk-1 (RNAi)* gonads (Fig. 3e). These results strongly suggest that transcriptional activity measured by 5-FU incorporation into the nascent RNA was increased in worms with depleted PIP2.

Obtained data showed that increased 5-FU incorporation is caused by the elevated transcription rate. Moreover, elevated transcription is consistent with increased localization of RNA pol I and II in the *C. elegans* gonad. All data together reveal PIP2 importance for the transcriptional regulation in meiotic germ cells nuclei of *C. elegans*.

PIP2 depletion increases germ cells apoptosis and DNA damage

We hypothesized that observed increased localization of RNA pol I, RNA pol II, increased 5-FU incorporation upon PIP2 depletion (Fig. 3) may cause DNA damage, and repair as the transcription is tightly regulated. Therefore, based on published data and obtained results in this study we decided to investigate the possible connection between PIP2 function and *C. elegans* genome stability.

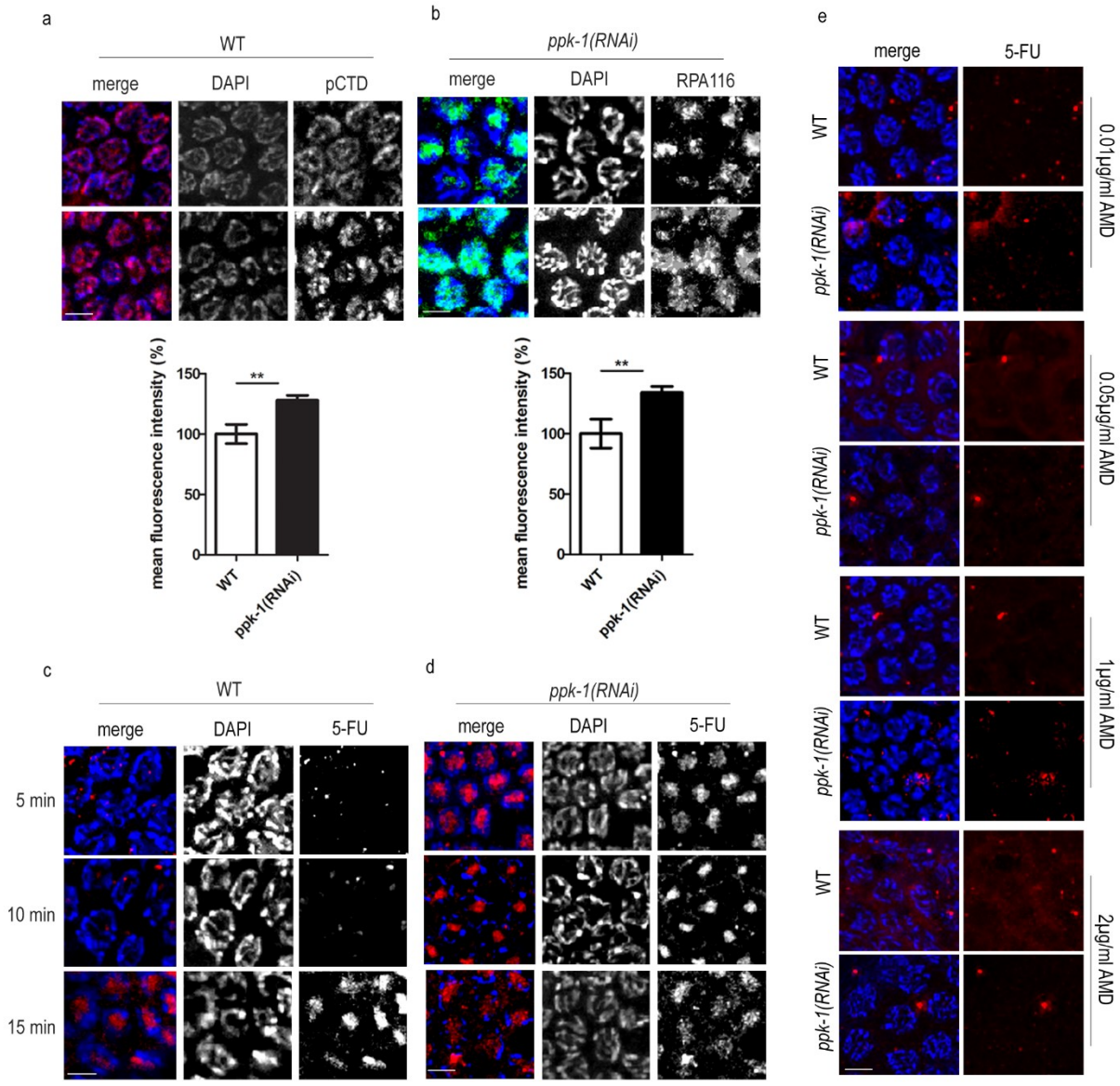

Figure 3. Increased transcription upon *ppk-1(RNAi).* (a) Indirect immunofluorescence of pCTD of RNA polymerase II in *ppk-1(RNAi)* or L4440 (WT) germ cell nuclei. Graph represents mean fluorescence intersity measured from N= 3, n= 60. (b) Indirect immunofluorescence of subunit 116 of RNA polymerase I in *ppk-1(RNAi)* or L4440 (WT) germ cell nuclei. Graph represents mean fluorescence intersity measured from N= 3, n= 60. (c-d)) Indirect immunofluorescence of 5-FU in *ppk-1(RNAi)* or L4440 (WT) background in the timecourse (N= 3, n=40). (e) Indirect immunofluorescence of 5-FU in *ppk-1(RNAi)* or L4440 (WT) background upon actinomycin D treatment (N= 3, n=40). Scale bars represent 5µm. Statistical comparisons between genotypes were performed using Student t-test: n.s. non-significant; * $P \leq 0.05$; ** $P \leq 0.01$; *** $P \leq 0.001$

First of all, we investigated the localization of γH2AX and RAD-51, markers of DNA double stands breaks and repair. We observed their localization upon *ppk-1(RNAi)* and wild-type control rrf-1(pk1417). By anti- γH2AX and anti-RAD-51 antibody, we observed increased localization of these proteins in nuclei with depleted PIP2 compare to WT rrf-1(pk1417) germ cells nuclei. The increase of signal was noticeable only in pachytene stage of prophase I, but not in the leptotene/zygotene (transition) or mitotic region (Fig. 4). *Ppk-1(RNAi)* worms exhibit elevated numbers of RAD-51 foci in pachytene nuclei compare to WT. 83% of *ppk-1(RNAi)* nuclei exhibit 4 and more RAD-51 foci per cell compare to 63% in WT worms. Additionally, 10% of *ppk-1(RNAi)* germ cells nuclei have more than 10 RAD-51 foci per cell, however we did not observed any nuclei with more than 10 RAD-51 foci in WT germ cells (Fig. 4).

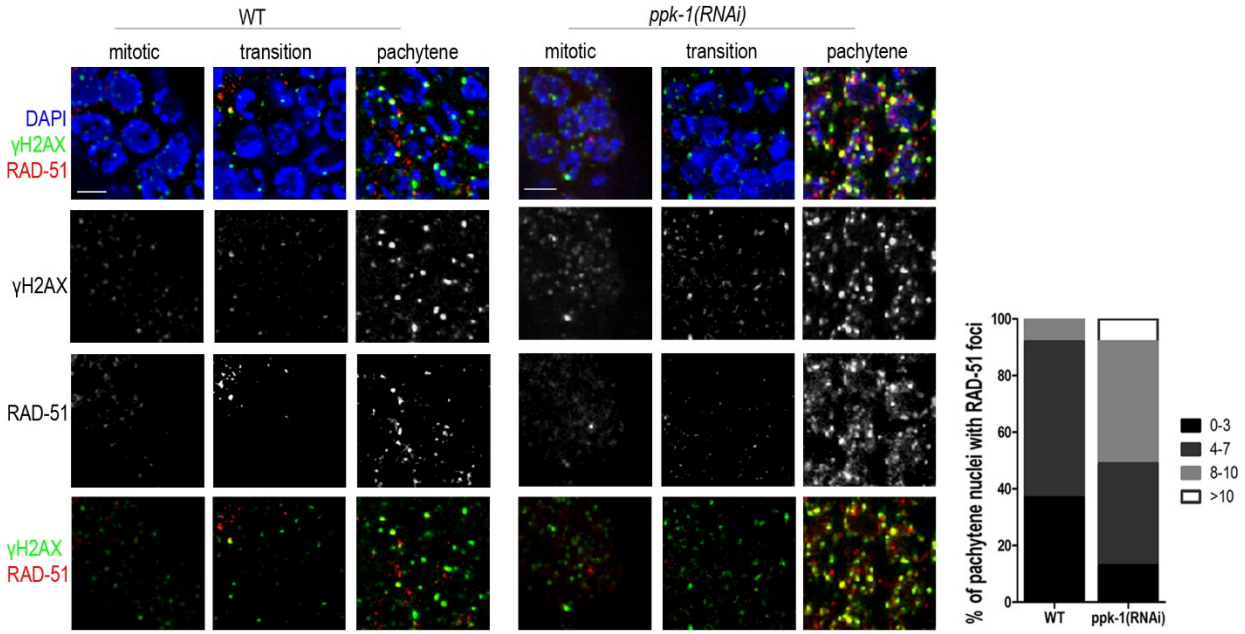

Figure 4. Increased DNA damage and repair upon *ppk-1(RNAi).* Indirect immunofluorescence of anti-RAD-51 and anti-γH2AX in mitotic, leptotene/zygotene (transition) or pachytene *ppk-1(RNAi)* and L4440 (WT) germ cell nuclei. Graph represents % of pachytene nuclei with counted number of RAD-51 foci (N= 3, n=30). Scale bar represents 5μm.

Next, we depleted PIP2 from *C. elegans* of CED-1::GFP transgenic line. CED-1 is a phagocytic receptor which localizes to plasma membrane during apoptosis [38]. We observed increased CED-1

localization to the plasma membrane in *ppk-1(RNAi)* worms compare to control worms. In *ppk-1(RNAi)* worms an average of 19 cells per germ line were positive for CED-1 compare to an average of 7 cells per WT germ line (Fig. 5a). Thus, we concluded that depletion of PIP2 is connected with the increase in apoptosis. To assess whether the observed increase in apoptosis is connected with the DNA damage we performed *ppk-1(RNAi)* in CED-1::GFP *C. elegans* transgenic strain with deleted CEP-1, a p53 mammalian homolog. We scored these worms for CED-1::GFP distribution. In CED-1::GFP worms with depleted CEP-1 and additionally knock-downed PPK-1, we detected background levels of apoptosis. The same background level of apoptosis was noticed in CED::GFP worms with depleted CEP-1 only (Fig. 5b). These observations firmly suggest that the apoptosis upon PIP2 depletion is caused by DNA damage.

Altogether, this supports a hypothesizes that the increased localization of RNA pol I and II in germ cells nuclei and subsequent DNA damage imply PIP2 function in genome stability.

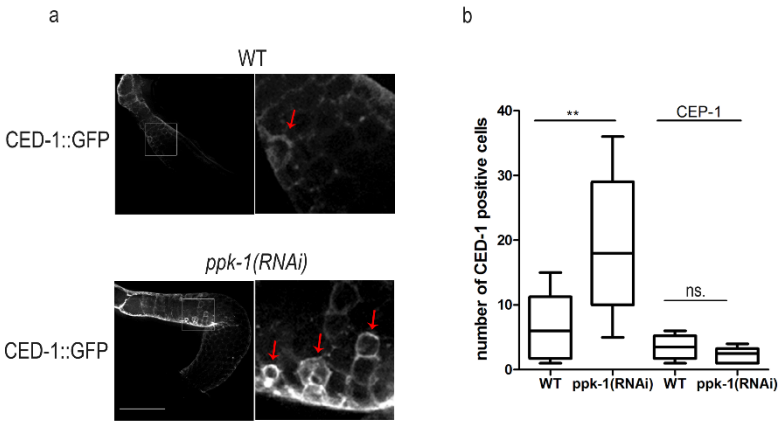

Figure 5. Increased apoptosis upon *ppk-1(RNAi)*. (a) CED-1::GFP immunofluorescence in *ppk-1(RNAi)* or L4440 (WT) background. Red arrows point to sheath cell localization of CED-1. Scale bars represent 50µm. (N= 3, n=30). (b) Graphical representation of number of CED-1 positive sheath cells in WT or *ppk-1(RNAi)* background with or without CEP-1 (N= 3, n=30). Statistical comparisons between genotypes were performed using Student t-test: n.s. non-significant; * $P \leq 0.05$; ** $P \leq 0.01$; *** $P \leq 0.001$

Impaired chromosome pairing and synapsis defect in ppk-1(RNAi) worms

It was previously published that the presence of univalents and altered chromatin structure in the nuclei of *C. elegans* oocytes is connected with defects in the synaptonemal complex formation and DNA

damage [39,40]. We have already observed the increase in DNA damage (Fig. 5) and altered chromatin structure (Fig. 2) which may cause impaired chromosomal pairing and weaken synaptonemal complex (SC) formation upon PIP2 depletion. Therefore, we decided to investigate SC complex formation. We depleted PIP2 by *ppk-1(RNAi)* in HIM-8::mCherry *C. elegans* transgenic line, and then visualized HIM-8 protein which localizes to pairing centers at X chromosome. We observed that after PIP2 depletion the pairing of X chromosomes was impaired in pachytene stage of the prophase I but not in transition stage. The statistical evaluation of HIM-8::mCherry foci revealed a significant increase (app. 20%) in non-paired HIM-8:mCherry foci in pachytene in *ppk-1(RNAi)* worms compare to the WT (Fig. 6a). The increase of HIM-8 foci upon *ppk-1(RNAi)* but not in control, propose PIP2 importance for proper chromosome pairing. To eliminate the possibility that observed PIP2 pairing effect is connected with PIP2 cytoplasmic role or its presence at nuclear membrane we depleted PIP2 in SUN-1::mRuby *C. elegans* strain. SUN-1 is part of SUN/KASH protein complex which link nucleoplasmic activities to the cytoskeleton [41]. We detected and evaluated SUN-1::mRuby localization upon *ppk-1(RNAi)* and compared it to mRuby signal in WT worms. We observed that SUN-1::mRuby localization is unchanged (Sup. Fig. 2a) and this suggests that PIP2 importance for chromosome pairing is not connected with its cytoplasmic but rather nuclear functions. Moreover, we investigated the nuclear periphery state by the localization of lamin in control and *ppk-1(RNAi)* worms by indirect immunofluorescence. We did not observed any change of lamin localization upon PIP2 depletion from *C. elegans* gonad (Sup. Fig. 2b). Unchanged SUN-1 and lamin localization confirmed that there are no major changes in the nuclear membrane and periphery structure.

In the next step, we used indirect immunofluorescence to visualize the synaptonemal complex (SC) formation in rrf-1(pk1417) *C. elegans* strain. We used anti-HTP-3 antibody and anti-SYP-1 antibody to visualize central and lateral elements of the SC. In *ppk-1(RNAi)* worms we observed uneven distribution of HTP-3 and SYP-1, with partial co-localization which confirmed that the synapsis is not fully formed (Fig. 6b). On the other hand, the synapsis in pachytene nuclei of WT worms was uniformly extended along the chromosomal axes with complete co-localization of both SC elements (Fig. 6c). These data suggested us that homolog pairs of chromosomes are not aligned properly thus SC cannot extend along full length of

chromosomes, showing the synapsis defect. From these observations, we can conclude that PIP2 is important for chromosome pairing and formation of the SC complex. Furthermore, by investigating of HTP-3 localization in diakinesis nuclei of WT and *ppk-1(RNAi)* in rrf-1(pk1417) strain, we confirmed a chromatin disorganization. HTP-3 has typical cruciform pattern in WT worms [42] however upon PIP2 depletion, HTP-3 is no longer localized to short but only to long chromosomal arms (Sup. Fig. 3). These results are apparently connected with the altered chromatin structure (Fig. 2) which is a probable cause of improperly paired homologs (lack of HTP-3 at short arms; Fig. 5 and Sup. Fig. 3) and subsequently increased number of DAPI stained bodies (Fig. 2).

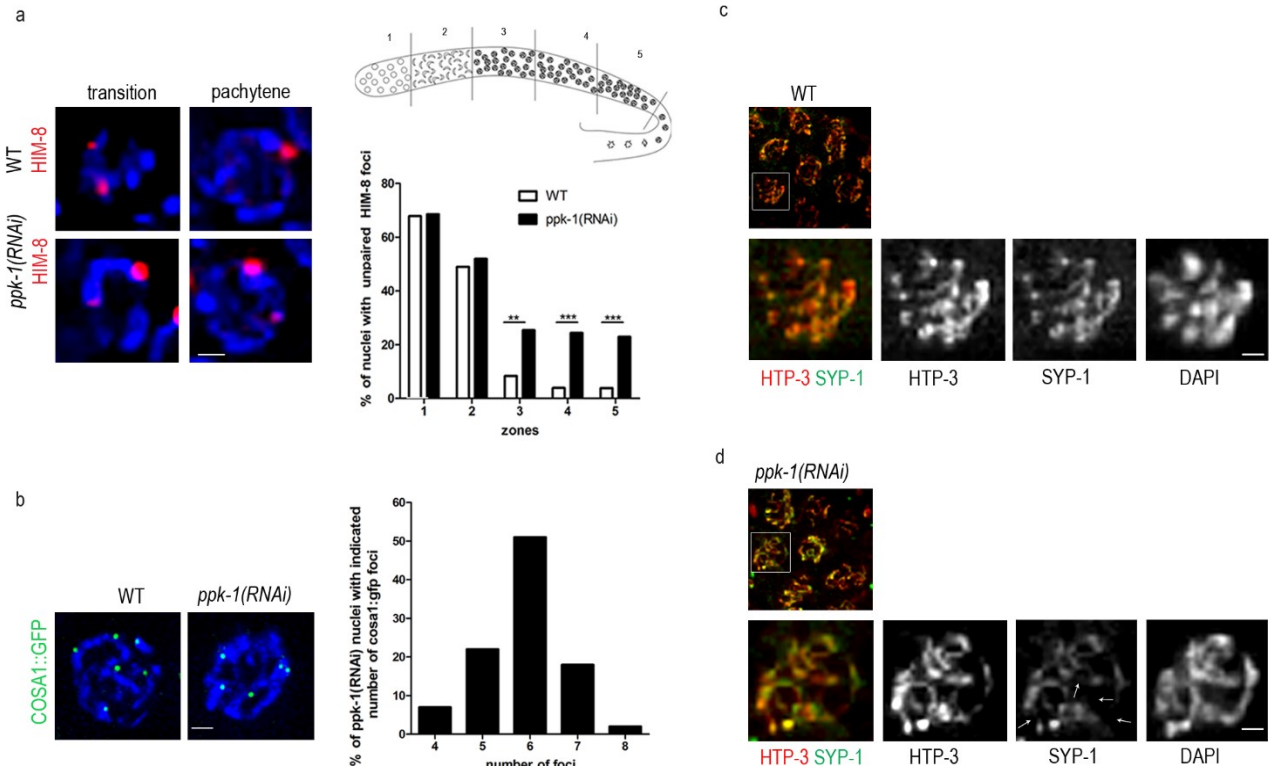

Figure 6. Meiotic defects upon *ppk-1(RNAi)*. (a) HIM-8::mCherry immunofluorescence in *ppk-1(RNAi)* or L4440 background. Graph represents number of observed HIM-8 foci during prophase I (N=3, n=30). (b-c) Indirect immunofluorescence of anti-HTP3 and anti-SYP1 in WT or *ppk-1(RNAi)* background. Arrows point to impaired anti-HTP3 and anti-SYP1 co-localization. (d) COSA-1::GFP foci immunofluorescence in *ppk-1(RNAi)* or L4440 background. Graph represents % of pachytene nuclei with observed numbers of COSA-1 foci (N=3, n=30). Scale bars represent 1µm. Statistical comparisons between genotypes were performed using Student t-test : n.s. non-significant; * $P \leq 0.05$; ** $P \leq 0.01$; *** $P \leq 0.001$

Pairing of homologs and formation of SC is tightly connected with crossover formation (CO). Disruption of SC formation between the paired chromosome result in abrogation of recombination. In context of previous data, we checked crossover formation in *C. elegans* where COSA-1 foci correspond to single CO [43]. After depletion of PIP2 from *C. elegans* gonad we observed a significant change in COSA-1::GFP foci compare to the WT gonad (Fig. 6d). Statistical evaluation of COSA-1::GFP foci revealed that approximately 50% of pachytene nuclei have less (4-5) or more (7-8) foci upon *ppk-1(RNAi)* compare to WT worms with 6 COSA-1::GFP foci per nucleus.

Overall, from this data we deduct that PIP2 plays an important role in the chromosome pairing and synaptonemal complex formation, which also affects crossover formation.

PIP2 interacts with proteins involved in the ubiquitin- proteasome pathway

To elucidate molecular mechanism behind observed effects upon *ppk-1(RNAi)* we decided to identify PIP2-binding partners in *C. elegans* germline. We performed mass-spectrometry analysis of the material immunoprecipitated either by anti-PIP2 or control mouse anti-IgM antibody from *C. elegans* lysate prepared from dissected gonads. By comparing control and anti-PIP2 antibody, we identified 65 putative PIP2-binding partners in *C. elegans* (Fig. 7) localized either in the cell nucleus and cytoplasm or exclusively in the cell nucleus.

In the next step, we tested PIP2 interactions in nuclear lysate by immunoprecipitation and partially confirmed data from mass-spectrometry. We endorsed that PIP2 is indeed a binding partner of lamin, proteasome subunit beta 4 (PBS-4) and leucine-rich repeat (LRR-1) protein which is known as a subunit of Cullin 2-RING E3 ligase complex ($CRL2^{LRR-1}$) [44,45]; (Fig. 8a) in *C. elegans*.

Interestingly, LRR-1 co-localizes with PIP2 in germ cell nuclei (Fig. 8b). As LRR-1 localization depends on CUL-2 [44], we tested PIP2 localization in worms with depleted CUL-2. We did not observe any change of PIP2 localization and therefore we conclude that PIP2 interacts with LRR-1 within the same nuclear compartment but its localization is not dependent on $CRL2^{LRR-1}$ in germ cell nuclei (Fig. 8b).

#	UNIPROT	protein name	#	UNIPROT	protein name
1	P90916	Probable histone-binding protein LIN53	34	O61792	Proteasome Regulatory Particle, Non-ATPase-like
2	Q9NLD1	HnRNP A1	35	V5XY55	Regulatory A subunit of protein phosphatase 2A
3	Q9TYV5	Nucleolar protein 1	36	P91495	Nuclear Pore complex Protein
4	Q18212	Spliceosome RNA helicase DDX39B	37	Q9XUV0	Proteasome subunit beta type
5	Q8I8G9	ADR-1E	38	Q18409	Probable splicing factor, arginine/serine-rich 6
6	Q9XTT9	Proteasome Regulatory Particle, ATPase-like	39	O44411	Nucleolar GTP-binding protein 1
7	Q04908	26S proteasome non-ATPase regulatory subunit 3	40	Q18787	26S protease regulatory subunit 7
8	V5XY55	Regulatory A subunit of protein phosphatase 2A	41	Q965V4	EXPOrtin (Nuclear export receptor) xpo-2
9	O16368	Probable 26S protease regulatory subunit 4	42	Q9NEW6	Probable splicing factor, arginine/serine-rich 3
10	O17915	GTP-binding nuclear protein ran-1	43	P04255	Histone H2B
11	G5ED41	Cullin-associated NEDD8-dissociated protein 1	44	Q09511	Probable splicing factor, arginine/serine-rich 4
12	P49632	Ubiquitin-60S ribosomal protein L40	45	Q23121	Probable splicing factor, arginine/serine-rich 1
13	Q21276	Uncharacterized NOP5 family protein K07C5.4	46	Q19973	C.Elegans Chromodomain protein/cec-4
14	P91306	C. Elegans Y-box cey-2	47	O17919	Putative H/ACA ribonucleoprotein complex subunit 4
15	O76371	Proteasome Regulatory Particle, ATPase-like	48	Q94045	Putative RNA polymerase II transcriptional coactivator
16	Q19328	Tudor Staphylococcal Nuclease homolog	49	Q9XTZ2	SR Protein Splicing factor
17	Q20938	Probable 26S proteasome regulatory subunit rpn-6.1	50	Q22053	rRNA 2-O-methyltransferase fibrillarin
18	Q9GZH5	Proteasome Regulatory Particle, Non-ATPase-like	51	P41932	14-3-3-like protein 1
19	Q21215	Guanine nucleotide-binding protein subunit beta-2-like 1	52	O62102	Proteasome subunit beta type
20	Q9N5V3	IMportin Beta family	53	O17586	Proteasome subunit alpha type-6
21	Q21443	Lamin-1	54	Q17361	Ubiquitin carboxyl-terminal hydrolase 14
22	P46502	Probable 26S protease regulatory subunit 6B	55	Q95005	Proteasome subunit alpha type-7
23	P62784	Histone H4	56	Q22037	Heterogeneous nuclear ribonucleoprotein A1
24	Q9BL61	Uncharacterized protein part of spliceosome	57	P34286	Proteasome subunit beta type-1
25	O17071	Probable 26S protease regulatory subunit 10B	58	P48727	Serine/threonine-protein phosphatase PP1
26	Q19007	Nucleosome Assembly Protein NAP-1	59	Q23089	EXPOrtin (Nuclear export receptor) xpo-1
27	Q18115	26S proteasome non-ATPase regulatory subunit 1	60	O44156	Proteasome subunit alpha type-1
28	Q3S1J5	UBA (Human ubiquitin) related	61	Q9U2U0	U2AF splicing factor
29	P48727	Serine/threonine-protein phosphatase PP1-beta	62	Q09583	Proteasome subunit alpha type-3
30	Q09475	Uncharacterized helicase C28H8.3	63	Q21633	UBiquitin Conjugating enzyme
31	Q27GU1	Chromosome-Segregation and RNAi deficient	64	Q95008	Proteasome subunit alpha type-5
32	G5EDV3	C. Elegans Y-box OS=Caenorhabditis elegans cey-4	65	P90868	Proteasome Beta Subunit
33	Q9U2X0	PRotein arginine MethylTransferase			

Figure 7. Protein identified in MS analysis as potential PIP2 binding partners. Proteins are listed based on number of identified unique peptides.

To focus on PIP2-LRR-1 complex importance, we investigated RNA polymerase II localization in CUL-2 depleted worms and observed increased localization compare to WT worms (Fig. 8c).

Here we identified PIP2-interacting partners in *C. elegans* and to our surprise, a great number of proteins are involved in the ubiquitin-proteasome pathway. Altogether these results prompt us to hypothesize that PIP2 might be targeting the RNA polymerase II for degradation by $CRL2^{LRR-1}$.

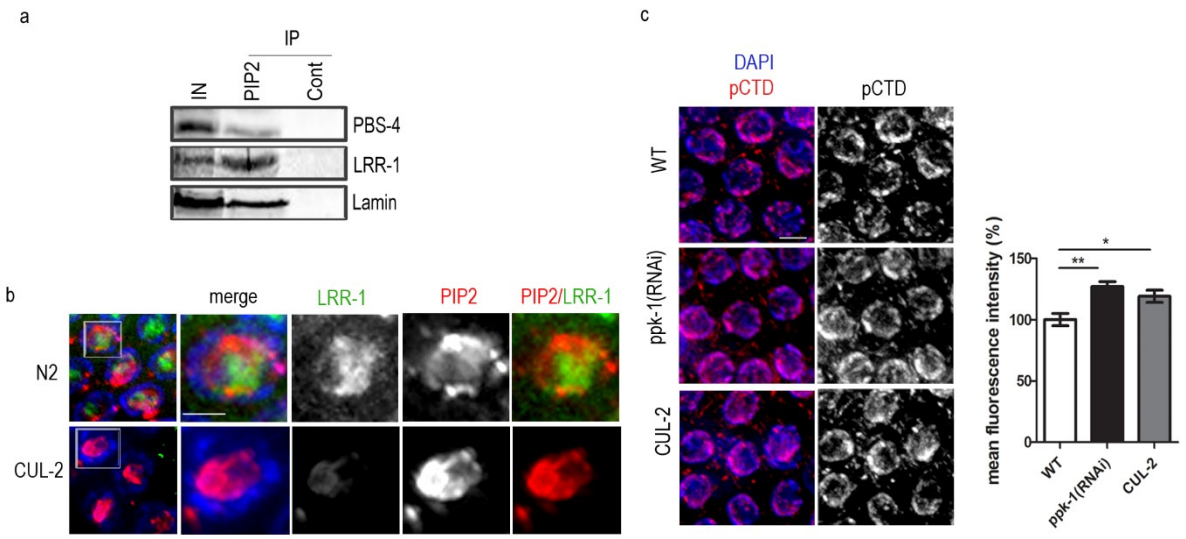

Figure 8. PIP2 interacts with LRR-1 and PBS-4. (a) Immunoprecipiation by anti-PIP2 and control mouse anti-IgM from *C. elegans* nuclear lysate. (b) Indirect immunofluorescence of anti-LRR-1 (green) and anti-PIP2 (red) in N2 and CUL-2 background germ cell nuclei. Scale bar represents 2µm. (c) Indirect immunofluorescence of pCTD of RNA polymerase II in *ppk-1(RNAi)* or L4440 (WT) germ cell nuclei. Graph represents mean fluorescence intersity measured from N= 3, n= 30. Scale bar represents 5µm. Statistical comparisons between genotypes were performed using Student t-test: n.s. non-significant; * $P \leq 0.05$; ** $P \leq 0.01$; *** $P \leq 0.001$

Discussion

PIP2 is implicated in various physiological processes therefore, it is very challenging to address its individual functions. Most studies of PIP2 and its synthetizing enzymes were performed in mammalian cells and only a few studies take advantage of the *C. elegans* simpler phosphoinositides metabolism. We decided to address specifically PIP2 function and thus we benefit from using *C. elegans* as a model organism for this study. Here we present that PIP2 influences chromatin structure, and is involved in processes such as transcriptional regulation, DNA-damage-driven apoptosis, chromosome condensation with subsequent pairing and the ubiquitin-proteasome degradation pathway. Based on our data we concluded that observed *C. elegans* phenotypes might be caused by (i) the altered chromatin structure (ii) impaired ubiquitin-proteasome pathway or (iii) disrupted binding of PIP2 to essential protein. We propose

that PIP2 is involved in the regulation of molecular processes at multiple levels and may be a part of many protein complexes in *C. elegans* germ cells nuclei.

PIP2 and its kinase PPK-1 have important functions in many physiological processes in *C. elegans* which are crucial in early development [30,31]. Here we described PIP2 localization in *C. elegans* gonad and embryo by anti-PIP2 antibody directly. PIP2 has a strong nuclear staining during prophase I, which differ from PPK-1 staining in the gonad. On the other hand, during *C. elegans* embryogenesis we observed nuclear, cytoplasmic and membranous localization of PIP2. Panbianco et al. suggested that PIP2 might be asymmetrically generated in *C. elegans* embryos because PPK-1 is enriched at the posterior site of embryo [46]. We did not observe asymmetrical localization of PIP2 in embryos thus we agree more with their other proposal that PPK-1 might influence spindle positioning independently from its function as a PIP2 producer. Similar suggestions about independent role of PI5PK and PIP2 were previously published by us [17] and Chakrabarti et al. for the regulation of RNA polymerase I transcription in mammalian cells [47].

We observed an increased incidence of males in *C. elegans* progeny upon PIP2 depletion (Fig. 1g). *C. elegans* male genotype is represent by the only one X chromosome (X0) therefore we suggest that increased incidence is dependent on the observed presence of univalent DAPI stained bodies in *ppk-1(RNAi)*; (Fig. 2) what is the most probable cause of increased male incidence [48]. Moreover, we observed oocytes mislocalization and the altered chromatin structure in diakinesis oocytes. The altered chromatin shape was also described after depletion of ZTF-8 and RAD-51 proteins, and both were shown to be important for *C. elegans* germ line genomic stability [40,39]. This is in an agreement with our observed data of increased RAD-51 and γH2AX localization in germ cell nuclei upon *ppk-1(RNAi)*. Therefore, we suggest that PIP2 is important for genomic stability in *C. elegans* germ line.

The presence of univalents and altered chromatin in nuclei of *C. elegans* oocytes are connected with defects in the synaptonemal complex formation and DNA damage [39,40]. Depletion of PIP2 resulted in the increase of genome instability, supported by defective SC formation, pointing out to the altered chromatin structure in our experiments. This altered chromatin structure results in synapsis defect, which

subsequently results in the increased presence of univalents. This is additionally supported by impaired crossover formation.

The transcription of germ cell specific but not somatic genes is ongoing in germ cell nuclei of *C. elegans*. Germ line transcription represents around ~21 % of all genes transcription, and ribosomal genes transcription is 4-fold higher in germ than in somatic cell nuclei [5]. Following investigation of altered chromatin upon PIP2 depletion revealed increased localization of RNA polymerase I, phosphorylated form of RNA polymerase II and 5-fluorouracil (FU) incorporation to the nascent RNA. As transcription is tightly regulated, the increased transcription rate together with altered chromatin structure is presumably a cause for DNA damage and repair, with following DNA-damage-driven apoptosis and genomic instability.

In mammalian cells it was proved that defects in the nuclear lamina may lead to misshapen nuclei [49]. Another important protein complex is SUN/KASH which is known to transmit forces from cytoplasm through nuclear envelope to the lamina and the chromatin [50]. Penkner et al. showed that active involvement of nuclear envelope is inevitable for homologous chromosome pairing and SUN-1 mutation leads to disruption of early meiosis chromatin reorganization. On the other hand, they proved that SUN-1 is not essential for SC formation [51]. Nevertheless, we did not observed any change in lamin localization or SUN-1 localization upon PIP2 depletion in the *C. elegans* gonad thus it is highly improbable that observed phenotypes are caused by cytoplasmic signaling or membranous PIP2.

We hypothesize that these observed impaired processes might originate from disruption of PIP2 interactions with protein partners. To discover more, we performed mass-spectrometry analysis of immunoprecipitated proteins in complex with PIP2. We identified 65 proteins as potential PIP2 binding partners, where the most striking partners are involved in the ubiquitin proteasome pathway. We showed that PIP2 interacts and co-localizes with LRR-1 protein in *C. elegans* germ cell nuclei. LRR-1 is described binding partner of CRL2 E3-ligase [45,44] and is important for proliferation and progression through *C. elegans* germline development. Burger et al. concluded that HTP-3 is likely a direct target for CRL-2^{LRR-1} E3 ligase as they observed its accumulation in distally located germ cells. We did not observed this phenotype (data not shown). However, they also showed that CRL-2^{LRR-1} acts at multiple levels of germ

cell development [45]. Based on different observed phenotypes upon PIP2 depletion we hypothesize that PIP2 interaction with CRL-2^{LRR-1} plays a role at different levels than CRL-2^{LRR-1} and HTP-3 complex. Most probably, PIP2 interaction targets CRL-2^{LRR-1} to RNA polymerase II as we observed increased RNA pol II localization in *ppk-1(RNAi)* and also CUL-2 depleted worms. Additionally, Merlet et al. observed DNA damage but did not detect RAD-51 foci in LRR-1 mutants [44]. Thus, this supports our suggestion that PIP2 may target CRL-2^{LRR-1} also to other proteins connected with disrupted phenotypes upon *ppk-1(RNAi)*. Interestingly, Jungmichel et al. identified Cullin-1 as possible specific interactor of nuclear PIP2 together with other proteins as ubiquitin-protein ligase, ubiquitin-like modifier-activating enzyme, ubiquitin-associated protein 2 in mammalian cells [52]. PIP2 has more protein binding partners (e.g. splicing factors) based on our mass-spectrometry data and therefore may play a role at various levels of C. *elegans* development regulation. Consistently, it was shown in mammalian cell lines that nuclear PIP2 regulates RNA polymerase I transcription at multiple levels by the interaction with several proteins [16].

On the other hand, PPK-1 *per se* may contribute to the regulation of these processes independently from its function as PIP2 producer and possibly by interaction with different protein binding partners, too. Previously a distinct role of PIP2 and its kinase has been described based on binding partners for mammalian cell lines [47,17]. Partially some of observed phenotypes might be indirect, caused by the decrease of second messengers produced by PIP2 cleavage. However, here we provide an evidence about PIP2 binding partners which are involved in the regulation of various processes thus we are inclined to conclude that observed phenotypes are connected directly with PIP2. Overall data confirmed PIP2 involvement and importance in the regulation of crucial processes in *C. elegans* germ cells.

Materials and methods

Strains and culture conditions

All strains were maintained and cultured under standard conditions at 20°C using *E. coli* OP50 as a food source [53], except when subjected to RNAi treatment. Used worm strains were obtained from the CGC

(Ceanorhabditis Genetics Center; Minnesota University,USA)**:** N2 (C. elegans var Bristol), rrf-1(PK1417) (NL2098), COSA-1::GFP (AV630), CED-1::GFP (MD701), SUN-1::mRuby (CA1219),CUL-2 (EU640; cultured at 15°C). We obtained H2B::GFP/HIM-8::mCherry [him-8(tm611)IV; ttTi5605 vv Is17 II; unc-119(ed3)III; H2B::GFP vvIs17[pie-1p::mCherry::him-8::unc- 54ter, unc-119(+)] strain from Monique Zetka (MacGill University, Canada). We obtained CED-1::GFP/CEP-1 [bcIs39 [lim-7p::ced-1::GFP + lin-15(+)]cep-1(ep347)I.] strain from Susan Gasser (FMI, Switzerland). Worm strain CUL-2 (EU640) from CGC was incubated at 15°C.

RNA interference

For RNAi of *ppk-1* we used the full coding sequence of 1836 bp (F55A12.3) from *C. elegans* cDNA. Used primers were: forward 5′- CCCGGGATGGCTTCTCGGTCCAC -3′ and reverse 5′ CCATGGTCAAGCGACAGGTGTGT- 3′. The sequence was cloned to L4440 feeding vector (pPD129.36) [54]. The resulting plasmid was transformed into the HT115(DE3) RNase Ill-deficient *E. coli* strain. Transformed bacteria were spread on an NGM plate with ampicillin (50 mg/ml) and IPTG (1mM). Hermaphrodite worms in L3/L4 stage were transferred onto the seeded plates and incubated at 20 °C for 48 hours. As a mock control we used empty L4440 plasmid transformed in *E.coli* HT115(DE3) bacteria and worms were incubated under the same conditions.

Antibodies

Following primary antibodies were used in this study: anti-PIP2 mouse monoclonal (Echelon Biosciences Inc. clone 2C11, Z-A045), anti-Polymerase I rabbit polyclonal (RPA116; gift from I. Grumt), anti-Polymerase II mouse monoclonal (gift from H. Kimura), anti-BrdU mouse monoclonal (Sigma, 094M4821V), anti-γH2AX mouse monoclonal (Millipore, 05-636), anti-RAD51 rabbit polyclonal (Santa Cruz, sc-8349), anti-Lamin rabbit polyclonal (Abcam, ab16048), anti-PPK-1 rabbit polyclonal (gift from D. Weinkove), anti-fibrillarin rabbit monoclonal (2639S, Cell signalling), anti-HTP3 rabbit polyclonal (gift from M. Zetka), anti-SYP-1 mouse monoclonal (gift from M. Zetka), control mouse anti-IgM (Abcam,

ab18401), control rabbit anti-IgG (Abcam, ab46540), anti-PBS-4 goat polyclonal (Abcam, ab166792), anti-LRR-1 rabbit monoclonal (gift from L. Pintard) antibody.

Following secondary antibodies were used in this study: goat anti-mouse IgM (μ-chain specific) antibody conjugated with Alexa Fluor 555 (Invitrogen, A21426), goat anti-mouse IgG (H+L) antibody conjugated with Alexa Fluor 488 (Invitrogen, A21202), goat anti-rabbit IgG (H+L) antibody conjugated with Alexa Fluor 488 (Invitrogen, A11034), goat anti-rabbit IgG (H+L) antibody conjugated with Alexa Fluor 555 (Invitrogen, A21429), IRDye 680 donkey anti-mouse IgG (H+L) antibody (LI-COR Biosciences, 926-68072), IRDye 800 donkey anti-mouse IgG (H+L) antibody (LI-COR Biosciences, 926-32212), IRDye 800 donkey anti-rabbit IgG (H+L) antibody (LI-COR Biosciences, 925-32213), IRDye 680 donkey anti-rabbit IgG (H+L) antibody (LI-COR, Biosciences, 926-68073), IRDye 800 Goat anti-Mouse IgM (μ chain specific) antibody (LI-COR Biosciences 926-32280), IRDye 800 donkey-anti Goat IgG (H+L) antibody (LI-COR Biosciences, 926-32214), IRDye 680 donkey-anti Goat IgG (H+L) antibody (LI-COR Biosciences, 926-68074).

Indirect immunofluorescence, 5-FU treatment and Actinomycin D inhibition

Immunofluorescence staining was performed according to the standard protocol [55]. Images were aquired at Delta Vision Image Restoration System (Applied Precission). Stacks of approximately 10 optical sections with 0.3 μm using 60x, 1.2 NA U Plan Apochromat objective (Olympus). We deconvolved the obtained images using the soft-WoRX 3.0 software (Applied Precision). The same imiging conditiones were used for WT or RNAi samples.

The rrf-1(pk1417) strain was subjected to RNAi feeding for 48 hours. After 48 hours adult worms *ppk-1(RNAi)* or WT were dissected and incubated in 8mM 5-FU in M9 (22 mM KH_2PO_4, 42 mM Na_2HPO_4, 86 mM NaCl, 1M $MgSO_4$) for 5, 10 or 15 minutes. After treatment, the standard protocol for indirect immunofluorescence was followed [55].

For AMD inhibition, NGM plates for RNAi knockdown with addition of different AMD concentration (0.01, 0.05, 1 or 2 μg/ml) were prepared. After 46 h of RNAi, rrf-1(pk1417) worms were replaced to fresh

dishes to continue RNAi effect with supplement of AMD. Worms were left on AMD containing plates for 2 hours at 20°C, than were subjected to 5-FU treatment and subsequent indirect immunofluorescence protocol.

Mass-spectrometry

For MS analysis we used material immunoprecipatated by anti-PIP2 or control anti-mouse antibody from synchronized adults. Gonads from at least 50 N2 worms were disected from body and collected to tube. The nuclear fraction was prepared according to Singh et al. [56]. After immunoprecipitation washed beads were resuspended in 100mM TEAB containing 1% SDC. Cysteins were reduced with 5mM final concentration of TCEP (60°C for 60 min) and blocked with 10mM final concentration of MMTS (10 min Room Temperature). Samples were cleaved on beads with 1µg of trypsin at 37°C overnight. After digestion, samples were centrifuged and supernatants were collected and acidified with TFA to 1% final concentration. SDC was removed by extraction to ethylacetate [57]. Peptides were desalted on Michrom C18 colum. Nano Reversed phase column (EASY-Spray column, 50 cm x 75 µm ID, PepMap C18, 2 µm particles, 100 Å pore size) was used for LC/MS analysis. Mobile phase buffer A was composed of water and 0.1% formic acid. Mobile phase B was composed of acetonitrile and 0.1% formic acid. Samples were loaded onto the trap column (Acclaim PepMap300, C18, 5 µm, 300 Å Wide Pore, 300 µm x 5 mm, 5 Cartridges) for 4 min at 15µl/min. Loading buffer was composed of water, 2% acetonitrile and 0.1% trifluoroacetic acid. Peptides were eluted with Mobile phase B gradient from 4% to 35% B in 60 min. Eluting peptide cations were converted to gas-phase ions by electrospray ionization and analyzed on a Thermo Orbitrap Fusion (Q-OT- qIT, Thermo). Survey scans of peptide precursors from 400 to 1600 m/z were performed at 120K resolution (at 200 m/z) with a 5×10^5 ion count target. Tandem MS was performed by isolation at 1,5 Th with the quadrupole, HCD fragmentation with normalized collision energy of 30, and rapid scan MS analysis in the ion trap. The MS 2 ion count target was set to 10^4 and the max injection time was 35ms. Only those precursors with charge state 2–6 were sampled for MS 2 . The dynamic exclusion duration was set to 45s with a 10 ppm tolerance around the selected precursor and its isotopes. Monoisotopic

precursor selection was turned on. The instrument was run in top speed mode with 2s cycles [58]. All data were analyzed and quantified with the MaxQuant software (version 1.5.3.8); [59]. The false discovery rate (FDR) was set to 1% for both proteins and peptides and we specified a minimum length of seven amino acids. The Andromeda search engine was used for the MS/MS spectra search against the *Caenorhabditis elegans* database (downloaded from Uniprot on April 2015, containing 25 527 entries). Enzyme specificity was set as C-terminal to Arg and Lys, also allowing cleavage at proline bonds and a maximum of two missed cleavages. Dithiomethylation of cysteine was selected as fixed modification and N- terminal protein acetylation and methionine oxidation as variable modifications. The "match between runs" feature of MaxQuant was used to transfer identifications to other LC-MS/MS runs based on their masses and retention time (maximum deviation 0.7 min) and this was also used in quantification experiments. Quantifications were performed with the label-free algorithms described recently. Data analysis was performed using Perseus 1.5.2.4 software.

Immunoprecipitation

The nuclear fraction was prepared according to Singh et al. [56]. For precipitation anti-PIP2 (2µg), control anti-mouse IgM antibody (2µg) and protein L magnetic beads (50µl of slurry) were used according to the manufacturer's protocol (Pierce, Thermo Scientific).

Dot blot

N2 worms were subjected to *ppk-1(RNAi)* or control RNAi for 48 hours. After RNAi treatment single worm was lysed in lysis buffer (50 mM KCl; 10 mM Tris (pH 8.3); 2.5 mM $MgCl_2$; 0.45% NP-40; 0.45% Tween-20) in total volume of 10 µl. The whole volume was spotted on PDVF membrane and anti-PIP2 antibody was used for detection.

Characterization of brood sizes and embryonic lethality

L3-L4 hermaphrodites were individually plated onto NGM plates seeded with *E.coli* HT115(DE3) transformed by L4440 or *ppk-1(RNAi)* at 20°C. After 24 hours, adult worms were removed from plates and

the progeny (laid eggs, L1) was counted. Subsequently we counted progeny (non-hatched eggs, L1,L2, L3) after 48 and 72 hours. We preformed experiment at least for 60 worms in three independent experiments.

Quantitation of COSA-1::GFP, HIM-8::mCherry and RAD-51 foci

Foci were quantified from deconvolved 3D data stacks of *C. elegans* WT or *ppk-1(RNAi)* germ cell nuclei. Foci we counted in at least 300 germ cell nuclei I from at least 10 gonads each. Quantification of RAD-51 foci was performed in whole gonad composing the mitotic tip to late pachytene regions [39]. COSA-1::GFP was quantified in late pachytene [43]. HIM-8::Cherry was quantified in TZ and late pachytene [60]. Statistical comparisons between genotypes were performed using Student t-test.

Detection of DAPI stained bodies in oocyte nuclei

Oocyte chromosomes were fixed with 4% formaldehyde and stained with DAPI [61]. In some oocyte nuclei the individual univalents or bivalents lie too close to each other to be resolved unambiguously, thus this method tends to underestimate the frequency of achiasmate chromosomes.

Supplementary Materials: Supplementary materials can be found at www.mdpi.com/link.

Acknowledgments

We are grateful to Dr. Monique Zetka (McGill University, Canada), Dr. Susan Gasser (Friedrich Miescher Institute, Switzerland), Dr. David Weinkove (Durham University, United Kingdom) and Dr. Lionel Pintard (Institut Jacques Monod, France) for sharing *C. elegans* strains or antibodies. Some strains were provided from the CGC, which is funded by National Institutes of Health - Office of Research Infrastructure Programs (P40 OD010440). Acknowledgment to Karel Harant and Pavel Talacko from Laboratory of Mass Spectrometry, Biocev, Charles University, Faculty of science, where proteomic and mass spectrometric analysis had been done. We acknowledge the Microscopy Centre - Light/Electron CF, IMG AS CR supported by the MEYS CR (LM2015062 Czech-BioImaging). This publication is supported by the project „BIOCEV – Biotechnology and Biomedicine Centre of the Academy of Sciences and Charles University“ (CZ.1.05/1.1.00/02.0109), from the European Regional Development Fund and by the Grant Agency of the

Czech Republic (17-09103S). The results achieved with institutional support were obtained with the support of long-term conceptual development of the scientific organization (RVO: 68378050). We thank members of the Hozak lab for critical reading of the manuscript.

Author Contributions: L.U. and J.R. conceived, designed and performed the experiments; L.U, J.R. and P.H. analyzed the data and wrote the paper.

Conflicts of Interest: The authors declare no conflict of interest.

REFERENCES:

1. MacQueen, A. V.; Villeneuve, A.M. Nuclear reorganization and homologous chromosome pairing during meiotic prophase require C. elegans chk-2. *Genes Dev* **2001,** *15* (13), 1674-87.
2. Nicklas, B.R. Chromosome segregation mechanisms. *Genetics* **1974,** *78* (1), 205-13.
3. Ostergren, G. The mechanism of co-orientation in bivalents and multivalents. *Hereditas* **1951,** *37*, 85-156.
4. Bell, O.; Tiwari, V.K; Thoma, N.H; Schubeler, D. Determinants and dynamics of genome accessibility. *Nat Rev Genet* **2011,** *12* (8), 554-64.
5. Wang, X; Zhao, Y; Wong, K; Ehlers, P; Kohara, Y; Jones, S.J; Marra, M.A; Holt, R.A; Moerman, D.G; Hansen, D. Identification of genes expressed in the hermaphrodite germ line of C. elegans using SAGE. *BMC Genomics* **2009,** *10*, 213.
6. Capitani, S.; Mazzotti, G.; Jovine, R.; Papa, S.; Maraldi, N.M.; Manzoli, F.A. Effect of phosphatidylcholine vesicles on the activity of DNA polymerase-alpha. *Mol Cell Biochem* **1979,** *27* (3), 135-8.
7. Capitani, S.; Caramelli, E.; Felaco, M.; Miscia, S.; Manzoli, F.A. Effect of phospholipid vesicles on endogenous RNA polymerase activity of isolated rat liver nuclei. *Physiol Chem Phys* **1981,** *13* (2), 153-8.
8. Manzoli, F.A.; Capitani, S.; Mazzotti, G.; Barnabei, O.; Maraldi, NM. Role of chromatin phospholipids on template availability and ultrastructure of isolated nuclei. *Adv Enzyme Regul* **1982,** *20*, 247-62.
9. Maraldi, N.M.; Capitani, S.; Caramelli, E.; Cocco, L.; Barnabei, O.; Manzoli, F.A. Conformational changes of nuclear chromatin related to phospholipid induced modifications of the template availability. *Adv Enzyme Regul* **1984,** *22*, 447-64.
10. Cocco, L.; Gilmour, R.S.; Maraldi, N.M.; Martelli, A.M.; Papa, S.; Manzoli, F.A. Increase of globin RNA synthesis induced by phosphatidylserine liposomes in isolated erythroleukemic cell nuclei. Morphological and functional features. *Biol Cell* **1985,** *54* (1), 49-56.
11. Capitani. S.; Cocco, L.; Maraldi, NM.; Papa, S.; Manzoli, F.A. Effect of phospholipids on transcription and ribonucleoprotein processing in isolated nuclei. *Adv Enzyme Regul* **1986,** *25*, 425-38.
12. Kuvichkin, V.V. DNA-lipid interactions in vitro and in vivo. *Bioelectrochemistry* **2002,** *58* (1), 3-12.

13. Mazzotti, G.; Zini, N.; Rizzi, E.; Rizzoli, R.; Galanzi, A.; Ognibene, A.; Santi, S.; Matteucci, A.; Martelli, A.M.; Maraldi, N.M. Immunocytochemical detection of phosphatidylinositol 4,5-bisphosphate localization sites within the nucleus. *J Histochem Cytochem* **1995,** *43* (2), 181-91.
14. Boronenkov, I.V.; Loijens, J.C.; Umeda, M.; Anderson, R.A. Phosphoinositide signaling pathways in nuclei are associated with nuclear speckles containing pre-mRNA processing factors. *Mol Biol Cell* **1998,** *9* (12), 3547-60.
15. Osborne, S.L.; Thomas, C.L.; Gschmeissner, S.; Schiavo, G. Nuclear PtdIns(4,5)P2 assembles in a mitotically regulated particle involved in pre-mRNA splicing. *J Cell Sci* **2001,** *114* (Pt 13), 2501-11.
16. Yildirim, S.; Castano, E.; Sobol, M.; Philimonenko, V.V.; Dzijak, R.; Venit, T.; Hozák, P. Involvement of phosphatidylinositol 4,5-bisphosphate in RNA polymerase I transcription. *J Cell Sci* **2013,** *126* (Pt 12), 2730-9.
17. Ulicna, L.; Kalendova, A.; Kalasova, I.; Vacik, T.; Hozák, P. PIP2 epigenetically represses rRNA genes transcription interacting with PHF8 *BBA Molecular and Cell Biology of Lipids* **2018,** *1863* (3), 266-275.
18. Yu, H.Y.; Fukami, K.; Watanabe, Y.; Ozaki, C.; Takenawa, T. Phosphatidylinositol 4,5-bisphosphate reverses the inhibition of RNA transcription caused by histone H1. *European Journal of Biochemistry* **1998,** *251* (1-2), 281-287.
19. Toska, E.; Campbell, H.A.; Shandilya, J.; Goodfellow, S.J.; Shore, P.; Medler, KF.; Roberts, S.G.E. Repression of Transcription by WT1-BASP1 Requires the Myristoylation of BASP1 and the PIP2-Dependent Recruitment of Histone Deacetylase. *Cell Reports* **2012,** *2* (3), 462-469.
20. Loijens, J.C.; Anderson, R.A. Type I phosphatidylinositol-4-phosphate 5-kinases are distinct members of this novel lipid kinase family. *J Biol Chem* **1996,** *271* (51), 32937-43.
21. Ogg, S.R.; Ruvkun, G. The C. elegans PTEN homolog, DAF-18, acts in the insulin receptor-like metabolic signaling pathway. *Mol Cell* **1998,** *2* (6), 887-93.
22. Blondeau, F.; Laporte, J.; Bodin, S.; Superti-Furga, G.; Payrastre, B.; Mandel, J.L. Myotubularin, a phosphatase deficient in myotubular myopathy, acts on phosphatidylinositol 3-kinase and phosphatidylinositol 3-phosphate pathway. *Hum Mol Genet* **2000,** *22* (9), 2223-9.
23. Klopfenstein, D.R.; Tomishige, M.; Stuurman, N.; Vale, R.D. Role of phosphatidylinositol(4,5)bisphosphate organization in membrane transport by the Unc104 kinesin motor. *Cell* **2002,** *109* (3), 347-58.
24. Nicot, A.S.; Fares, H.; Payrastre, B.; Chisholm, AD.; Labouesse, M.; Laporte, J. The phosphoinositide kinase PIKfyve/Fab1p regulates terminal lysosome maturation in Caenorhabditis elegans. *Mol Biol Cell* **2006,** *17* (7), 3062-74.
25. Bae, Y.K.; Kim, E.; L´hernault, S.W.; Barr, M.M. The CIL-1 PI 5-phosphatase localizes TRP Polycystins to cilia and activates sperm in C. elegans. *Curr Biol* **2009,** *19* (19), 1599-607.
26. Padmanabhan, S.; Mukhopadhyay, A.; Narasimhan, S.D.; Tesz, G.; Czech, M.P.; Tissenbaum, H.A. A PP2A regulatory subunit regulates C. elegans insulin/IGF-1 signaling by modulating AKT-1 phosphorylation. *Cell* **2009,** *136* (5), 939-51.
27. Liu, Z.; Klaavuniemi, T.; Ono, S. Distinct roles of four gelsolin-like domains of Caenorhabditis elegans gelsolin-like protein-1 in actin filament severing, barbed end capping, and phosphoinositide binding. *Biochemistry* **2010,** *49* (20), 4349-60.
28. Lu, N.; Shen, Q.; Mahoney, T.R.; Neukomm, L.J.; Wang, Y.; Zhou, Z. Two PI 3-kinases and one PI 3-phosphatase together establish the cyclic waves of phagosomal PtdIns(3)P critical for the degradation of apoptotic cells. *Plos Biol* **2012,** *10* (1), e1001245.

29. Cheng, S.; Wang, K.; Zou, W.; Miao, R.; Huang, Y.; Wang, H.; Wang, X. PtdIns(4,5)P_2 and PtdIns3P coordinate to regulate phagosomal sealing for apoptotic cell clearance. *The Journal of cell biology* **2015,** *210* (3), 485-502.
30. Weinkove, D.; Bastiani, M.; Chessa, T.A.M.; Joshi, D.; Hauth, L.; Cooke, F.T.; Divecha, N.; Kim, S. Overexpression of PPK-1, the C. elegans Type 1 PIP kinase, inhibits growth cone collapse in the developing nervous system and causes axonal degeneration in adults. *Dev Biol* **2008,** *313* (1), 384–397.
31. Xu, X.; Guo, H.; Wycuff, D. L.; Lee, M., Role of phosphatidylinositol-4-phosphate 5′ kinase (ppk-1) in ovulation of Caenorhabditis elegans. *Experimental Cell Research* **2007,** *313* (11), 2465-75.
32. Sobol, M.; Yildirim, S.; Philimonenko, V.V.; Marasek, P.; Castano, E.; Hozak, P. UBF complexes with phosphatidylinositol 4,5-bisphosphate in nucleolar organizer regions regardless of ongoing RNA polymerase I activity. *Nucleus* **2013,** *4* (6), 478-86.
33. Osborne, S. L.; Thomas, C. L.; Gschmeissner, S.; Schiavo, G. Nuclear PtdIns(4,5)P2 assembles in a mitotically regulated particle involved in pre-mRNA splicing. *J Cell Sci* **2001,** *114* (Pt 13), 2501-11.
34. Mellman, D. L.; Gonzales, M. L.; Song, C.; Barlow, C. A.; Wang, P.; Kendziorski, C.; Anderson, R. A. A PtdIns4,5P2-regulated nuclear poly(A) polymerase controls expression of select mRNAs. *Nature* **2008,** *451* (7181), 1013-7.
35. Kumsta, C.; Hansen, M.C. elegans rrf-1 mutations maintain RNAi efficiency in the soma in addition to the germline. *Plos One* **2012,** *7* (5).
36. Tang, L.; Machacek, T.; Mamnum, Y.M.; Penkner, A.; Gloggnitzer, J.; Wegrostek, C.; Konrat, R.; Jantsch, M.F.; Loidl, J.; Jantsch, V. Mutations in Caenorhabditis elegans him-19 show meiotic defects that worsen with age. *Mol Biol Cell* **2010,** *21* (6), 885-96.
37. Cortes, D.B.; McNally, K.L.; Mains, P.E.; McNally, F.J. The asymmetry of female meiosis reduces the frequency of inheritance of unpaired chromosomes. *Elife* **2015**, 4:e06056.
38. Zhou, Z.; Hartwieg, E.; Horvitz, H.R. CED-1 is a transmembrane receptor that mediates cell corpse engulfment in C. elegans. *Cell* **2001,** *104* (1), 43-56.
39. Colaiacovo, M.P.; MacQueen, A.J.; Martinez-Perez, E.; McDonald, K.; Adamo, A.; La Volpe, A.; Villeneuve, A.M., Synaptonemal complex assembly in C. elegans is dispensable for loading strand-exchange proteins but critical for proper completion of recombination. *Dev Cell* **2003,** *5* (3).
40. Kim, HM.; Colaiacovo, M.P. ZTF-8 interacts with the 9-1-1 complex and is required for DNA damage response and double-strand break repair in the C. elegans germline. *PLoS Genet* **2014,** *10* (10), e1004723.
41. Tzur, Y.B.; Wilson, K.L.; Gruenbaum, Y. SUN-domain proteins: 'Velcro' that links the nucleoskeleton to the cytoskeleton. *Nat Rev Mol Cell Biol* **2006,** *7* (10), 782-8.
42. Goodyer, W.; Kaitna, S; .Couteau, F.; Ward, J.D.; Boulton, S.J.; Zetka, M. HTP-3 links DSB formation with homolog pairing and crossing over during C. elegans meiosis. *Dev Cell* **2008,** *14* (2), 263-74.
43. Yokoo, R.; Zawadzki, K.A.; Nabeshima, K.; Drake, M.; Arur, S.; Villeneuve, A.M. COSA-1 Reveals Separable Licensing and Reinforcement Steps and Efficient Homeostasis Governing Meiotic Crossovers. *Cell* **2012,** *149* (1), 75-87.
44. Merlet, J.; Burger, J.; Tavernier, N.; Richaudeau, B.; Gomes, J.E.; Pintard, L. The CRL2LRR-1 ubiquitin ligase regulates cell cycle progression during C. elegans development. *Development* **2010,** *137* (22), 3857-66.
45. Burger, J.; Merlet, J.; Tavernier, N.; Richaudeau ,B.; Arnold, A.; Ciosk, R.; Bowerman, B.; Pintard, L. CRL2(LRR-1) E3-ligase regulates proliferation and progression through meiosis in the Caenorhabditis elegans germline. *PLoS Genet* **2013,** *9* (3), e1003375.

46. Panbianco, C.; Weinkove, D.; Zanin, E.; Jones, D.; Divecha, N.; Gotta, M.; Ahringer, J. A casein kinase 1 and PAR proteins regulate asymmetry of a PIP(2) synthesis enzyme for asymmetric spindle positioning. *Dev Cell* **2008,** *15* (2), 198-208.
47. Chakrabarti, R.; Sanyal, S.; Ghosh, A.; Bhar, K.; Das, C.; Siddhanta, A. Phosphatidylinositol-4-phosphate 5-Kinase 1α Modulates Ribosomal RNA Gene Silencing through Its Interaction with Histone H3 Lysine 9 Trimethylation and Heterochromatin Protein HP1-α. **2015,** *290* (34), 20893-903.
48. Hodgkin, J.; Horovitz, HR.; Brenner, S. Nondisjunction mutants of the nematode Caenorhabditis elegans. *Genetics* **1979,** *91*, 67-94.
49. Sullivan, T.; Escalante-Alcalde, D.; Bhatt, H.; Anver, M.; Bhat, N.; Nagashima, K.; Stewart, C.L.; Burke, B. Loss of A-type lamin expression compromises nuclear envelope integrity leading to muscular dystrophy. *The Journal of cell biology* **1999,** *147* (5), 913-20.
50. Starr, D.A. A nuclear-envelope bridge positions nuclei and moves chromosomes. *The Journal of cell biology* **2009,** *122* (5), 577-86.
51. Penkner, A.; Tang, L.; Novatchkova, M.; Ladurner, M.; Fridkin, A.; Gruenbaum, Y.; Schweizer, D.; Loidl, J.; Jantsch, V. The nuclear envelope protein Matefin/SUN-1 is required for homologous pairing in C. elegans meiosis. *Dev Cell* **2007,** *12* (6), 873-86.
52. Jungmichel, S.; Sylvestersen, K. B.; Choudhary, C.; Nguyen, S.; Mann, M.; Nielsen, M. L. Specificity and commonality of the phosphoinositide-binding proteome analyzed by quantitative mass spectrometry. *Cell Rep* **2014,** *6* (3), 578-91.
53. Brenner, S. The genetics of Caenorhabditis elegans. *Genetics* **1974,** *77* (1), 71-94.
54. Timmons, L.; Fire, A. Specific interference by ingested dsRNA. *Nature* **1998,** *395* (6705), 854.
55. Martinez-Perez, E., and Villeneuve, A.M. HTP-1-dependent constraints coordinate homolog pairing and synapsis and promote chiasma formation during *C. elegans* meiosis. *Genes and Development* **2005,** *19*, 2727–2743.
56. Singh, V. A Aballay, A. Regulation of DAF-16-mediated Innate Immunity in Caenorhabditis elegans. *J Biol Chem* **2009,** *284* (51), 35580-7.
57. Masuda, T.; Tomita, M.; Ishihama, Y. Phase Transfer Surfactant-Aided Trypsin Digestion for Membrane Proteome Analysis. *Journal of Proteome Research* **2008,** *7*, 731-740
58. Hebert, A.; Richards, A.L.; Bailey, D.J.; Ulbrich, A.; Coughlin, E.E.; Westphall, M.S.; Coon, J.J. The one hour yeast proteome. *Mol Cell Proteomics* **2014,** *13* (1), 339-47.
59. Cox, J.; Hein, M.Y.; Luber, C.A.; Paron, I.; Nagaraj, N.; Mann, M. Accurate proteome-wide label-free quantification by delayed normalization and maximal peptide ratio extraction, termed MaxLFQ. *Mol Cell Proteomics* **2014,** *13* (9), 2513-26.
60. Harper, N.; Rillo, R.; Jover-Gil, S.; Assaf, Z.J.; Bhalla, N.; Dernburg, A.F. Pairing centers recruit a Polo-like kinase to orchestrate meiotic chromosome dynamics in C. elegans. *Dev Cell* **2011,** *21* (5), 934-47.
61. Villeneuve, A. A cis-acting locus that promotes crossing over between X chromosomes in Caenorhabditis elegans. *Genetics* **1994,** *136*, 887-902.

Supplemental data

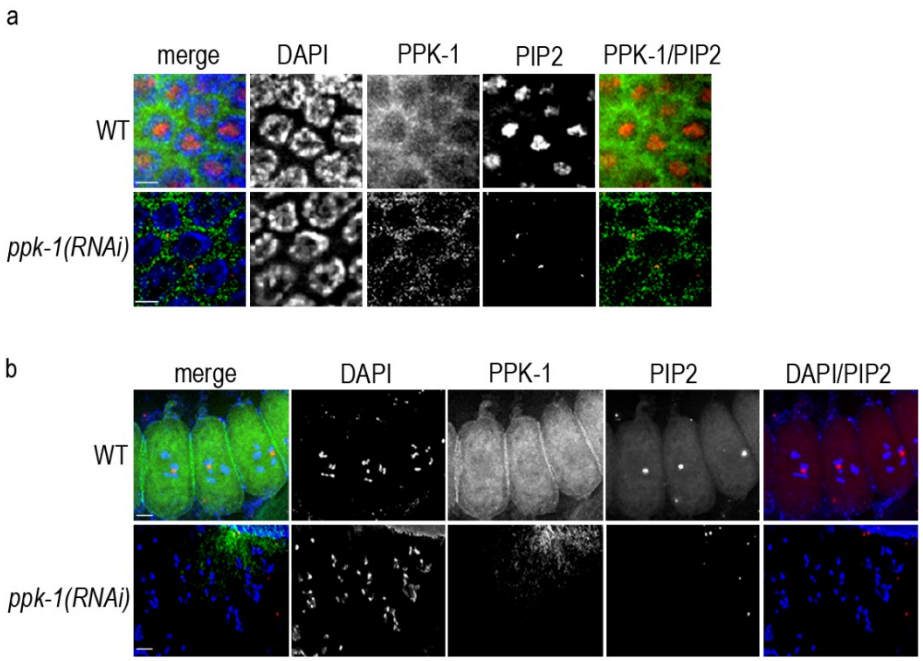

Sup. Figure 1. PIP2 and PPK-1 localization. (a) Indirect immunofluorescence of anti-PIP2 and anti-PPK-1 in WT or ppk-1(RNAi) germ cell nuclei background. Scale bar represents 5µm. (b) Indirect immunofluorescence of anti-PIP2 and anti-PPK-1 in WT or ppk-1(RNAi) background in oocytes. Scale bar represents 10µm.

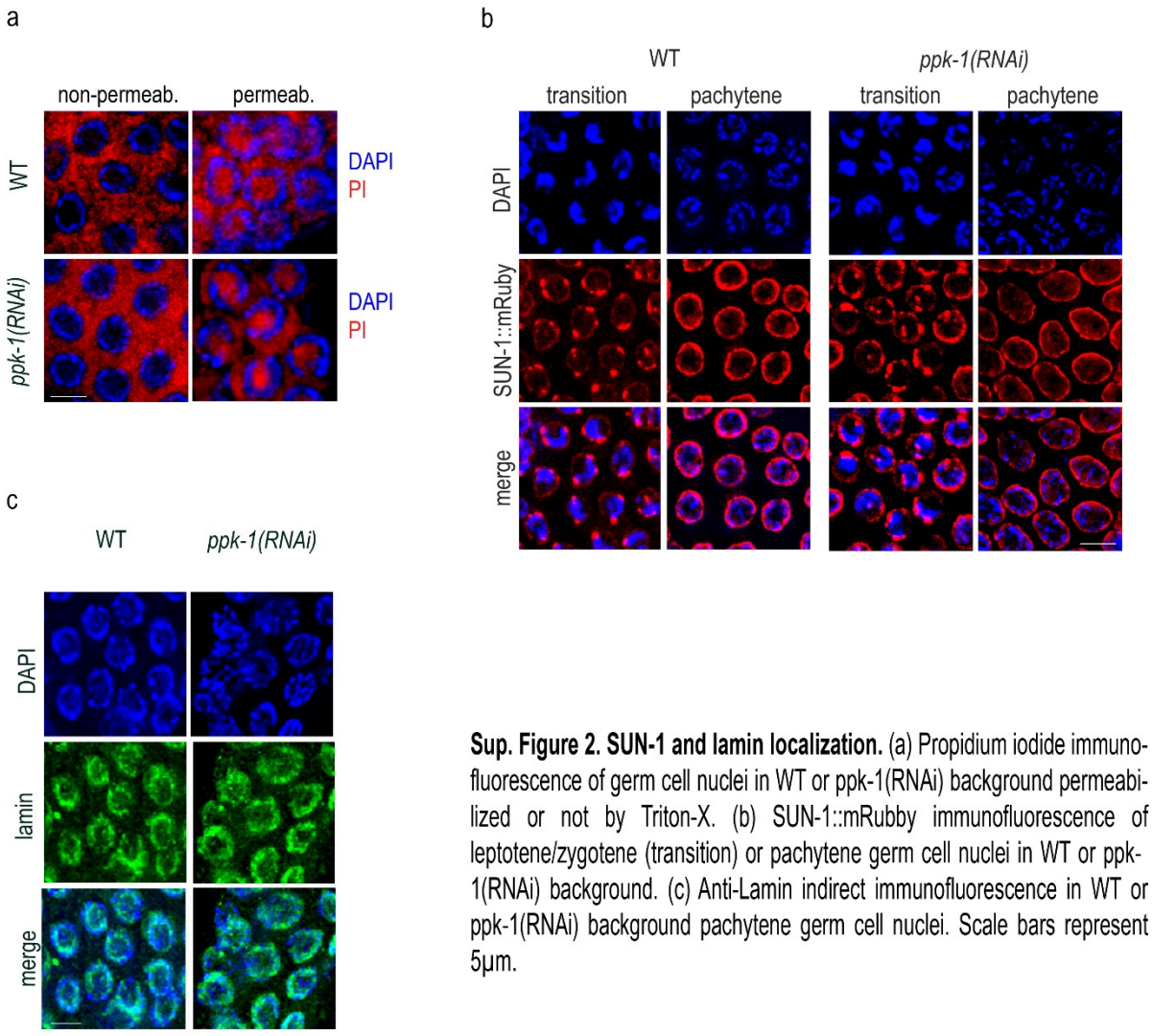

Sup. Figure 2. SUN-1 and lamin localization. (a) Propidium iodide immunofluorescence of germ cell nuclei in WT or ppk-1(RNAi) background permeabilized or not by Triton-X. (b) SUN-1::mRubby immunofluorescence of leptotene/zygotene (transition) or pachytene germ cell nuclei in WT or ppk-1(RNAi) background. (c) Anti-Lamin indirect immunofluorescence in WT or ppk-1(RNAi) background pachytene germ cell nuclei. Scale bars represent 5µm.

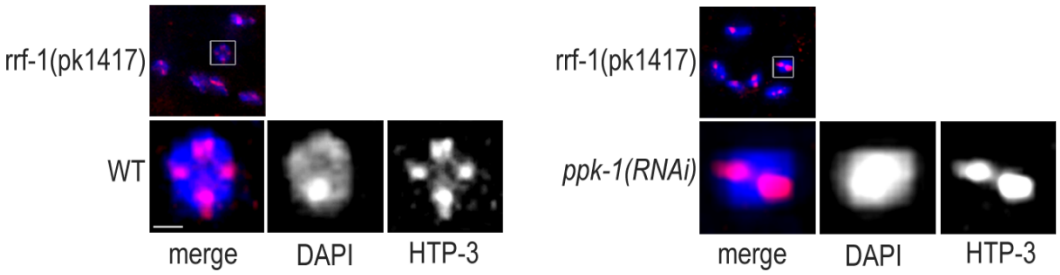

Sup. Figure 3. HTP-3 localization in DAPI stained bodies. Indirect immunofluorescence of anti-HTP-3 in WT or ppk-1(RNAi) background. Scale bar represents 2µm.

3.4 Nuclear actin filaments recruit cofilin and Arp3 and their formation is connected with a mitotic block

Kalendová A, Kalasová I, Yamazaki S, Uličná L, Harata M and Hozák P

Histochem Cell Biol. 2014 Aug;142(2):139-52. doi: 10.1007/s00418-014-1243-9.

IF: 3.054 (2014)

L.U. performed experiments (indirect immunofluorescence)

Histochem Cell Biol (2014) 142:139–152
DOI 10.1007/s00418-014-1243-9

ORIGINAL PAPER

Nuclear actin filaments recruit cofilin and actin-related protein 3, and their formation is connected with a mitotic block

Alžběta Kalendová · Ilona Kalasová · Shota Yamazaki · Lívia Uličná · Masahiko Harata · Pavel Hozák

Accepted: 25 June 2014 / Published online: 8 July 2014

Abstract Although actin monomers polymerize into filaments in the cytoplasm, the form of actin in the nucleus remains elusive. We searched for the form and function of β-actin fused to nuclear localization signal and to enhanced yellow fluorescent protein (EN-actin). Our results reveal that EN-actin is either dispersed in the nucleoplasm (homogenous EN-actin) or forms bundled filaments in the nucleus (EN-actin filaments). Formation of such filaments was not connected with increased EN-actin levels. Among numerous actin-binding proteins tested, only cofilin is recruited to the EN-actin filaments. Overexpression of EN-actin causes increase in the nuclear levels of actin-related protein 3 (Arp3). Although Arp3, a member of actin nucleation complex Arp2/3, is responsible for EN-actin filament nucleation and bundling, the way cofilin affects nuclear EN-actin filaments dynamics is not clear. While cells with homogenous EN-actin maintained unaffected mitosis during which EN-actin re-localizes to the plasma membrane, generation of nuclear EN-actin filaments severely decreases cell proliferation and interferes with mitotic progress. The introduction of EN-actin manifests in two mitotic-inborn defects—formation of binucleic cells and generation of micronuclei—suggesting that cells suffer aberrant cytokinesis and/or impaired chromosomal segregation. In interphase, nuclear EN-actin filaments passed through chromatin region, but do not co-localize with either chromatin remodeling complexes or RNA polymerases I and II. Surprisingly presence of EN-actin filaments was connected with increase in the overall transcription levels in the S-phase by yet unknown mechanism. Taken together, EN-actin can form filaments in the nucleus which affect important cellular processes such as transcription and mitosis.

Keywords Nuclear actin · Transcription · Mitosis · Actin-related protein 3 · Cofilin

A. Kalendová · I. Kalasová · L. Uličná · P. Hozák (✉)
Department of Biology of the Cell Nucleus, Institute of Molecular Genetics of the Academy of Sciences of the Czech Republic, v.v.i., Vídeňská 1083, 142 20 Prague, Czech Republic
e-mail: hozak@img.cas.cz

S. Yamazaki · M. Harata
Laboratory of Molecular Biology, Graduate School of Agricultural Science, Tohoku University, Tsutsumidori-Amamiyamachi 1-1, Aoba-ku, Sendai 981-8555, Japan

Introduction

Actin is a highly abundant intracellular protein essential for maintenance of many cellular functions. It is widely expressed across the species and present in all eukaryotic cell types. In the cytoplasm, actin is present in the form of monomers (globular actin, G-actin), which can polymerize to form filaments (F-actin) that can be specifically visualized by phalloidin. The formation of F-actin is driven by the availability of G-actin subunits—a filament grows when G-actin levels exceed the critical concentration required for polymerization, and a filament shrinks if the critical concentration was not reached. Actin filaments are highly dynamic structures that can assemble or disassemble rapidly based on cell needs.

There are many actin-binding proteins available in the cytoplasm. Depending on their relative binding affinities, they can promote, block or alter the formation of actin filaments. In addition, various actin-binding proteins cross-link actin filaments to form bundles or networks (reviewed in Winder and Ayscough 2005). Such structures are important for the maintenance of cell shape, polarity, mechanical resistance, adhesion and movement.

Actin shuttles between cytoplasm and nucleus employing importin 9 and exportin 6 (Dopie et al. 2012). In the nucleus, actin is present in the form of monomers (Jockusch et al. 2006; Kukalev et al. 2005; McDonald et al. 2006; Obrdlik et al. 2008; Pendleton et al. 2003), yet its ability to form nuclear filaments has been questioned for a long time due to the lack of nuclear phalloidin staining. Eventually, several conditions leading to the formation of nuclear actin polymers have been described. Under various stress conditions (e.g., heat shock, DMSO treatment, virus infection etc.), nuclear actin rods and paracrystals were observed in numerous cell types (reviewed in Hofmann 2009). Moreover, a recent study revealed the presence of actin filaments in nuclei of NIH3T3 cells after overexpression of LifeAct, an F-actin marker, fused to nuclear localization signal (NLS). These filaments were formed after serum induction in a formin-dependent manner (Baarlink et al. 2013). Accumulation and subsequent polymerization of the overexpressed actin in the nucleus was also reported after the disruption of the actin export (Dopie et al. 2012; Stuven et al. 2003). Additionally, Miyamoto et al. (2011) detected actin filaments in nuclei of somatic cells transplanted into oocytes of *Xenopus leavis* using an actin-binding domain of utrophin fused to NLS. Interestingly, the same probe revealed the presence of punctate structures in the nuclei of U2OS cells under physiological conditions which were moreover susceptible to phalloidin staining (Belin et al. 2013). Even though these polymeric structures do not co-localize with any actin-binding proteins, they are found predominantly in the interchromatin space and probably serve as a structural platform that facilitates nuclear organization (Belin et al. 2013).

Even though the state of nuclear actin is not entirely clear, its functional importance has been known for some time. Actin is together with the actin-related proteins required for chromatin remodeling (Ikura et al. 2000; Kapoor et al. 2013; Mizuguchi et al. 2004; Shen et al. 2000; Szerlong et al. 2008; Zhao et al. 1998). Actin also associates with all three RNA polymerases (Hofmann et al. 2004; Hu et al. 2004; Philimonenko et al. 2004) and in cooperation with nuclear myosin 1 (NM1) facilitates transcription initiation and recruitment of chromatin modifying complexes during the elongation phase (reviewed in de Lanerolle and Serebryannyy 2011). Furthermore, actin also participates in RNA processing and export by interacting with heterogenous ribonucleoproteins (hnRNPs; Obrdlik et al. 2008; Percipalle et al. 2002).

From the data available, it seems that the state of nuclear actin engaged in chromatin remodeling complexes and in complex with hnRNPs (Kapoor et al. 2013; Obrdlik et al. 2008; Percipalle et al. 2002) is rather monomeric, whereas in transcription both forms seem to be involved (Miyamoto et al. 2011; Obrdlik and Percipalle 2011; Qi et al. 2011; Wu et al. 2006; Ye et al. 2008; Yoo et al. 2007). Similarly, actin in its polymeric form is essential for the movement of genomic loci throughout the nucleus during transcriptional activation (Dundr et al. 2007; Hu et al. 2008). The presence of polymeric actin in the nucleus is also supported by the findings that various proteins known to bind F-actin in the cytoplasm also localize to the nucleus (reviewed in Castano et al. 2010)) and are implicated in nuclear processes such as transcription (Baarlink et al. 2013; Miyamoto et al. 2011; Obrdlik and Percipalle 2011; Wu et al. 2006; Yoo et al. 2007).

Kokai et al. (2014) have previously reported that ectopically expressed β-actin fused to NLS is imported into the nucleus, where it forms filamentous network. Detailed analysis of the network revealed that distinct actin filaments are branched and cross-linked into parallel bundles. The formation of such structures alters the shape of neuronal-like rat PC12 cells and activates serum response factor (SRF)-mediated transcription. In this study, we employed a similar fusion protein, β-actin fused to enhanced yellow fluorescent protein (EYFP) and to NLS (EN-actin), aiming to explore (1) the formation of EN-actin filaments in the nucleus, (2) contribution of actin-binding proteins to the EN-actin filaments formation and dynamics, (3) association of nuclear EN-actin filaments with complexes where endogenous actin is known to localize, and (4) an effect of the nuclear EN-actin filaments formation on cell cycle and transcription in human osteosarcoma cells (U2OS).

Materials and methods

Cells and transfections

U2OS, H1299, HEK293 and human skin fibroblasts were cultured in D-MEM supplemented with 10 % FBS in 5 % CO2/air, 37 °C and humidified atmosphere. Cells were transfected with Lipofectamine 2000 (Life Technologies) and TurboFect (Thermo Scientific) according to manufacturer's protocol. 2 μg of DNA and 5 μl of Lipofectamine or 3 μl of TurboFect was used to transfect 5×10^5 cells. Cells were incubated for 6 to 12 h with a transfection mix and additional 36 h before fixation and imaging. Linear polyethylenimine (PEI), 25 kDa, was purchased from Polysciences. 1 mg/ml stock solution was prepared and pH adjusted to 7. 9 μl of this solution was mixed with 1.5 μg DNA in serum-free media and incubated for 15 min at room temperature. 5×10^5 cells were incubated with transfection mix for 4 h and then grown for 48 h before imaging.

5 μg of exogenous DNA was delivered into 5×10^5 primary mouse skin fibroblasts by nucleofection using Amaxa nucleofector (Lonza), programme C005. Cells were seeded onto coverslips and imaged 48 h after nucleofection.

Constructs used in this study

EN-actin was generated as described previously (Hofmann et al. 2009). Shortly, NLS was inserted between the EYFP and actin into the plasmid pEYFP-actin (Clontech). cDNA of mouse NM1 was cloned into pCDNA3.1-mCherry using NheI and HindIII by standard methods of molecular biology.

Indirect immunofluorescence and confocal fluorescence microscopy

U2OS cells seeded on glass coverslips were fixed with 4 % paraformaldehyde in PBS for 20 min and permeabilized with 0.1 % Triton X-100 in PBS for 10 min afterward. Non-specific labeling was further blocked with 5 % BSA in PBS for 30 min. After washes with PBS, coverslips were incubated with the respective primary antibodies diluted in PBS for 1 h at RT in a wet chamber and washed with PBST (PBS supplemented with 0.05 % Tween 20). Subsequently, coverslips were incubated with corresponding secondary antibodies for 1 h at RT in a wet chamber. After final washes in PBST, coverslips were mounted in ProLong Gold anti-fade reagent with DAPI. For detection of emerin, cells were fixed with ice-cold methanol for 5 min without additional permeabilization. Images were acquired using confocal microscope Leica TCS SP5 AOBS TANDEM with 63× (NA 1.4) immersion oil objective lens with 405, 512, 561 and 631 laser excitations, and LAS AF software.

Antibodies

Following primary antibodies were used in this study: lamin B (Santa Cruz cat. no. sc-6217); filamin (Santa Cruz cat. no. sc-28284); alpha-actinin-4 (Abcam cat. no. ab96866); spectrin (Sigma Aldrich cat. no. S1390); paxillin (Millipore cat. no. 05-471); vinculin (Sigma Aldrich cat. no. V4505); mDia1 (BD Biosciences cat. no. P66520-050); SUN2 (Abcam cat. no. ab124916); emerin (Abcam cat. no. ab40688); Arp3 (Welch et al. 1997); cofilin (Abcam cat. no. ab11062); P-cofilin (Cell Signaling cat. no. 3313); Arp6 (Sigma Aldrich cat. no. R35554); Arp5 (Kitayama et al. 2009); Arp8 (Aoyama et al. 2008); Brg1 (Abcam cat. no. ab70558); hnRNP U (Santa Cruz, clone 3G6); H3K9Me2 (Millipore cat. no. 17-648); H3K4Me2 (Millipore cat. no. 07-030); CTD-phosphoS2 (Abcam cat. no. ab24758); RPA194 (Santa Cruz, cat. no. sc-28714); and BrdU (Sigma Aldrich, clone BU-33).

Secondary antibodies used in this study are donkey anti-rabbit IgG conjugated with Alexa Fluor 568 (A10042), goat anti-mouse IgG conjugated with Alexa Fluor 647 (A21236) and donkey anti-goat IgG cojugated with Alexa Fluor 647 (A21447) all purchased from Life Sciences.

5-Fluorouridine, 5-ethynyl-2′-deoxyuridine incorporation and EN-actin fluorescence measurements

U2OS cells grown on coverslips were transfected with EN-actin using Lipofectamine as described above. 48 h after the transfection, cells were incubated for 30 min or 1 h at 37 °C, 5 % CO_2/air with 2 mM 5-fluorouridine (FU) or 5-ethynyl-2′-deoxyuridine (EdU), respectively. After this time period, cells were washed, fixed and permeabilized as mentioned above. FU incorporated into nascent transcripts was detected using anti-BrdU antibody as described above. EdU was directly labeled in a click reaction using ClickiT EdU Alexa Fluor 647 Flow Cytometry Assay kit (Life Technologies). Images were acquired as four 200-nm optical stacks of a total thickness of 2 μm using the above mentioned fluorescence confocal microscope. Total intensity of FU/EdU fluorescence in the nucleus was integrated from 3D reconstruction (maximal projection) of all four optical stacks in LAS AF, background subtracted and normalized to the nuclear area. The measurement was repeated three times, and fluorescence intensities of the cells expressing EN-actin were in each replicate normalized to the controls to prevent variations caused by antibodies dilutions, etc. Results are presented as a mean of three experiments ± standard deviation (SD) and were plotted using Prism GraphPad. *T* test was used to determine the statistical significance. Each cell imaged was manually classified according to the EN-actin expression pattern as G-actin (homogenous signal), F-actin (nuclear filaments) or control (no expression of EN-actin). Fluorescence of EN-actin was quantified in the same way.

Results

EN-actin forms filaments in the nucleus

We studied the behavior of exogenous β-actin in the nucleus. In order to achieve its nuclear localization, we fused β-actin with NLS and EYFP (EN-actin). It has been observed previously that the overexpression of NLS-β-actin leads to the formation of filamentous structures inside of the nucleus in various cell lines (Kokai et al. 2014). When we overexpressed EN-actin in human osteosarcoma cell line (U2OS), majority of cells (95 to 99 %) exhibited homogenously dispersed nuclear signal, apparently corresponding to the free G-actin or short actin polymers (Fig. 1a). However, in 1–5 % of cells, EN-actin assembled into filamentous structures which stretched through the whole nuclear volume with the exception of nucleoli (Fig. 1b, c). The EN-actin filaments adopt various shapes from straight long (Fig. 8h) to curved (Fig. 1b), or they form a dense meshwork (Fig. 1c). These nuclear actin filaments are phalloidin-positive structures (Fig. 2a) which in some cases run at the nuclear periphery

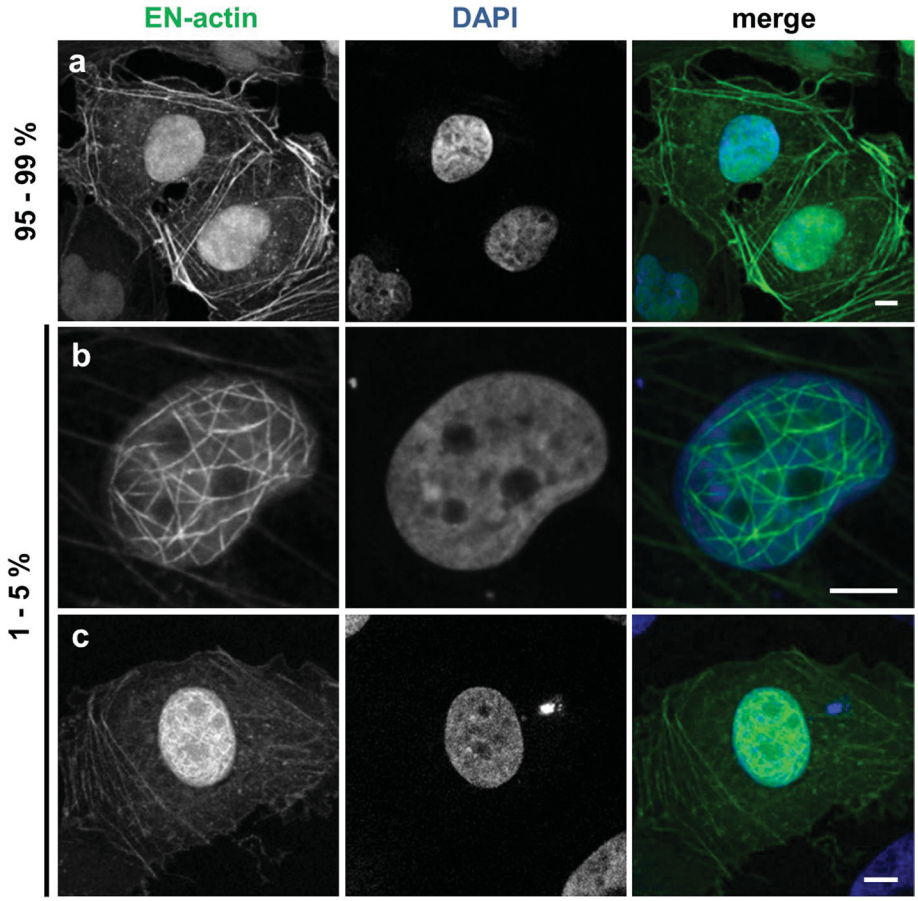

Fig. 1 Overexpressed EN-actin forms filaments in the nucleus of U2OS cells. In vast majority of cells (95–99 %), EN-actin was imported into the nucleus, where it was homogenously dispersed throughout the nucleoplasm (**a**). Minority of cells (1–5 %) displayed EN-actin assembled into thick nuclear filaments (**b**). At the same time, EN-actin was also incorporated into cytoplasmic filaments (**a**, **c**). Single focal plane in the equatorial position (**b**) and 3D reconstructions of the entire cells (**a**, **c**) are shown. *Scale bars* 5 μm

along the nuclear lamina (Fig. 2b, white arrows), occasionally even reaching the nuclear lamina (Fig. 2c, d). The thickness of and the length of the filaments range from 50 to 100 nm and 1 to 15 μm, respectively, which corresponds to actin bundles rather than single filaments, as has been concluded previously (Kokai et al. 2014).

In parallel to its nuclear localization, EN-actin was also incorporated into canonical cytoplasmic filaments in both cells with homogenous nuclear pattern (Fig. 1a), as well as in the cells that contained nuclear EN-actin filaments (Fig. 1c). This suggests that the presence of cytoplasmic EN-actin filaments does not restrict nuclear EN-actin filaments formation, and vice versa.

Since nuclear EN-actin filaments are present only in a small fraction of cells, this raises the question which stimulus triggers their formation. One could predict that when the critical concentration of actin monomers inside a compartment is reached, the polymerization process starts. To find out whether there is a difference in the amount of EN-actin in the nucleus between the cells forming filaments and those having homogenous dispersion of EN-actin, we measured the total fluorescence intensity of EN-actin in the nuclei of those cells. Because there is a variability in size of the nuclei among the cells, we normalized total fluorescence intensity to the nuclear area after background subtraction. We found that there is no significant difference in normalized fluorescence intensity between nuclei with homogenously dispersed EN-actin (G-actin) and filaments-forming nuclei (F-actin; Fig. 2e).

In addition, we tested the impact of transfection method on the filament formation. For this purpose, we used Lipofectamine 2000 (Life Technologies), TurboFect (Thermo Scientific) and linear polyethylenimine (Polysciences) according to the manufacturers' protocols (see Materials and methods). Even though the efficiencies of the transfections varied, the percentage of transfected cells containing nuclear actin filaments did not change significantly (data not shown).

Taken together, after overexpression of EN-actin, 1–5 % of cells contain nuclear EN-actin filaments assembled into bundles. Formation of these filaments is dependent neither on the intranuclear concentration of EN-actin nor on the transfection method.

Formation of nuclear EN-actin filaments varies among cell types

We analyzed the formation of nuclear EN-actin filaments in various cell types. The pattern of overexpressed EN-actin

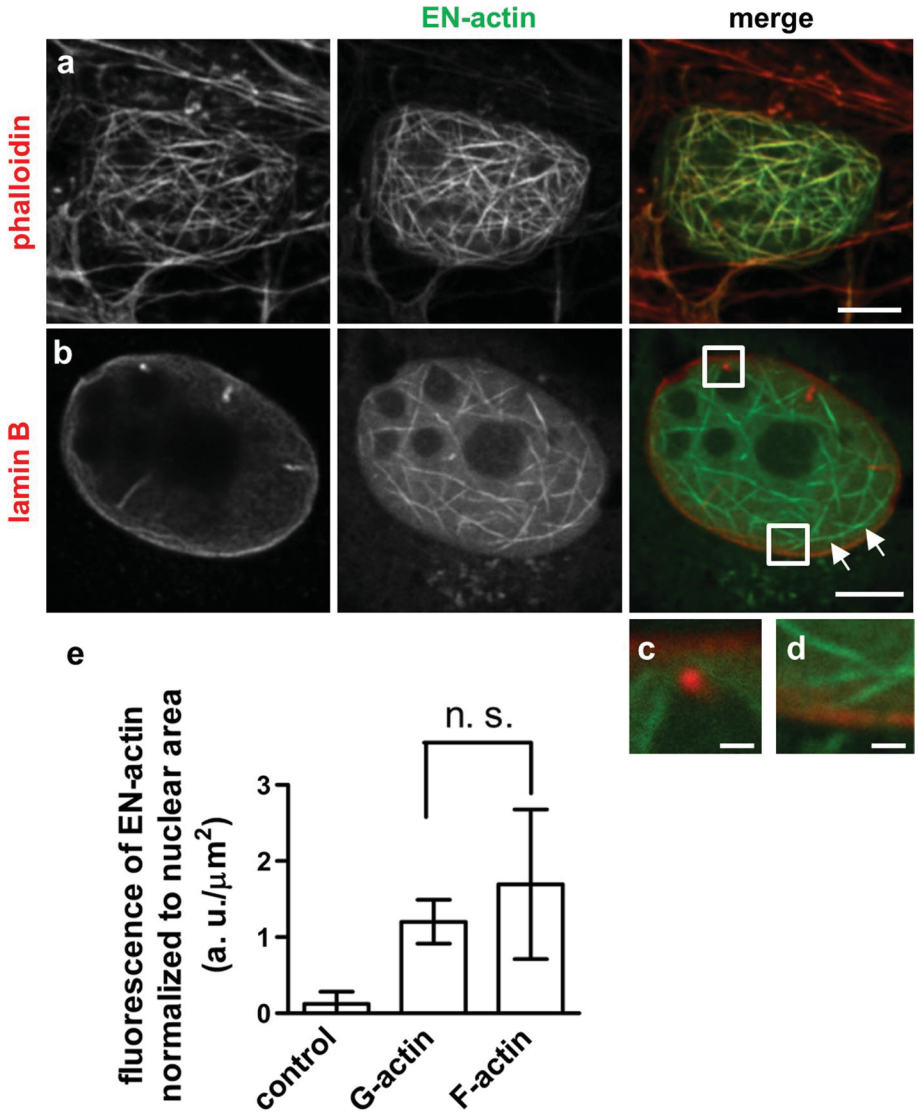

Fig. 2 Properties of nuclear EN-actin filaments formed in U2OS cells. Nuclear EN-actin filaments are susceptible to phalloidin staining (**a**), run along the nuclear lamina (**b** *white arrows*) and occasionally join the nuclear lamina (**c**–**d**). No significant difference in the total nuclear fluorescence intensity of EN-actin normalized to the nuclear area was found between the cells forming EN-actin filaments (F-actin; **e**) and cells containing homogenously dispersed EN-actin (G-actin; **e**). As a control, cells having no expression of EN-actin but present within the same coverslip were used. Results are presented as mean ± SD of three independent experiments, whiskers indicate minimal and maximal values. In total, 30 cells for F-actin, 69 cells for G-actin and 130 control cells were analyzed (**e**). *Scale bars* 5 μm (**a**–**e**), 1.25 μm (**f**–**g**), *n. s. p*>0.05

was inspected in immortalized human embryonic kidney cell line (HEK293), human cervical carcinoma cell line (HeLa), human non-small cell lung carcinoma cell line (H1299) and primary mouse skin fibroblasts. Formation of nuclear actin filaments was noticed in all immortalized human cell lines (HEK293, HeLa, H1299; Fig. 3c–e); however, no nuclear filaments were found in primary mouse fibroblasts (Fig. 3a, b). In mouse fibroblasts, EN-actin was preferentially incorporated into cytoplasmic fibers (Fig. 3a, optical section focused to the cytoplasmic fibers), while only a small portion was imported into the nucleus, where it stayed homogenously dispersed in the monomeric form (Fig. 3b, the same cell—optical section in the equatorial position).

However, we noticed some differences between the immortalized cell lines. HEK293 cells (Fig. 3e) formed nuclear actin filaments more readily than U20S cells, reaching up to 10–20 % of cells with filaments. On the other hand, the proportion of H1299 cells forming nuclear actin filaments was only around 0.5 % (Fig. 3d). Even though we found nuclear EN-actin filaments in some H1299 cells, EN-actin was not imported into the nucleus efficiently; it rather stayed in the cytoplasmic filaments in majority of cells (not shown).

Altogether, we conclude that the ability to translocate EN-actin into the nucleus and form nuclear EN-actin filaments is cell-type specific and reflects diverse nuclear environment and/or nucleocytoplasmic transport properties.

Cells with nuclear EN-actin filaments undergo a mitotic block

In order to investigate the behavior of nuclear EN-actin during cell cycle, we observed localization of homogenously dispersed EN-actin and EN-actin incorporated into the filaments at various stages of mitosis by light

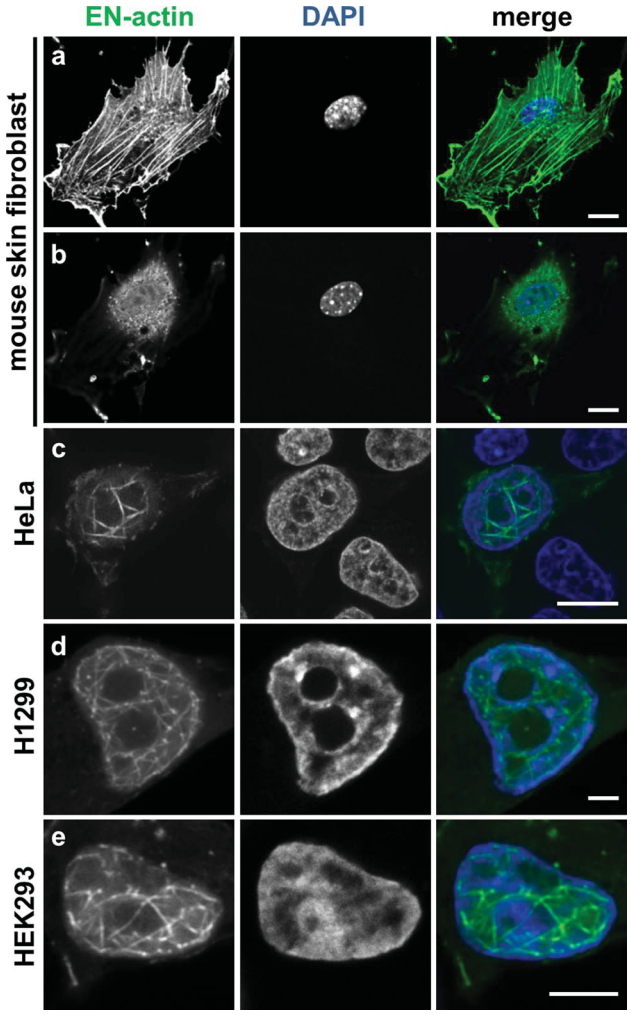

Fig. 3 Formation of nuclear EN-actin filaments varies among cell types. In primary mouse skin fibroblasts, EN-actin (delivered by nucleofection) incorporates preferentially into cytoplasmic fibers (**a** optical section focused on the cytoplasmic fibers) and does not form filaments in the nucleus (**b** optical section of the same cell in the equatorial position). EN-actin, delivered by transfection, assembled into filaments in the nuclei of Hela (**c**), H1299 (**d**) and HEK293 (**e**) cells. *Scale bars* 10 μm (**a**–**c**), 5 μm (**d**–**e**)

microscopy (Fig. 4a–f). We revealed that homogenously dispersed EN-actin is at the onset of mitosis exported from the nucleus (Fig. 4b). In later phases of mitosis, EN-actin is not associated with chromosomes; it is enriched at the plasma membrane and in plasma membrane protrusions instead (Fig. 4c–e). EN-actin is imported into the nucleus after the re-assembly of the nuclear envelope during cytokinesis (Fig. 4f).

Interestingly, when we monitored cells by a long-term live-cell observations, we did not observe any cells containing EN-actin filaments to progress through mitosis. At the same time, other cells in the field of view which contained cytoplasmic EN-actin filaments or homogenous nuclear EN-actin divided normally (data not shown). This suggests a block in mitosis caused by the presence of EN-actin filaments in the nucleus. Indeed, when we measured proliferation rate by EdU incorporation, 53 % of the control or homogenous nuclear EN-actin containing cells incorporated EdU (Fig. 5c, control and G-actin, respectively). After the formation of nuclear EN-actin filaments, the EdU incorporation decreased by a half, to 24 % (Fig. 5c, F-actin). We furthermore noticed that many cells carrying nuclear actin filaments exhibited two types of morphological abnormalities: in the first case, additional micronuclei was formed. This micronuclei contained DAPI-stainable chromatin and also a homogenous or filamentous EN-actin (Fig. 5a). Second, some cells did not complete cytokinesis resulting in retention of both daughter nuclei within one cell (Fig. 5b). Of the binucleic cells, 90 % contained nuclear EN-actin filaments in both nuclei, while only 10 % of cells had homogenous EN-actin. The other way around, of all the nuclear EN-actin filament-containing cells, 10 % were binucleic, while only 1 % of cells with homogenous nuclear EN-actin were binucleic. In the binucleic cells, both nuclei always contained the same pattern of EN-actin—either filamentous or homogenous.

Based on the results, we propose that the presence of the EN-actin filaments in the cell nucleus may disturb progress into mitotic phase of a cell cycle. In case the cell still undergoes mitosis, irregularities in structure of daughter cells or aberrant cytokinesis appear as a consequence.

Cofilin co-localizes with nuclear EN-actin filaments, and Arp3 is enriched in cells with EN-actin

The initial experiment (Fig. 2e) showed that the concentration of EN-actin is not the only factor which triggers assembly of nuclear EN-actin filaments. To see whether actin-binding proteins participate in the regulation of EN-actin filaments formation in the nucleus, we observed their localization in respect of the nuclear EN-actin filaments by confocal light microscopy (Fig. 6). We considered particular protein as co-localizing when it was accumulated or enriched at the EN-actin filaments or in their close vicinity.

As we have established that EN-actin does not form individual filaments but bundles instead, we explored the localization of F-actin cross-linking proteins filamin, α-actinin and spectrin (Fig. 6a–c) which are known to localize to the nucleus (Bedolla et al. 2009; Dingova et al. 2009). None of these actin cross-linkers, however, showed preferential co-localization with nuclear EN-actin filaments; therefore, it remains unclear by which mechanism nuclear EN-actin filaments become bundled.

Next, we explored the localization of the F-actin-binding proteins paxillin and vinculin (Fig. 6d, e). These two proteins typically associate with focal adhesions, where

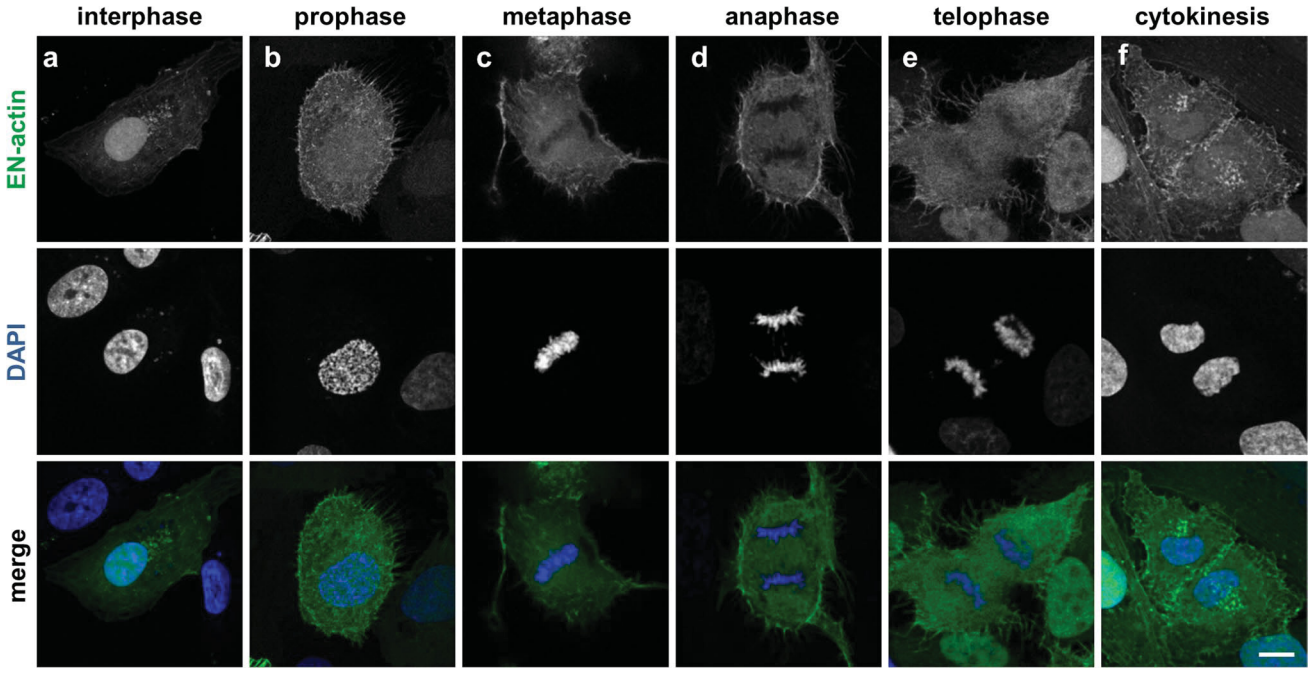

Fig. 4 EN-actin is enriched at the plasma membrane during mitosis. Localization of overexpressed EN-actin was observed at various stages of mitosis in U2OS cells (**a**–**f**). At the onset of mitosis, EN-actin is exported from the nucleus to the plasma membrane (**b**–**e**). When the nuclear envelope re-assembles, EN-actin is imported back into the nucleus (**f**). Maximal projections of five optical sections are shown. *Scale bars* 10 μm

vinculin mediates the association between integrin and F-actin and binds also paxillin (Turner et al. 1990). Despite the fact that both vinculin and paxillin were previously reported to localize in the nucleus (Dingova et al. 2009; Dong et al. 2009; Kano et al. 1996), we detected only a negligible amount of nuclear paxillin. Yet, neither of them co-localized with the nuclear filaments formed after the overexpression of EN-actin (Fig. 6d, e). Therefore, we speculate that nuclear-specific isoforms of actin-bundling proteins assist in cross-linking of EN-actin filaments.

In a recent study, Baarlink et al. (2013) showed that formation of the actin filaments in the nucleus is dependent on the presence of nuclear formins. Since we observed neither co-localization of formin mDia1 with the EN-actin filaments nor any change in pattern of mDia upon EN-actin filaments formation (Fig. 6f), we concluded that mDia1 does not assist in EN-actin polymerization.

Our results show that nuclear EN-actin filaments join nuclear lamina occasionally (Fig. 2b–d). Therefore, we also tested their association with two other nuclear envelope-associated proteins—SUN2, a member of linker of nucleoskeleton and cytoskeleton complex (LINC; Fig. 6g); and emerin, an inner nuclear membrane protein, which binds lamin A/C (Fig. 7a, b). Of these proteins, nuclear EN-actin filaments join in some cases emerin (Fig. 7a, b) in a similar manner as lamin B (Fig. 2b–d).

Next, we investigated the localization of proteins which affect F-actin assembly. First of them, cofilin binds to the pointed end of F-actin filaments and causes their disassembly. Surprisingly, cofilin co-localized with the nuclear EN-actin filaments (Fig. 7c, arrowheads) not only at the ends, but along the entire length of the filament (Fig. 7d, arrowheads). On the contrary, phosphorylated form of cofilin (P-cofilin), which becomes incapable of F-actin binding, did not co-localize with EN-actin filaments (Fig. 7e), even though it was present in the nucleus.

Since the previous study suggested that NLS-actin filaments are branched (Kokai et al. 2014), we explored also localization of branching proteins which area able to bind to the existing filaments in order to trigger nucleation and growth of new branches of the actin filaments. We found that levels of Arp3, a member of Arp2/3 nucleation complex (Pantaloni et al. 2000), are increased upon expression of EN-actin (Fig. 7f, g). It is therefore plausible that Arp3 re-localizes to the nucleus after elevation of EN-actin to assist in the growth of new filaments.

Among the actin-binding proteins analyzed, only Arp3 and cofilin seem to be in relation with the nuclear EN-actin filaments. Such limited co-localization indicates that assembly and bundling of nuclear EN-filaments are controlled by nuclear-specific regulators or nuclear-specific isoforms of actin-associated proteins.

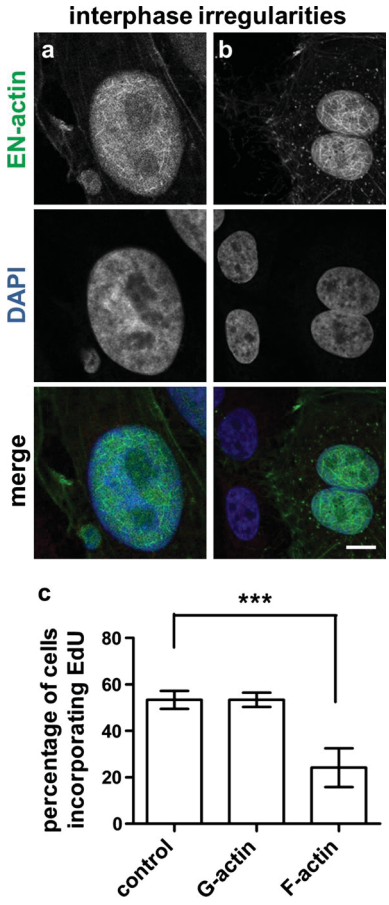

Fig. 5 Cells with EN-actin filaments exhibit irregularities in the interphase. U2OS cells with EN-actin filaments exhibit two phenomena originated in mitosis—presence of DAPI-stainable micronuclei (**a**) and retention of both daughter nuclei within a single cell (**b**). Cell proliferation was measured by EdU incorporation. After labeling, fluorescence of EdU was measured and percentage of EdU-positive cells is shown for cells containing EN-actin filaments (F-actin, **c**), homogenous EN-actin (G-actin, **c**) and control. Results are presented as mean ± SD of three independent experiments. More than 50 cells were analyzed in each experiment (**c**). *Scale bars* 10 μm, ***$p < 0.001$

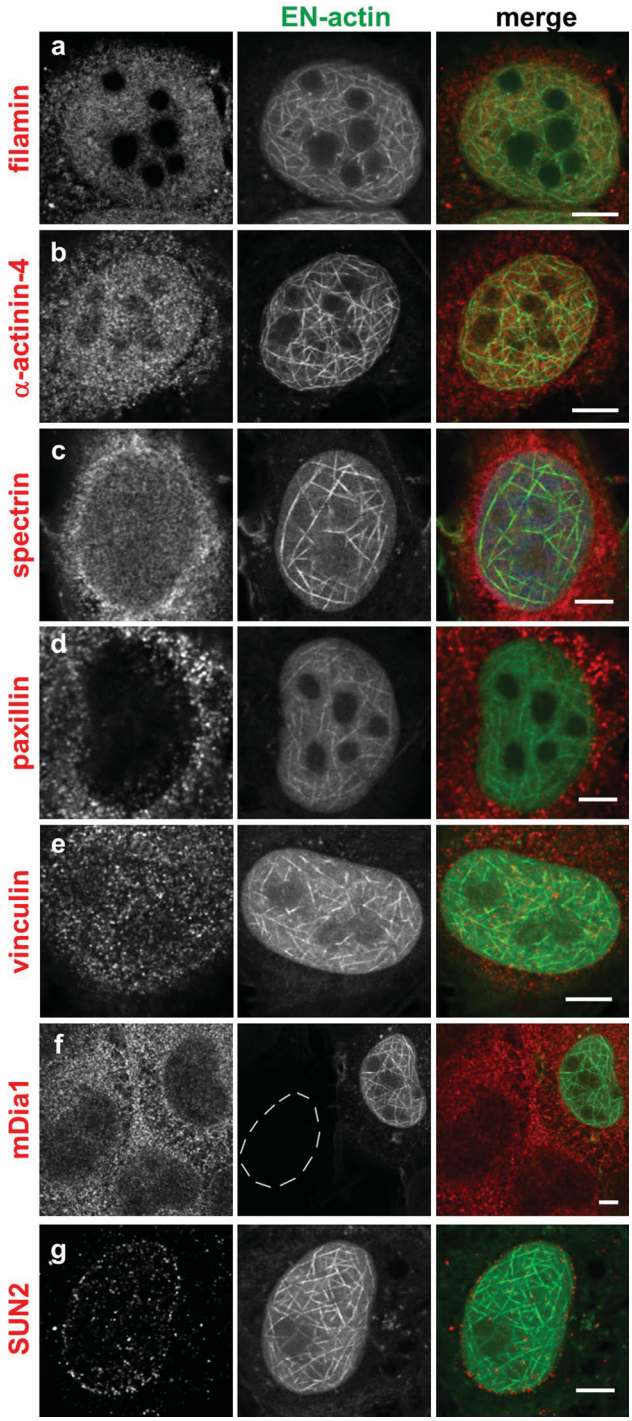

Fig. 6 Nuclear EN-actin filaments do not co-localize with the actin-binding proteins tested. Co-localization of the nuclear EN-actin filaments with various actin-binding proteins was tested by indirect immunofluorescence microscopy in the U2OS cells (**a**–**g**). A protein was considered as co-localizing when it predominantly accumulated at the nuclear EN-filaments or was enriched in their close vicinity. Nucleus of cell with no EN-actin expression is labelled by a *dashed line*. *Scale bars* 5 μm

Nuclear EN-actin filaments formation enhances transcription in the S-phase

It is known that actin is found in chromatin remodeling complexes (Szerlong et al. 2008; Zhao et al. 1998). To test the functional involvement of the EN-actin filaments in chromatin remodeling, we performed co-localization studies with protein hallmarks of chromatin remodeling using confocal microscopy. However, no significant co-localization was observed with the actin-related proteins (Arp5, Arp8 and Arp6), brahma-related gene 1 (Brg1) or hnRNP U (Fig. 8a–e).

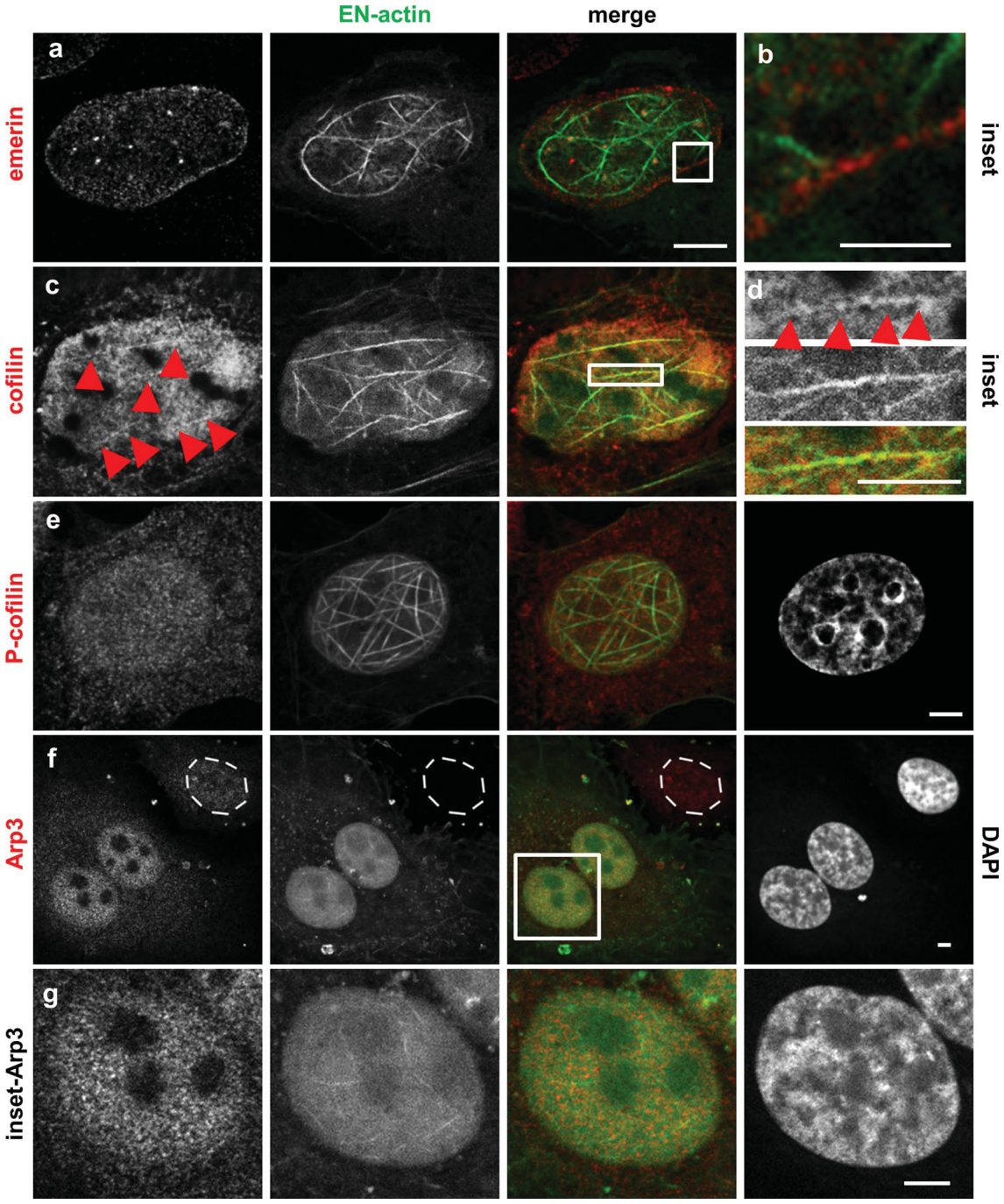

Fig. 7 Nuclear EN-actin filaments recruit Arp3 and cofilin. Co-localization of the nuclear EN-actin filaments with various actin-binding proteins was tested by indirect immunofluorescence microscopy in the U2OS cells (**a**–**g**). EN-actin filaments occasionally come into contact with emerin (**a** and **b** *inset*). EN-actin filaments co-localize with cofilin in the nucleus (**c** and **d**, *arrowheads*). *Inset* of the EN-actin filaments (**d**). EN-actin filaments do not co-localize with P-cofilin (**e**), but recruit Arp3 into the nucleus (**f**). Nucleus of cell with no expression of EN-actin is labeled by dashed line (**f**). *Inset* of the cell with increased Arp3 levels and EN-actin filaments (**g**). *Scale bars* 2.5 μm

Numerous studies have repeatedly emphasized the importance of actin in transcription (Hofmann et al. 2004; Hu et al. 2004; Philimonenko et al. 2004). NM1 is a transcription factor, which exerts its function in cooperation with actin (Ye et al. 2008). Even though one would expect NM1, which requires oligo- or polymeric actin for its function, to be predominantly found on the EN-actin filaments, it is not the case (Fig. 8f). Overexpressed NM1-mCherry is in the nucleoplasm present in the vicinity of the EN-actin filaments, but no evidence points toward their association.

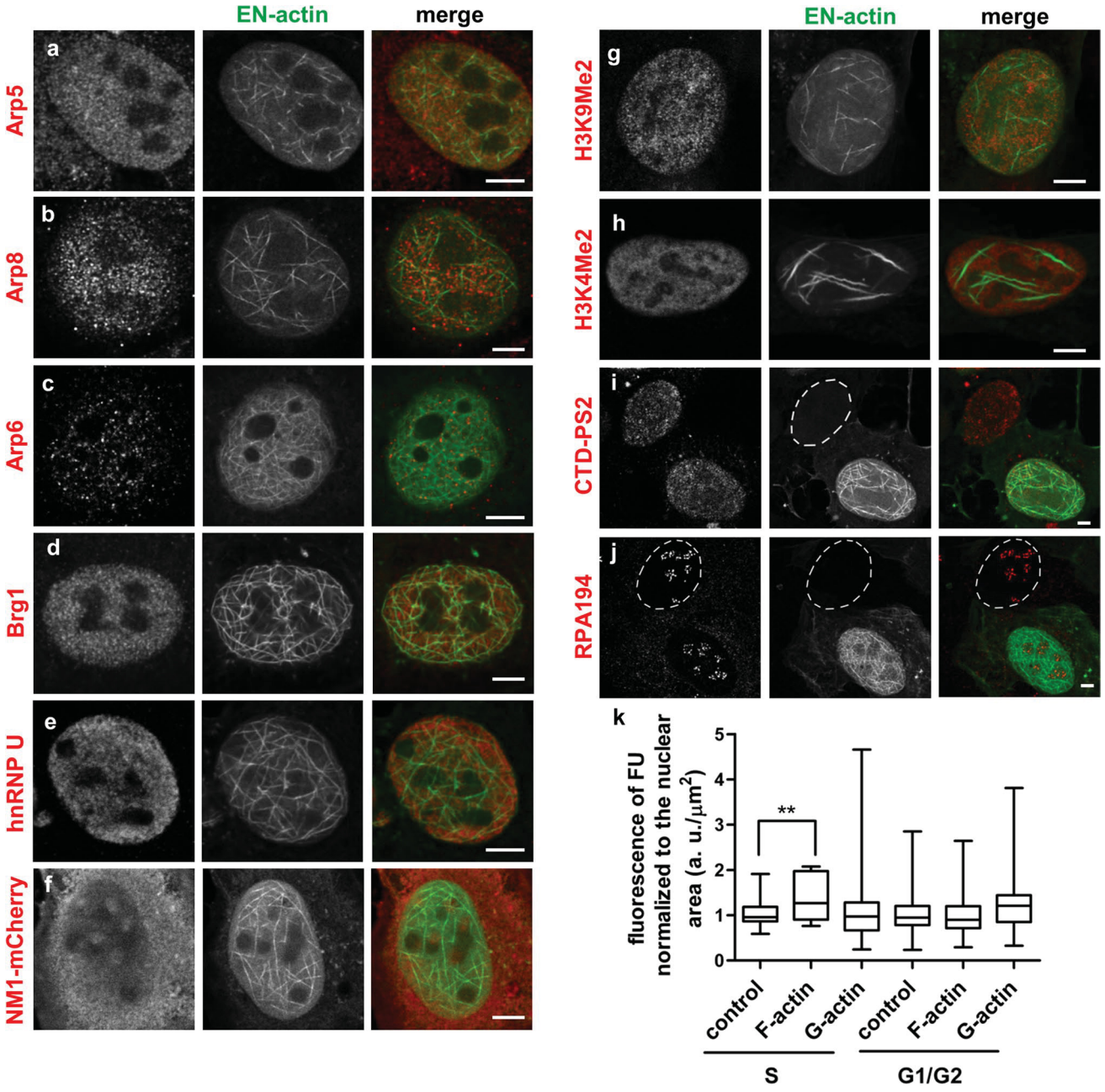

Fig. 8 Nuclear EN-actin filaments enhance DNA transcription. Co-localization of overexpressed nuclear EN-actin and hallmarks of various nuclear functional complexes was observed in U2OS cells by indirect immunofluorescence microscopy. A protein was considered as co-localizing when it predominantly accumulated at the nuclear EN-filaments or was enriched in their close vicinity. Nuclear EN-actin filaments do not co-localize with components of chromatin remodeling complexes (**a**–**f**), but passed through both transcriptionally inactive (**g**) and active chromatin (**h**). Formation of EN-actin filaments does not affect either localization of C-terminal domain of RNA polymerase II phosporylated on serine 2 (CTD-PS2, **i**) or the catalytic subunit of RNA polymerase I (RPA194, **j**). Generation of nuclear EN-actin filaments causes increase in the overall transcription levels in the S-phase (**k**). In this experiment, transcription levels of cells containing EN-actin filaments (**k** F-actin) were compared to cells with homogenous EN-actin (**k** G-actin) and to cells with no expression of EN-actin, which resided within the same coverslips (**k** control). Nascent transcripts were labeled by FU in the U2OS cells and their amounts were then quantified by indirect immunofluorescence using anti-BrdU antibody. Total fluorescence intensity in the nucleus was normalized to the nuclear area. The experiment was repeated three times and the values in each replicate were further normalized to the control. Normalized mean values ± SD of three independent experiments are shown in the graph where whiskers represent the minimum and maximum values. More than 20 cells were analyzed in each experiment. S and G1/G2 phases of the cell cycle were analyzed separately. No significant changes ($p < 0.05$) were observed unless indicated by *asterisks*. **$p = 0.01$-0.001. *Scale bars* 5 μm

We then proceeded with the study of participation of EN-actin in transcription and observed its occurrence in transcriptionally inactive and active chromatin regions, marked by H3K9Me2 and H3K4Me2 histone modification, respectively. Nuclear EN-actin filaments did not show any preferential enrichment in either type of chromatin, neither did homogenously dispersed EN-actin (Fig. 8g, h). On the other hand, EN-actin filaments did not avoid either type of chromatin; they passed through both chromatin regions instead. Therefore, we asked whether EN-actin filaments or free EN-actin do indeed affect transcription as has been previously published (Miyamoto et al. 2011; Wu et al. 2006; Ye et al. 2008). To answer this question, we explored the presence of the catalytic subunit of RNA polymerase I (RPA194) as well as the active form of RNA polymerase II phosphorylated on serine 2 (CTD-PS2), as these would indicate active transcription. Both CTD-PS2 and RPA194 were present in the cells containing nuclear EN-actin filaments (Fig. 8i, j), and no obvious changes in their localization were noticed in comparison with non-transfected cells. In order to assess the impact of homogenous and filamentous EN-actin on transcription, we compared transcription levels of those cells with cells having no overexpression of actin (control). As it is known that transcription is inactivated during mitosis, gradually activated during G1 and its levels are maximal in S and G2 phases (Klein and Grummt 1999; Oelgeschlager 2002; White et al. 1995), we measured the transcription levels in different stages of the cell cycle based on the proliferating cell-nuclear antigen (PCNA) pattern. Nascent transcripts were labeled with fluorouridine (FU) in vivo, which was then detected by indirect immunofluorescence microscopy. Total fluorescence intensity of FU in the nucleus was quantified and normalized to the nuclear area. Transcription levels of cells expressing either homogenous EN-actin (Fig. 8k, G-actin) or EN-actin filaments (Fig. 8k, F-actin) did not significantly differ from the control (Fig. 8k, control) cells in the G1 and G2 phases of the cell cycle. However, we detected changes in transcription in the S-phase when cells forming nuclear EN-actin filaments significantly increased their transcription levels by 30 % (Fig. 8k) in comparison with control cells. On the other hand, S-phase transcription of cells having homogenous nuclear EN-actin did not significantly differ either from control cells or from the cells with EN-actin filaments.

In conclusion, nuclear EN-actin filaments do not participate in chromatin remodeling, do not preferentially associate with transcriptionally active or inactive chromatin, but their presence causes increase in general transcription levels in the S-phase in comparison with control cells.

Discussion

The fundamental ability of actin is to form polymers. Although polymeric structures are long known to exist in the cytoplasm, their presence and form in the nucleus remains unclear.

We showed that the overexpression of EN-actin triggers formation of bundled filaments in the nucleus bearing various shapes from straight long (Figs. 7e, 8h) to curved (Fig. 7a) and dense meshwork (Figs. 1c, 6e). This observation is in agreement with a previous work by Kokai et al. (2014), which moreover proposed that some of the filaments are even branched. Even though we did not study this feature in greater detail, we support the notion that some of the filaments are indeed branched, not only crossing each other (Fig. 2b–c).

In U2OS cells, EN-actin localizes not only to the nucleus, but is also incorporated into cytoplasmic filaments (Fig. 1a and c). The incorporation of EN-actin into the cytoplasmic fibers affected neither formation of EN-actin nuclear filaments nor its nuclear translocation, which was indeed favored (Fig. 1c). The distribution of EN-actin within a cell seems to be cell-type specific, because cytoplasmic retention was not observed in rat PC12 cells (Kokai et al. 2014), whereas in primary mouse skin fibroblasts (Fig. 3a, b) EN-actin resided preferentially in the cytoplasm and did not form nuclear filaments. At the same time, EN-actin was readily imported into the nucleus of HEK293 cells (Fig. 3e). This may reflect differential requirements of actin in the nuclear processes in various cell types.

The formation of nuclear filaments after expression of exogenous EN-actin is relatively rare in U2OS cells, since only 1–5 % of cells show such phenomenon. Such a low incidence of EN-actin filament formation suggests that specific conditions are required to trigger polymerization. It is known that actin begins to polymerize when the critical concentration of free actin monomers is achieved. However, we did not observe such concentration dependency, since the expression levels of EN-actin normalized to nuclear area did not differ significantly in cells with homogenous EN-actin versus cells containing EN-actin filaments (Fig. 2e). This indicates that the amount of actin in the nucleus is not the only factor determining the filament formation, but seems to be a prerequisite. In agreement, blocking the actin export has been reported to cause actin polymerization inside of the nucleus (Dopie et al. 2012; Stuven et al. 2003).

While we observed that cells containing homogenous EN-actin progressed through mitosis (Fig. 4), during which EN-actin mimicked localization of the endogenous actin (Yang et al. 2004), the presence of nuclear EN-actin filaments decreased cell proliferation rate by a half (Fig. 5c). Moreover, we observed two abnormalities in the interphase

cells which seem to originate in mitosis—formation of additional micronuclei or retention of both daughter nuclei within one cell (Fig. 5a, b). These two irregularities were previously observed by Moulding et al. (2007) as a consequence of increase in cytoplasmic F-actin assembly, which caused its mislocalization and led to delay in mitosis and defects in cytokinesis. Besides, both micronuclei formation and bridging the two daughter nuclei together are also results of improper chromosome segregation, which is caused by aberrant centromeric incidence (reviewed in Fenech et al. 2011). Because F-actin is as well required for the anchoring of mitotic spindle to the cell cortex and moreover to establish the direction of spindle movement (Woolner and Bement 2009), it is plausible that the excessive amount of overexpressed EN-actin (which may form filaments during mitosis) prevents correct spindle positioning and manifests in chromosome segregation errors. Since 90 % of the binucleic cells contained nuclear EN-actin filaments, whereas only 10 % of the cells contained homogenous nuclear EN-actin, we speculate that the effect is reinforced with increasing filamentous EN-actin levels. In conclusion, multiple aspects seem to contribute to the defects in mitosis; however, the severity is related to the amount of EN-actin which is available for polymerization into nuclear filaments.

It has been shown that the increase in cofilin expression causes arrest in G1 phase of a cell cycle by a mechanism which involves cyclin-dependent kinase inhibitor $p27^{Kip1}$ (Tsai et al. 2009). Although we did not observe elevated levels of cofilin, we showed a co-localization between cofilin and the nuclear EN-actin filaments (Fig. 7c, d). Therefore, we speculate that cofilin might trigger the nuclear $p27^{Kip1}$ leading to G1 arrest. In conclusion, the defective mitosis is probably a result of more than one aspect and additional experiments need to be performed to understand this issue clearly.

Numerous actin-binding proteins localize and exert their functions in the nucleus (reviewed in Castano et al. 2010). Among those tested in this study, cofilin co-localized with the nuclear EN-actin filaments (Fig. 7c, d,), whereas its phosphorylated form (P-cofilin) did not (Fig. 7e). Besides its involvement in cell cycle progression, cofilin employs multiple modes of action—upon increase in G-actin amount, cofilin maintains actin import into the nucleus (Pendleton et al. 2003) and, at the same time, regulates actin dynamics. Cofilin severs actin filaments at low actin concentrations and nucleates actin filaments at high actin concentrations (Andrianantoandro and Pollard 2006). When filaments are bundled, they become more resistant to cofilin severing (Michelot et al. 2007). Therefore, we suggest that cofilin promotes EN-actin filament formation.

We also found Arp3 upregulated upon EN-actin overexpression (Fig. 7f, g). Arp3 is a member of Arp2/3 complex, which triggers nucleation of the new or branching of the existing actin filaments (Pantaloni et al. 2000). Although we did not study branching of the EN-actin filaments, analysis of nuclear NLS-actin filaments performed by Kokai et al. (2014) revealed that the filaments are most likely branched. Hence, we propose that Arp3 might assist in EN-actin filament nucleation and branching.

Besides cofilin and Arp3, we did not identify any other actin-associated protein to co-localize with the EN-actin filaments, despite testing many potential candidates. However, as recent studies identified nuclear actin filament formation being dependent on nuclear formin (Baarlink et al. 2013), Toca-1, (Miyamoto et al. 2011), N-WASP (Wu et al. 2006) and JMY (Zuchero et al. 2009), we assume that other nuclear-specific actin-binding proteins assist in EN-actin dynamics too.

We showed here that both homogenous and filamentous forms of EN-actin are preferentially neither enriched nor excluded from the chromatin regardless of its transcriptional state (Fig. 8g, h). Noteworthy, we observed that EN-actin filaments seem to avoid only densely packed heterochromatin (Figs. 1c, 3c–e, 7g), which indeed occurs rarely in the U2OS cells as revealed by the electron microscopy (not shown). Based on the absence of co-localization between nuclear EN-actin filaments and chromatin remodeling complexes (Fig. 8a–f), we support the notion that the actin in chromatin remodeling complexes and in complex with hnRNPs is monomeric (Obrdlik et al. 2008; Percipalle et al. 2002) and nuclear EN-actin filaments do not seem to affect chromatin state.

Similarly, formation of nuclear EN-actin filaments did not affect the gross localization of active forms of RNA polymerases I and II (Fig. 8i, j), which were concentrated in discrete foci throughout the nucleolus and nucleoplasm, respectively. The pattern of transcription foci was identical to the control cells, and all the cells were transcriptionally active. After we quantified transcription levels, we found that there is an elevation in the S-phase of the cell cycle in the presence of nuclear EN-actin filaments by 30 % in comparison with control, whereas the presence of homogenous EN-actin did not affect transcription significantly (Fig. 8k). In G1 and G2 phases, the transcription levels did not differ significantly from control. It is plausible that recruitment of EN-actin filaments to the transcription complexes in the S-phase is enabled by a more permissive state of chromatin in the S-phase. This finding also points toward the possibility that polymeric state of actin is required for transcription as has been suggested previously (Miyamoto et al. 2011; Obrdlik and Percipalle 2011; Wu et al. 2006; Ye et al. 2008; Yoo et al. 2007). Up to date, numerous studies focused on the involvement of actin in transcription of SRF-regulated genes. To trigger transcription, SRF requires its cofactor

MAL which is only imported into the nucleus when free of G-actin (Miralles et al. 2003; Vartiainen et al. 2007). Collectively, these studies revealed that formation of F-actin in the nucleus or in the cytoplasm depletes levels of G-actin, which cannot sequester MAL. MAL is in turn imported into the nucleus leading to upregulation of SRF-mediated transcription (Baarlink et al. 2013; Kokai et al. 2014; Stern et al. 2009; Vartiainen et al. 2007). It is therefore reasonable to speculate that the elevation of transcription upon EN-actin filaments formation that we observed occurs via exhaustion of free G-actin monomers. However, to answer this clearly, more experiments need to be performed.

To sum up, our study documents a potential for EN-actin to form filaments in the nucleus closely resembling actin filaments in the cytoplasm. Generation of nuclear EN-actin filaments recruits cofilin and Arp3 into the nucleus and affects cellular processes. Since our observations of the EN-actin polymerization, its behavior during cell cycle, co-localization with actin-binding proteins and transcriptional activity are in agreement with previous studies, we suggest that EN-actin fusion protein mimics the endogenous actin and may be used as a tool for future challenging research focusing on actin functions in the nucleus.

Acknowledgments P. H., A. K. and L. U. were supported by the Grant agency of the Czech Republic (P305/11/2232), P. H. and I. K. were supported by the Ministry of Youth, Sports and Education of the Czech Republic (LD12063); P. H., L. U. and M. H. were supported by Human Frontier Science Program (RGP0017/2013). A. K., I. K. and L. U. were supported by the Charles University in Prague. This publication is supported by the project "BIOCEV – Biotechnology and Biomedicine Centre of the Academy of Sciences and Charles University" (CZ.1.05/1.1.00/02.0109), from the European Regional Development Fund. This research was performed with support of the Institute of Molecular Genetics, Academy of Sciences of the Czech Republic (RVO: 68378050). We are very grateful to Prof. Primal de Lanerolle (University of Illinois at Chicago) for providing us the EN-actin plasmid and Prof. Matthew Welch (University of California, Berkeley) for providing us the Arp3 antibody. We would like to thank Iva Jelínková for excellent technical assistance and Irina Studenyak for critical reading of the manuscript.

References

Andrianantoandro E, Pollard TD (2006) Mechanism of actin filament turnover by severing and nucleation at different concentrations of ADF/cofilin. Mol Cell 24:13–23. doi:10.1016/j.molcel.2006.08.006

Aoyama N, Oka A, Kitayama K, Kurumizaka H, Harata M (2008) The actin-related protein hArp8 accumulates on the mitotic chromosomes and functions in chromosome alignment. Exp Cell Res 314:859–868. doi:10.1016/j.yexcr.2007.11.020

Baarlink C, Wang H, Grosse R (2013) Nuclear actin network assembly by formins regulates the SRF coactivator MAL. Science 340:864–867. doi:10.1126/science.1235038

Bedolla RG et al (2009) Nuclear versus cytoplasmic localization of filamin A in prostate cancer: immunohistochemical correlation with metastases Clinical cancer research : an official journal of the American Association for. Cancer Res 15:788–796. doi:10.1158/1078-0432.CCR-08-1402

Belin BJ, Cimini BA, Blackburn EH, Mullins RD (2013) Visualization of actin filaments and monomers in somatic cell nuclei. Mol Biol Cell 24:982–994. doi:10.1091/mbc.E12-09-0685

Castano E et al (2010) Actin complexes in the cell nucleus: new stones in an old field. Histochem Cell Biol 133:607–626. doi:10.1007/s00418-010-0701-2

de Lanerolle P, Serebryannyy L (2011) Nuclear actin and myosins: life without filaments. Nat Cell Biol 13:1282–1288. doi:10.1038/ncb2364

Dingova H, Fukalova J, Maninova M, Philimonenko VV, Hozak P (2009) Ultrastructural localization of actin and actin-binding proteins in the nucleus. Histochem Cell Biol 131:425–434. doi:10.1007/s00418-008-0539-z

Dong JM, Lau LS, Ng YW, Lim L, Manser E (2009) Paxillin nuclear-cytoplasmic localization is regulated by phosphorylation of the LD4 motif: evidence that nuclear paxillin promotes cell proliferation. Biochem J 418:173–184. doi:10.1042/BJ20080170

Dopie J, Skarp KP, Rajakyla EK, Tanhuanpaa K, Vartiainen MK (2012) Active maintenance of nuclear actin by importin 9 supports transcription. Proc Natl Acad Sci USA 109:E544–E552. doi:10.1073/pnas.1118880109

Dundr M et al (2007) Actin-dependent intranuclear repositioning of an active gene locus in vivo. J Cell Biol 179:1095–1103. doi:10.1083/jcb.200710058

Fenech M et al (2011) Molecular mechanisms of micronucleus, nucleoplasmic bridge and nuclear bud formation in mammalian and human cells. Mutagenesis 26:125–132. doi:10.1093/mutage/geq052

Hofmann WA (2009) Cell and molecular biology of nuclear actin. Int Rev Cell Mol Biol 273:219–263. doi:10.1016/S1937-6448(08)01806-6

Hofmann WA et al (2004) Actin is part of pre-initiation complexes and is necessary for transcription by RNA polymerase II. Nat Cell Biol 6:1094–1101. doi:10.1038/ncb1182

Hofmann WA, Arduini A, Nicol SM, Camacho CJ, Lessard JL, Fuller-Pace FV, de Lanerolle P (2009) SUMOylation of nuclear actin. J Cell Biol 186:193–200. doi:10.1083/jcb.200905016

Hu P, Wu S, Hernandez N (2004) A role for beta-actin in RNA polymerase III transcription. Genes Dev 18:3010–3015. doi:10.1101/gad.1250804

Hu Q et al (2008) Enhancing nuclear receptor-induced transcription requires nuclear motor and LSD1-dependent gene networking in interchromatin granules. Proc Natl Acad Sci USA 105:19199–19204. doi:10.1073/pnas.0810634105

Ikura T et al (2000) Involvement of the TIP60 histone acetylase complex in DNA repair and apoptosis. Cell 102:463–473

Jockusch BM, Schoenenberger CA, Stetefeld J, Aebi U (2006) Tracking down the different forms of nuclear actin. Trends Cell Biol 16:391–396. doi:10.1016/j.tcb.2006.06.006

Kano Y, Katoh K, Masuda M, Fujiwara K (1996) Macromolecular composition of stress fiber-plasma membrane attachment sites in endothelial cells in situ. Circ Res 79:1000–1006

Kapoor P, Chen M, Winkler DD, Luger K, Shen X (2013) Evidence for monomeric actin function in INO80 chromatin remodeling. Nat Struct Mol Biol 20:426–432. doi:10.1038/nsmb.2529

Kitayama K et al (2009) The human actin-related protein hArp5: nucleo-cytoplasmic shuttling and involvement in DNA repair. Exp Cell Res 315:206–217. doi:10.1016/j.yexcr.2008.10.028

Klein J, Grummt I (1999) Cell cycle-dependent regulation of RNA polymerase I transcription: the nucleolar transcription factor UBF is inactive in mitosis and early G1. Proc Natl Acad Sci USA 96:6096–6101

Kokai E et al (2014) Analysis of nuclear actin by overexpression of wild-type and actin mutant proteins. Histochem Cell Biol 141:123–135. doi:10.1007/s00418-013-1151-4

Kukalev A, Nord Y, Palmberg C, Bergman T, Percipalle P (2005) Actin and hnRNP U cooperate for productive transcription by RNA polymerase II. Nat Struct Mol Biol 12:238–244. doi:10.1038/nsmb904

McDonald D, Carrero G, Andrin C, de Vries G, Hendzel MJ (2006) Nucleoplasmic beta-actin exists in a dynamic equilibrium between low-mobility polymeric species and rapidly diffusing populations. J Cell Biol 172:541–552. doi:10.1083/jcb.200507101

Michelot A, Berro J, Guerin C, Boujemaa-Paterski R, Staiger CJ, Martiel JL, Blanchoin L (2007) Actin-filament stochastic dynamics mediated by ADF/cofilin. Curr Biol: CB 17:825–833. doi:10.1016/j.cub.2007.04.037

Miralles F, Posern G, Zaromytidou AI, Treisman R (2003) Actin dynamics control SRF activity by regulation of its coactivator MAL. Cell 113:329–342

Miyamoto K, Pasque V, Jullien J, Gurdon JB (2011) Nuclear actin polymerization is required for transcriptional reprogramming of Oct4 by oocytes. Genes Dev 25:946–958. doi:10.1101/gad.615211

Mizuguchi G, Shen X, Landry J, Wu WH, Sen S, Wu C (2004) ATP-driven exchange of histone H2AZ variant catalyzed by SWR1 chromatin remodeling complex. Science 303:343–348. doi:10.1126/science.1090701

Moulding DA et al (2007) Unregulated actin polymerization by WASp causes defects of mitosis and cytokinesis in X-linked neutropenia. J Exp Med 204:2213–2224. doi:10.1084/jem.20062324

Obrdlik A, Percipalle P (2011) The F-actin severing protein cofilin-1 is required for RNA polymerase II transcription elongation. Nucleus 2:72–79. doi:10.4161/nucl.2.1.14508

Obrdlik A, Kukalev A, Louvet E, Farrants AK, Caputo L, Percipalle P (2008) The histone acetyltransferase PCAF associates with actin and hnRNP U for RNA polymerase II transcription. Mol Cell Biol 28:6342–6357. doi:10.1128/MCB.00766-08

Oelgeschlager T (2002) Regulation of RNA polymerase II activity by CTD phosphorylation and cell cycle control. J Cell Physiol 190:160–169. doi:10.1002/jcp.10058

Pantaloni D, Boujemaa R, Didry D, Gounon P, Carlier MF (2000) The Arp2/3 complex branches filament barbed ends: functional antagonism with capping proteins. Nature Cell Biol 2:385–391. doi:10.1038/35017011

Pendleton A, Pope B, Weeds A, Koffer A (2003) Latrunculin B or ATP depletion induces cofilin-dependent translocation of actin into nuclei of mast cells. J Biol Chem 278:14394–14400. doi:10.1074/jbc.M206393200

Percipalle P, Jonsson A, Nashchekin D, Karlsson C, Bergman T, Guialis A, Daneholt B (2002) Nuclear actin is associated with a specific subset of hnRNP A/B-type proteins. Nucleic Acids Res 30:1725–1734

Philimonenko VV et al (2004) Nuclear actin and myosin I are required for RNA polymerase I transcription. Nat Cell Biol 6:1165–1172. doi:10.1038/ncb1190

Qi T, Tang W, Wang L, Zhai L, Guo L, Zeng X (2011) G-actin participates in RNA polymerase II-dependent transcription elongation by recruiting positive transcription elongation factor b (P-TEFb). J Biol Chem 286:15171–15181. doi:10.1074/jbc.M110.184374

Shen X, Mizuguchi G, Hamiche A, Wu C (2000) A chromatin remodelling complex involved in transcription and DNA processing Nature 406:541–544. doi:10.1038/35020123

Stern S, Debre E, Stritt C, Berger J, Posern G, Knoll B (2009) A nuclear actin function regulates neuronal motility by serum response factor-dependent gene transcription. J Neurosci 29:4512–4518. doi:10.1523/JNEUROSCI.0333-09.2009

Stuven T, Hartmann E, Gorlich D (2003) Exportin 6: a novel nuclear export receptor that is specific for profilin. Actin complexes. EMBO J 22:5928–5940. doi:10.1093/emboj/cdg565

Szerlong H, Hinata K, Viswanathan R, Erdjument-Bromage H, Tempst P, Cairns BR (2008) The HSA domain binds nuclear actin-related proteins to regulate chromatin-remodeling ATPases. Nat Struct Mol Biol 15:469–476. doi:10.1038/nsmb.1403

Tsai CH, Chiu SJ, Liu CC, Sheu TJ, Hsieh CH, Keng PC, Lee YJ (2009) Regulated expression of cofilin and the consequent regulation of p27(kip1) are essential for G(1) phase progression. Cell Cycle 8:2365–2374

Turner CE, Glenney JR Jr, Burridge K (1990) Paxillin: a new vinculin-binding protein present in focal adhesions. J Cell Biol 111:1059–1068

Vartiainen MK, Guettler S, Larijani B, Treisman R (2007) Nuclear actin regulates dynamic subcellular localization and activity of the SRF cofactor MAL. Science 316:1749–1752. doi:10.1126/science.1141084

Welch MD, Iwamatsu A, Mitchison TJ (1997) Actin polymerization is induced by Arp2/3 protein complex at the surface of Listeria monocytogenes. Nature 385:265–269. doi:10.1038/385265a0

White RJ, Gottlieb TM, Downes CS, Jackson SP (1995) Cell cycle regulation of RNA polymerase III transcription. Mol Cell Biol 15:6653–6662

Winder SJ, Ayscough KR (2005) Actin-binding proteins. J Cell Sci 118:651–654. doi:10.1242/jcs.01670

Woolner S, Bement WM (2009) Unconventional myosins acting unconventionally. Trends Cell Biol 19:245–252. doi:10.1016/j.tcb.2009.03.003

Wu X, Yoo Y, Okuhama NN, Tucker PW, Liu G, Guan JL (2006) Regulation of RNA-polymerase-II-dependent transcription by N-WASP and its nuclear-binding partners. Nat Cell Biol 8:756–763. doi:10.1038/ncb1433

Yang X, Yu K, Hao Y, Li DM, Stewart R, Insogna KL, Xu T (2004) LATS1 tumour suppressor affects cytokinesis by inhibiting LIMK1. Nat Cell Biol 6:609–617. doi:10.1038/ncb1140

Ye J, Zhao J, Hoffmann-Rohrer U, Grummt I (2008) Nuclear myosin I acts in concert with polymeric actin to drive RNA polymerase I transcription. Genes Dev 22:322–330. doi:10.1101/gad.455908

Yoo Y, Wu X, Guan JL (2007) A novel role of the actin-nucleating Arp2/3 complex in the regulation of RNA polymerase II-dependent transcription. J Biol Chem 282:7616–7623. doi:10.1074/jbc.M607596200

Zhao K, Wang W, Rando OJ, Xue Y, Swiderek K, Kuo A, Crabtree GR (1998) Rapid and phosphoinositol-dependent binding of the SWI/SNF-like BAF complex to chromatin after T lymphocyte receptor signaling. Cell 95:625–636

Zuchero JB, Coutts AS, Quinlan ME, Thangue NB, Mullins RD (2009) p53-cofactor JMY is a multifunctional actin nucleation factor. Nat Cell Biol 11:451–459. doi:10.1038/ncb1852

4 DISCUSSION

4.1 Localization of nuclear PIs

For better understanding of nuclear PIs roles, we decided to investigate their nuclear localization. Concerning the detection of nuclear PIs, we tested several antibodies and protein domains recognizing PIs conjugated with GFP. Overexpression of PIs-binding domains tagged with GFP not only showed membranous localization as expected, but additionally also nuclear localization, most probably caused by accumulation of GFP-fusion construct in the cell nucleus (Hammond and Balla, 2015). We confirmed this unspecific accumulation as most of mutated PIs-binding domains (incapable of binding to PIs) displayed the same nuclear pattern as their wild-type forms. EEA1-FYVE was the only domain fused with GFP capable to detect specifically PI(3)P foci in the nucleoli of U2OS cells. Gillooly et al. (2000) have previously shown PI(3)P presence in nucleoli of human fibroblasts and baby hamster kidney cells which confirmed our observation.

To overcome the effect of GFP-fusion construct overexpression, we purified recombinant PLCδ1-PH, Tubby and OSH1-PH domains fused with eGFP and used them for PIs detection on fixed cells. PLCδ1-PH and Tubby domains recognize PI(4,5)P2, and OSH1-PH domain recognizes PI(4)P. By using the purified OSH1-PH domain together with specific anti-PI(4)P antibody, we demonstrated for the first time that nuclear PI(4)P can be visualized in the cell nucleus. In detail, PI(4)P localizes to the nuclear membrane, nuclear speckles and forms small foci in the nucleoplasm. We observed that PI(4)P forms distinct small foci inside and at the edges of nuclear speckles, where the active transcription takes place (reviewed in Spector and Lamond, 2011), which suggests that PI(4)P may have a role in DNA transcription. Using purified PLCδ1-PH and Tubby domains together with anti-PI(4,5)P2 antibody we detected PI(4,5)P2 in the nucleoli, nuclear speckles and nucleoplasm. Supporting our data, localization of PI(4,5)P2 in the nuclear speckles and nucleoli has been described previously (Osborne et al. 2001; Yildirim et al. 2013; Sobol et al. 2016). Our results revealing localization of PI(4)P and PI(4,5)P2 will help us to better understand the roles of these PIs in the cell nucleus. Based on our localization study we hypothesized that their functions are connected with DNA transcription.

By comparing antibodies and protein binding domains staining patterns, we have described useful tools for visualization of PI(4,5)P2 and PI(4)P in the cell nucleus. Our future plans are thus to modify and optimize this approach to detect the rest of PIs present in the cell

nucleus. Moreover, we would like to use this approach to reveal undescribed functions of nuclear PIs in a greater detail.

4.2 PI(4,5)P2 function in regulation of gene expression at epigenetic level

Nuclear PIs can associate or bind directly to many proteins (Lewis et al. 2011; Jungmichel et al. 2014), and most probably through this interaction PIs contribute to nuclear processes, such as chromatin remodelling, DNA modifications, and transcription. However, molecular mechanisms of their nuclear functions have been poorly described.

Here we showed that PI(4,5)P directly binds to histone lysine demethylase PHF8 (PHD finger protein 8)**,** which demethylates H3K9me2/1, H3K27me3, H4K20me1 (Feng et al. 2010; Liu et al. 2010; Zhu et al. 2010). Since these are all repressive histone marks, PHF8 activates the transcription of its target genes (Bannister and Kouzarides, 2011; Kouzarides, 2007). PI(4,5)P2 binding to PHF8 changes conformation. Subsequently, PHF8 affinity toward H3K9me2 is decreased. Both PI(4,5)P2 and PHF8 influence rRNA genes transcription and are in complex with proteins involved in RNA polymerase I transcription (Feng et al. 2010; Yildirim et al. 2013; Zhu et al. 2010). The decrease of H3K9me2 levels caused by PI(4,5)P2-PHF8 interaction increases expression of pre-rRNA genes. We concluded that PI(4,5)P2 acts as RNA polymerase I transcriptional regulator at the epigenetic level trough interaction with PHF8. Typically, around 50% of rRNA genes are actively transcribed in cells and thus we hypothesized that PI(4,5)P2 contributes to this regulation by fine-tuning of PHF8 activity, i.e. to "block" its activity as transcription activator to sustain normal levels of rRNA genes transcription and prevent their upregulation. In agreement, it has been previously shown that PI(4,5)P2 influences chromatin remodelling, mRNA splicing and export, regulation of RNA polymerase I transcription at initiation level (Osborne et al. 2001; Rando et al. 2002; Yildirim et al. 2013; Zhao et al. 1998). Moreover, consistently with our data PIs influencing proteins function by conformational change were previously reported by Yildirim et al. (2013) for UBF and fibrillarin and by Gelato et al. (2015) for UHRF1.

Furthermore, we confirmed that PI(4,5)P2 acts as a regulator of cellular processes at multiple levels in *C. elegans.* We decreased PI(4,5)P2 levels by RNAi mediated knockdown of PPK-1 kinase. PPK-1 kinase was described as the only *C. elegans* PI(4,5)P2 kinase capable to produce PI(4,5)P2 *in vitro* and *in vivo* (Weinkove et al. 2008; Xu et al. 2007). The decrease of PI(4,5)P2 from *C. elegans* gonad was connected with phenotypes, such as increased male incidence in the progeny or decreased brood size. Similar results upon *ppk-1* RNAi depletion observed Xu et al. (2007) however, they concluded that the observed decrease in number of

progeny is caused by impaired function of cytoplasmic PI(4,5)P2 and its function in muscles important for ovulation. Importantly, we also observed increased presence of DAPI stained bodies, decondensed chromatin, increased levels of DNA transcription and DNA damage. These observations suggest that PI(4,5)P2 depletion influences various cellular processes of *C. elegans*, which are connected with gene expression.

Up to date, there has been no study about PI(4,5)P2 interacting partners in germ cell nuclei of *C. elegans*. Therefore we identified possible PI(4,5)P2 interacting partners involved in these processes. We observed that PI(4,5)P2 interacts with various proteins present in the nuclei of germ cells thus by depletion of PI(4,5)P2 we disturbed these interactions and in turn influenced processes, such as chromosome pairing, DNA damage, apoptosis, transcription and chromatin shape. Possible PI(4,5)P2 binding partners are e.g. proteasome subunits which are important for regulation of molecular processes including DNA transcription (reviewed in Geng et al. 2012). We confirmed that PI(4,5)P2 interacts with proteasome subunits (PBS-4) and ubiquitin-proteasome interacting protein leucine rich repeat protein 1 (LRR-1) and through this interaction most probably contribute to the regulation of physiological and molecular processes in *C. elegans*. Based on our observation from mammalian cell lines, there is however a possibility that some phenotypes might be caused by decrease of H3K9me2 connected with PI(4,5)P2 depletion in *C. elegans*. We will thus investigate this possibility that PI(4,5)P2 acts as a transcriptional regulator at the epigenetic level in *C. elegans* in our future studies.

4.3 Nuclear actin

Actin can be present in two forms, monomeric globular actin (G-actin), or filamentous actin (F-actin) in the cytoplasm. F-actin is formed by polymerization of G-actin. It is known that in the cell nucleus actin is present as G-actin (reviewed in Jockusch et al. 2006) and more recently, several studies reported that also G-actin polymerization can occur in the cell nucleus (Miyamoto et al. 2011; Belin et al. 2013; Baarlink et al. 2013; Kokai et al. 2014). Therefore, we investigated whether nuclear F-actin recruits actin-binding proteins and thus affects the nuclear processes e.g. DNA transcription. After over-expression of EYEP-NLS-actin (EN-actin) construct in U2OS cells, we observed that 1 to 5 % of cells formed long thick nuclear filaments. These filaments resembled by the length and thickness cytoplasmic F-actin filaments, the majority of cells however displayed diffused nuclear actin signal. Cofilin, an actin-depolymerizing factor, and Arp3, a component of actin nucleation complex Arp2/3, are known actin binding proteins (reviewed in Bamburg and Bernstein, 2010) and we therefore investigated their co-localization with nuclear F-actin. We showed that both co-localize with

nuclear actin filaments. Next, we confirmed that EN-actin filaments did not preferentially localize to either active or inactive chromatin. Also, EN-actin did not co-localize with RNA polymerases, but on the other hand the level of transcription increases in S-phase of cell cycle in the presence of EN-actin filaments. Consistently with these data, presence of polymeric actin increases transcription in the cell nucleus (Ye et al. 2008; Baarlink et al. 2013; Kokai et al. 2014).

Additionally, the formation of EN-actin filaments causes a decrease of cell proliferation rate and an increase of additional micronuclei formation or retention of both daughter nuclei in one cell. Moulding et al. (2007) previously reported similar results as a consequence of cytoplasmic F-actin assembly. The co-localization with actin-binding proteins and changes in transcriptional activity are in an agreement with previous studies (Yoo et al. 2007; Obrdlik and Percipalle, 2011; reviewed in Miyamoto and Gurdon, 2013). Thus, we suggest that EN-actin could be used as a tool in the future research regarding actin functions in the cell nucleus. Further, we will use EN-actin to investigate role of PI(4,5)P2 -actin complex in the regulation of gene expression and to identify, whether PI(4,5)P2 is important for nuclear F-actin interaction with Arp3 or cofilin.

5 SUMMARY AND CONCLUSIONS

5.1 PCδ1-PH, Tubby and OSH1-PH domains recognize nuclear PIs

For the first time we visualized the presence of PI(4)P in the nucleus by OSH1-PH domain. We observed a specific localization of PI(4)P at the nuclear membrane, nuclear speckles and small foci in the nucleoplasm. PLCδ1-PH and Tubby domains detect PI(4,5)P2 in nucleoli, nuclear speckles and nucleoplasm.

5.2 PHF8 is PI(4,5)P2 binding partner

We showed that PHF8 and PI(4,5)P2 are direct interacting partners. The C-terminal K/R rich motif of PHF8 is the PI(4,5)P2 binding site. PHF8 and PI(4,5)P2 co-localize in the cell nucleus and nucleolus.

5.3 PI(4,5)P2 regulates rRNA genes expression at the epigenetic level interacting with PHF8

We demonstrated that PI(4,5)P2 decreases PHF8 activity as H3K9me2 histone lysine demethylase. binding of PI(4,5)P2 to PHF8 triggers conformational change in PHF8. This conformational change results in decrease of PHF8 activity as transcriptional activator and thus subsequently leads to a decrease in rRNA genes expression.

5.4 PI(4,5)P2 influences chromatin shape in germ cell nuclei *C. elegans*

We investigated PI(4,5)P2 function in *C. elegans*. After PPk-1 knockdown mediated by RNAi and subsequent depletion of PI(4,5)P2, we observed misshapen chromatin in *C. elegans* gonad. PI(4,5)P2-depleted worms exhibited phenotypes such as decreased brood size, increased male progeny incidence and an increase of univalent chromosomes.

5.5 PI(4,5)P2 influences molecular processes in *C. elegans* germ cell nuclei.

PI(4,5)P2 influences chromatin shape, and is involved in processes such as transcriptional regulation, DNA-damage-driven apoptosis, chromosome pairing and ubiquitin-proteasome degradation pathway. Based on our data, we concluded that these *C. elegans* phenotypes might be caused by (i) misshapen chromatin (ii) impaired ubiquitin-proteasome pathway or (iii) disrupted binding to essential protein. We proposed that PI(4,5)P2 is involved in regulation of molecular processes at multiple levels and as a part of many protein complexes in *C. elegans*.

5.6 Nuclear actin filaments change cellular processes

Overexpression of EN-actin caused that 1-5 % of cells form nuclear actin filaments. Nuclear F-actin filaments recruited only cofilin and Arp3, known actin binding proteins. Formation of nuclear F-actin filaments led to an increase in transcription during S-phase, decrease in cell proliferation and caused aberrant mitosis.

6 FUTURE PROSPECTS

Our results demonstrate that nuclear PI(4,5)P2 has functions as regulator of important processes. PI(4,5)P2 regulates rRNA genes expression interacting with PHF8 in mammalian cell line. Moreover, PI(4,5)P2 depletion influences molecular and physiological processes in *C. elegans*. Therefore, we plan to focus on the following questions:

6.1 Is PI(4)P involved in DNA transcription?

PI(4)P localizes in the cell nucleus to nuclear speckles where it forms small foci inside and at the edges of speckles. Based on the published data, the active transcription takes place here (reviewed in Spector and Lamond 2011). This suggests that PI(4)P may have a role in DNA transcription. Therefore we would like to confirm this assumption by identifying PI(4)P interacting partners involved in transcription and further reveal PI(4)P importance.

6.2 Can the PI(4,5)P2-PHF8 complex modulate RNA polymerase II transcription?

Here we showed that PI(4,5)P2 regulates expression of genes transcribed by RNA polymerase I through binding to PHF8. In the future, we would like to investigate whether PI(4,5)P2-PHF8 complex influences also transcription of PHF8 target genes transcribed by RNA polymerase II. PHF8 target genes are often involved in craniofacial and neural development, cell cycle progression and other important cellular processes.

6.3 Does PI(4,5)P2 decrease H3K9me2 level through interaction with PHF8 in *C. elegans*?

In the mammalian cell line, we showed that PI(4,5)P2 influences H3K9me2 level through the interaction with PHF8. Importantly, we observed an increase of DNA transcription upon PI(4,5)P2 depletion in *C. elegans* gonad. We will thus investigate the levels of H3K9me2 upon PI(4,5)P2 depletion. So far it is not known whether PI(4,5)P2 interacts with a homolog of PHF8 (Lee et al., 2015) or other similar proteins, such as jmjd-2 demethylase (Whetstine et al., 2006) or met-2 methyltransferase (Checchi and Engebrecht, 2011) in *C. elegans*. Thus we will investigate also the possibility that PI(4,5)P2 acts as an epigenetic regulator of DNA transcription in *C. elegans*.

6.4 Can PI(4,5)P2-actin complex regulate gene expression?

Here we showed that EN-actin can be used as a tool for investigation of nuclear actin function. Also, nuclear actin filaments decrease cell proliferation rate and increase formation

of additional micronuclei or retention of both daughter nuclei in one cell. Recently, Le et al. (2016) showed that nuclear actin determines global transcriptional activity. We will thus investigate role of PI(4,5)P2 in actin-mediated DNA transcription regulation.

7 REFERENCES

Alvarez-Venegas R, Sadder M, Hlavacka A, Baluska F, Xia Y, Lu G, Firsov A, Sarath G, Moriyama H, Dubrovsky JG, Avramova Z (2006) The Arabidopsis homolog of trithorax, ATX1, binds phosphatidylinositol 5-phosphate, and the two regulate a common set of target genes. Proc Natl Acad Sci U S A 103: 6049-6054

Anderson RA, Boronenkov IV, Doughman SD, Kunz J, Loijens JC (1999) Phosphatidylinositol phosphate kinases, a multifaceted family of signaling enzymes. J Biol Chem 247:9907-10.

Baarlink C, Wang H, Grosse R (2013) Nuclear actin network assembly by formins regulates the SRF coactivator MAL. Science 340:864–7. doi: 10.1126/science.1235038

Bacqueville D, Déléris P, Mendre C, et al (2001) Characterization of a G protein-activated phosphoinositide 3-kinase in vascular smooth muscle cell nuclei. J Biol Chem 276:22170–6. doi: 10.1074/jbc.M011572200

Balla T (2013) Phosphoinositides: Tiny Lipids With Giant Impact on Cell Regulation. Physiol Rev 93:1019–1137. doi: 10.1152/physrev.00028.2012

Bamburg J.R and Bernstein B.W (2010) Roles of ADF/cofilin in actin polymerization and beyond. F1000 Biol Rep 2: 62. doi: 10.3410/B2-62

Bannister A.J, and Kouzarides T (2011) Regulation of chromatin by histone modifications. Cell Research 21:381–395.

Belin BJ, Cimini BA, Blackburn EH, Mullins RD (2013) Visualization of actin filaments and monomers in somatic cell nuclei. Mol Biol Cell 24:982–94. doi: 10.1091/mbc.E12-09-0685

Bell SP, Learned RM, Jantzen HM, Tjian R (1988) Functional cooperativity between transcription factors UBF1 and SL1 mediates human ribosomal RNA synthesis. Science 241:1192–7.

Bertagnolo V, Marchisio M, Capitani S, Neri LM (1997) Intranuclear translocation of phospholipase C beta2 during HL-60 myeloid differentiation. Biochem Biophys Res Commun 235:831–7. doi: 10.1006/bbrc.1997.6893

Bertagnolo V, Mazzoni M, Ricci D, et al (1995) Identification of PI-PLC beta 1, gamma 1, and delta 1 in rat liver: subcellular distribution and relationship to inositol lipid nuclear signalling. Cell Signal 7:669–78.

Bertagnolo V, Neri LM, Marchisio M, et al (1999) Phosphoinositide 3-Kinase Activity Is Essential for all- trans -Retinoic Acid-induced Granulocytic Differentiation of HL-60 Cells Granulocytic Differentiation of HL-60 Cells. Cancer Res 59:542–546.

Blind RD, Sablin EP, Kuchenbecker KM, et al (2014) The signaling phospholipid PIP3 creates a new interaction surface on the nuclear receptor SF-1. Proc Natl Acad Sci U S A 111:15054–9. doi: 10.1073/pnas.1416740111

Blind RD, Suzawa M, Ingraham HA (2012) Direct modification and activation of a nuclear receptor-PIP_2 complex by the inositol lipid kinase IPMK. Sci Signal 5:ra44. doi: 10.1126/scisignal.2003111

Boronenkov I V, Loijens JC, Umeda M, Anderson R a (1998) Phosphoinositide signaling pathways in nuclei are associated with nuclear speckles containing pre-mRNA processing factors. Mol Biol Cell 9:3547–3560.

Boucrot E, Ferreira APA, Almeida-Souza L, et al (2015) Endophilin marks and controls a clathrin-independent endocytic pathway. Nature 517:460–5. doi: 10.1038/nature14067

Bourachot B, Yaniv M, Muchardt C (1999) The activity of mammalian brm/SNF2alpha is dependent on a high-mobility-group protein I/Y-like DNA binding domain. Mol Biol Cell 19: 3931-3939.

Bridges D, Ma JT, Park S, Inoki K,Weisman LS, Saltiel AR. (2012) Phosphatidylinositol 3,5-bisphosphate plays a role in the activation and subcellular localization of mechanistic target of rapamycin 1. Mol Biol Cell 23:2955-2962.

Bua DJ, Martin GM, Binda O, Gozani O (2013) Nuclear phosphatidylinositol-5-phosphate regulates ING2 stability at discrete chromatin targets in response to DNA damage. Sci Rep 3:2137. doi: 10.1038/srep02137

Capitani S, Cocco L, Maraldi NM, Papa S, Manzoli FA (1986) Effect of phospholipids on transcription and ribonucleoprotein processing in isolated nuclei. Adv Enzyme Regul 25: 425-438.

Checchi PM, Engebrecht J (2011) Caenorhabditis elegans histone methyltransferase MET-2 shields the male X chromosome from checkpoint machinery and mediates meiotic sex chromosome inactivation. PLoS Genet. 7(9):e1002267. doi: 10.1371/journal.pgen.1002267

Clarke JH, Emson PC, Irvine RF (2009) Distribution and neuronal expression of phosphatidylinositol phosphate kinase IIγ in the mouse brain. J Comp Neurol 517:296–312. doi: 10.1002/cne.22161

Clarke JH, Irvine RF (2012) The activity, evolution and association of phosphatidylinositol 5-phosphate 4-kinases. Adv Biol Regul 52:40–5. doi: 10.1016/j.advenzreg.2011.09.002

Cocco L, Gilmour RS, Ognibene A, et al (1987) Synthesis of polyphosphoinositides in nuclei of Friend cells. Evidence for polyphosphoinositide metabolism inside the nucleus which changes with cell differentiation. Biochem J 248:765–70.

Cooney MA, Malcuit C, Cheon B, et al (2010) Species-specific differences in the activity and nuclear localization of murine and bovine phospholipase C zeta 1. Biol Reprod 83:92–101. doi: 10.1095/biolreprod.109.079814

Cozier GE, Carlton J, McGregor AH, Gleeson PA,Teasdale RD, Mellor H, Cullen PJ (2002) The phox homology (PX) domain-dependent, 3-phosphoinositide-mediated association of sorting nexin-1 with an early sorting endosomal compartment is required for its ability to regulate epidermal growth factor receptor degradation. J Biol Chem 277:48730-48736.

Crjlen V,Visnjic D, Banfic H (2004) Presence of different phospholipase C isoforms in the nucleus and their activation during compensatory liver growth. FEBS Lett 571:35-42.

de Graaf P, Klapisz EE, Schulz TKF, et al (2002) Nuclear localization of phosphatidylinositol 4-kinase beta. J Cell Sci 115:1769–75.

de Lartigue J, Polson H, Feldman M, et al (2009) PIKfyve regulation of endosome-linked pathways. Traffic 10:883–893. doi: 10.1111/j.1600-0854.2009.00915.x

De Vries KJ, Westerman J, Bastiaens PI, et al (1996) Fluorescently labeled phosphatidylinositol transfer protein isoforms (alpha and beta), microinjected into fetal bovine heart endothelial cells, are targeted to distinct intracellular sites. Exp Cell Res 227:33–9. doi: 10.1006/excr.1996.0246

Déléris P, Bacqueville D, Gayral S, et al (2003) SHIP-2 and PTEN are expressed and active in vascular smooth muscle cell nuclei, but only SHIP-2 is associated with nuclear speckles. J Biol Chem 278:38884–91. doi: 10.1074/jbc.M300816200

Didichenko SA, Thelen M (2001) Phosphatidylinositol 3-kinase c2alpha contains a nuclear localization sequence and associates with nuclear speckles. J Biol Chem 276:48135–42. doi: 10.1074/jbc.M104610200

Divecha N.R, Rhee SG, Letcher, AJ. Irvine, RF (1993) Phosphoinositide signalling enzymes in rat liver nuclei: phosphoinositidase C isoform beta 1 is specifically, but not predominantly, located in the nucleus. Biochem J 289:617-620.

Downes C.P, Gray A, Lucocq JM (2005) Probing phosphoinositide functions in signaling and membrane trafficking. Trends Cell Biol 15:259-268.

Dupuis-Coronas S, Lagarrigue F, Ramel D, et al (2011) The nucleophosmin-anaplastic lymphoma kinase oncogene interacts, activates, and uses the kinase PIKfyve to increase invasiveness. J Biol Chem 286:32105–14. doi: 10.1074/jbc.M111.227512

Ehm P, Nalaskowski MM, Wundenberg T, Jücker M (2015) The tumor suppressor SHIP1 colocalizes in nucleolar cavities with p53 and components of PML nuclear bodies. Nucleus 6:154–164. doi: 10.1080/19491034.2015.1022701

Ellson CD, Gobert-Gosse S, Anderson KE, et al (2001) PtdIns(3)P regulates the neutrophil oxidase complex by binding to the PX domain of p40(phox). Nat Cell Biol 3:679–82. doi: 10.1038/35083076

Elong Edimo W, Derua R, Janssens V, et al (2011) Evidence of SHIP2 Ser132 phosphorylation, its nuclear localization and stability. Biochem J 439:391–401. doi: 10.1042/BJ20110173

Feng W, Yonezawa M, Ye J, Jenuwein T, and Grummt I (2010) PHF8 activates transcription of rRNA genes through H3K4me3 binding and H3K9me1/2 demethylation. Nat Struct Mol Biol 17:445-450.

Fiume R, Ramazzotti G, Faenza I, et al (2012) Nuclear PLCs affect insulin secretion by targeting PPARγ in pancreatic β cells. FASEB J 26:203–10. doi: 10.1096/fj.11-186510

Follo MY, Bosi C, Fiume R, Faenza I, Ramazzotti G, Gaboardi GC, Manzoli L, Cocco L (2006) Real-time PCR as a tool for quantitative analysis of PI-PLCbeta1 gene expression in myelodysplastic syndrome. Int J Mol Med 18:267-271.

Fuke H, Ohno M (2008) Role of poly (A) tail as an identity element for mRNA nuclear export. Nucleic Acids Res 36:1037–49. doi: 10.1093/nar/gkm1120

Fukumoto M, Ijuin T, Takenawa T (2017) PI(3,4)P2 plays critical roles in the regulation of focal adhesion dynamics of MDA-MB-231 breast cancer cells. Cancer Sci. 108(5): 941–951. doi: 10.1111/cas.13215

Garcia-Ramirez M, Rocchini C, Ausio J (1995) Modulation of chromatin folding by histone acetylation. J Biol Chem 270:17923–8.

Gaullier JM, Simonsen A, D'Arrigo A, et al (1998) FYVE fingers bind PtdIns(3)P. Nature 394:432–3. doi: 10.1038/28767

Gelato KA, Tauber M, Ong MS, et al (2014) Accessibility of different histone H3-binding domains of UHRF1 is allosterically regulated by phosphatidylinositol 5-phosphate. Mol Cell 54:905–19. doi: 10.1016/j.molcel.2014.04.004

Geng F, Wenzel S, Tansey W.P (2012) Ubiquitin and Proteasomes in Transcription. Annu Rev Biochem 81: 177–201. doi: 10.1146/annurev-biochem-052110-120012

Gillooly DJ, Morrow IC, Lindsay M, et al (2000) Localization of phosphatidylinositol 3-phosphate in yeast and mammalian cells. EMBO J 19:4577–4588. doi: 10.1093/emboj/19.17.4577

Godi A, Di Campli A, Konstantakopoulos A, et al (2004) FAPPs control Golgi-to-cell-surface membrane traffic by binding to ARF and PtdIns(4)P. Nat Cell Biol 6:393–404. doi: 10.1038/ncb1119

Gonzales ML, Anderson RA (2006) Nuclear phosphoinositide kinases and inositol phospholipids. J Biol Chem 97:252-260.

Gozani O, Karuman P, Jones DR, et al (2003) The PHD finger of the chromatin-associated protein ING2 functions as a nuclear phosphoinositide receptor. Cell 114:99–111. doi: 10.1016/S0092-8674(03)00480-X

Halstead JR, Jalink K, Divecha N (2005) An emerging role for PtdIns(4,5)P2-mediated signalling in human disease. Trends Pharmacol Sci 26:654-60. doi: 10.1016/j.tips.2005.10.004

Hammond G, Thomas C, Schiavo G (2004) Nuclear phosphoinositides and their functions. Curr Top Microbiol Immunol, 177-206.

Hammond GR V, Balla T (2015) Polyphosphoinositide binding domains: Key to inositol lipid biology. Biochim Biophys Acta 1851:746–758. doi: 10.1016/j.bbalip.2015.02.013.Polyphosphoinositide

Han BK, Emr SD (2011) Phosphoinositide [PI(3,5)P2] lipid-dependent regulation of the general transcriptional regulator Tup1. Genes Dev 25:984–995. doi: 10.1101/gad.1998611

Heo WD, Inoue T, Park WS, Kim ML, Park BO,Wandless TJ, Meyer T (2006) PI(3,4,5)P3 and PI(4,5)P2 lipids target proteins with polybasic clusters to the plasma membrane. Science 314:1458-1461.

Chang CJ, Mulholland DJ, Valamehr B, Mosessian S, Sellers WR, Wu H (2008) PTEN nuclear localization is regulated by oxidative stress and mediates p53-dependent tumor suppression. Mol Biol Cell 28:3281-3289.

Cheever ML, Sato TK, de Beer T, et al (2001) Phox domain interaction with PtdIns(3)P targets the Vam7 t-SNARE to vacuole membranes. Nat Cell Biol 3:613–8. doi: 10.1038/35083000

Choi S, Thapa N, Hedman AC, Li Z, Sacks DB, Anderson RA (2013) IQGAP1 is a novel phosphatidylinositol 4,5 bisphosphate effector in regulation of directional cell migration. Embo J 32:2617-2630.

Irvine R.F, Divecha N (1992) Phospholipids in the nucleus--metabolism and possible functions. Semin Cell Biol 3:225-235.

Ivetac I, Munday AD, Kisseleva M V, et al (2005) The type Ialpha inositol polyphosphate 4-phosphatase generates and terminates phosphoinositide 3-kinase signals on endosomes and the plasma membrane. Mol Biol Cell 16:2218–33. doi: 10.1091/mbc.E04-09-0799

Ivetac I, Gurung R, Hakim S, Horan KA, Sheffield DA, Binge LC, Majerus PW, Tiganis T, Mitchell CA (2009) Regulation of PI(3)K/Akt signalling and cellular transformation by inositol polyphosphate 4-phosphatase-1. EMBO Rep 10:487-493.

Jiang K, Liu Y , Fan J , Zhang J, Li X-A, Evers B. M, Zhu H, Jia J (2016) PI(4)P Promotes Phosphorylation and Conformational Change of Smoothened through Interaction with Its C-terminal Tail. Plos Biol 14(2):e1002375. doi: 10.1371/journal.pbio.1002375

Jockusch BM, Schoenenberger C-A, Stetefeld J, Aebi U (2006) Tracking down the different forms of nuclear actin. Trends Cell Biol 16:391–6. doi: 10.1016/j.tcb.2006.06.006

Jones DR, Bultsma Y, Keune W-J, et al (2006) Nuclear PtdIns5P as a Transducer of Stress Signaling: An In Vivo Role for PIP4Kbeta. Mol Cell 23:685–695. doi: 10.1016/j.molcel.2006.07.014

Jones DR, Foulger R, Keune W-J, et al (2013) PtdIns5P is an oxidative stress-induced second messenger that regulates PKB activation. FASEB J 27:1644–56. doi: 10.1096/fj.12-218842

Jungmichel S, Sylvestersen KB, Choudhary C, et al (2014) Specificity and commonality of the phosphoinositide-binding proteome analyzed by quantitative mass spectrometry. Cell Rep 6:578–91. doi: 10.1016/j.celrep.2013.12.038

Juris L, Montino M, Rube P, Schlotterhose P, Thumm M, Krick R (2015) PI3P binding by Atg21 organises Atg8 lipidation. Embo J 34:955-973.

Kakuk A, Friedländer E, Vereb G, et al (2006) Nucleolar localization of phosphatidylinositol 4-kinase PI4K230 in various mammalian cells. Cytometry A 69:1174–83. doi: 10.1002/cyto.a.20347

Kanai F, Liu H, Field SJ, et al (2001) The PX domains of p47phox and p40phox bind to lipid products of PI(3)K. Nat Cell Biol 3:675–8. doi: 10.1038/35083070

Karlsson T, Altankhuyag A, Dobrovolska O, Turcu D.C, Lewis A.E (2016) A polybasic motif in ErbB3-binding protein 1 (EBP1) has key functions in nucleolar localization and polyphosphoinositide interaction. Biochem J 473:2033–2047.

Kavran JM, Klein DE, Lee A, Falasca M, Isakoff SJ, Skolnik EY, Lemmon MA (1998) Specificity and promiscuity in phosphoinositide binding by pleckstrin homology domains. J Biol Chem 273:30497-30508.

Kim CG, Park D, Rhee SG (1996) The role of carboxyl-terminal basic amino acids in Gqalpha-dependent activation, particulate association, and nuclear localization of phospholipase C-beta1. J Biol Chem 271:21187–92.

Klein BM, Andrews JB, Bannan BA, et al (2008) Phospholipase C beta 4 in mouse hepatocytes: rhythmic expression and cellular distribution. Comp Hepatol 7:8. doi: 10.1186/1476-5926-7-8

Kokai E, Beck H, Weissbach J, et al (2014) Analysis of nuclear actin by overexpression of wild-type and actin mutant proteins. Histochem Cell Biol 141:123–35. doi: 10.1007/s00418-013-1151-4

Kouzarides T (2007) Chromatin Modifications and Their Function. Cell 128:693–670.

Kuvichkin, V.V (2002) DNA-lipid interactions in vitro and in vivo. Bioelectrochemistry 58:3-12.

Lalli E, Doghman M, Latre de Late P, et al (2013) Beyond steroidogenesis: novel target genes for SF-1 discovered by genomics. Mol Cell Endocrinol 371:154–9. doi: 10.1016/j.mce.2012.11.005

Larman MG, Saunders CM, Carroll J, et al (2004) Cell cycle-dependent Ca2+ oscillations in mouse embryos are regulated by nuclear targeting of PLCzeta. J Cell Sci 117:2513–21. doi: 10.1242/jcs.01109

Le HQ, Ghatak S, Yeung CY, Tellkamp F, Günschmann C, Dieterich C, Yeroslaviz A, Habermann B, Pombo A, Niessen CM, Wickström SA (2016) Mechanical regulation of transcription controls Polycomb-mediated gene silencing during lineage commitment. Nat Cell Biol 18:864-75. doi: 10.1038/ncb3387.

Lee DY, Hayes JJ, Pruss D, Wolffe AP (1993) A positive role for histone acetylation in transcription factor access to nucleosomal DNA. Cell 72:73–84.

Lewis A.E, Sommer L, Arntzen M, Strahm Y, Morrice N.A, Divecha N, D'Santos C.S (2011) Identification of nuclear phosphatidylinositol 4,5-bisphosphate-interacting proteins by neomycin extraction. Mol Cell Proteomics 10: M110.003376. doi: 10.1074/mcp.M110.003376

Lin A, Hu Q, Li C, Xing Z, Ma G, Wang C, Li J, Ye Y, Yao J, Liang K, Wang S, Park PK, Marks JR, Zhou Y, Zhou J, Hung MC, Liang H, Hu Z, Shen H, Hawke DH, Han L, Zhou Y, Lin C, Yang L (2017) The LINK-A lncRNA interacts with PtdIns(3,4,5)P3 to hyperactivate AKT and confer resistance to AKT inhibitors. Nat Cell Biol 19(3):238-251. doi: 10.1038/ncb3473.

Lindsay Y, McCoull D, Davidson L, Leslie NR, Fairservice A, Gray A, Lucocq J, Downes CP (2006) Localization of agonist-sensitive PtdIns(3,4,5)P3 reveals a nuclear pool that is insensitive to PTEN expression. J Cell Sci 119(24):5160-8. doi:10.1242/jcs.000133

Ling, K, Schill NJ, Wagoner MP, Sun Y, Anderson RA (2006) Movin' on up: the role of PtdIns(4,5)P(2) in cell migration. Trends Cell Biol 16:276-284.

Liu N, Fukami K, Yu H, Takenawa T (1996) A new phospholipase C delta 4 is induced at S-phase of the cell cycle and appears in the nucleus. J Biol Chem 271:355–60.

Liu W, Tanasa B, Tyurina O.V, Zhou T.Y, Gassmann R, Liu W.T, Ohgi K.A, Benner C, Garcia-Bassets I, Aggarwal A.K, *et al.* (2010). PHF8 mediates histone H4 lysine 20 demethylation events involved in cell cycle progression. Nature 466:508-512.

Lukinovic-Skudar V, Donlagic L, Banfic H, Visnjic D (2005) Nuclear phospholipase C-beta1b activation during G2/M and late G1 phase in nocodazole-synchronized HL-60 cells. Biochim Biophys Acta 1733:148-156.

Maag D, Maxwell MJ, Hardesty DA, et al (2011) Inositol polyphosphate multikinase is a physiologic PI3-kinase that activates Akt/PKB. Proc Natl Acad Sci USA 108:1391–6. doi: 10.1073/pnas.1017831108

Malave TM, Dent SY (2006) Transcriptional repression by Tup1-Ssn6. Biochem Cell Biol 84:437-443.

Manzoli L, Martelli AM, Billi AM, Fiume R, Cocco L (2005) Nuclear phospholipase C: involvement in signal transduction. Prog Lipid Res 44:185-206.

Martelli A.M, Gilmour RS, Bertagnolo V, Neri LM, Manzoli L, Cocco L (1992) Nuclear localization and signalling activity of phosphoinositidase C beta in Swiss 3T3 cells. Nature 358:242-245.

McCartney AJ, Zhang Y, Weisman LS (2014) Phosphatidylinositol 3,5-bisphosphate: low abundance, high significance. Bioessays 36:52–64. doi: 10.1002/bies.201300012

McLaughlin S, Smith SO, Hayman MJ, Murray D (2005) An electrostatic engine model for autoinhibition and activation of the epidermal growth factor receptor (EGFR/ErbB) family. J Gen Physiol 126:41-53.

Mellman DL, Gonzales ML, Song C, et al (2008) A PtdIns4,5P2-regulated nuclear poly(A) polymerase controls expression of select mRNAs. Nature 451:1013–1017. doi: 10.1038/nature06666

Metjian A, Roll RL, Ma AD, Abrams CS (1999) Agonists cause nuclear translocation of phosphatidylinositol 3-kinase gamma. A Gbetagamma-dependent pathway that requires the p110gamma amino terminus. J Biol Chem 274:27943–7.

Mills IG, Praefcke GJK, Vallis Y, et al (2003) EpsinR: an AP1/clathrin interacting protein involved in vesicle trafficking. J Cell Biol 160:213–22. doi: 10.1083/jcb.200208023

Miyamoto K and Gurdon J. B (2013) Transcriptional regulation and nuclear reprogramming: roles of nuclear actin and actin-binding proteins. Cell Mol Life Sci. 70(18): 3289–3302. doi: 10.1007/s00018-012-1235-7

Miyamoto K, Pasque V, Jullien J, Gurdon JB (2011) Nuclear actin polymerization is required for transcriptional reprogramming of Oct4 by oocytes. Genes Dev 25:946–58. doi: 10.1101/gad.615211

Morris JB, Hinchliffe KA, Ciruela A, et al (2000) Thrombin stimulation of platelets causes an increase in phosphatidylinositol 5-phosphate revealed by mass assay. FEBS Lett 475:57–60. doi: 10.1016/S0014-5793(00)01625-2

Moulding DA, Blundell MP, Spiller DG, et al (2007) Unregulated actin polymerization by WASp causes defects of mitosis and cytokinesis in X-linked neutropenia. J Exp Med 204:2213–24. doi: 10.1084/jem.20062324

Nady N, Lemak A,Walker JR, Avvakumov GV, Kareta MS, Achour M, Xue S, Duan S, Allali-Hassani A, Zuo X, Wang YX, Bronner C, Chédin F, Arrowsmith CH, Dhe-Paganon S (2011) Recognition of multivalent histone states associated with heterochromatin by UHRF1 protein. J Biol Chem 286:24300-24311.

Nalaskowski MM, Deschermeier C, Fanick W, Mayr GW (2002) The human homologue of yeast ArgRIII protein is an inositol phosphate multikinase with predominantly nuclear localization. Biochem J 366:549–56. doi: 10.1042/BJ20020327

Nalaskowski MM, Metzner A, Brehm MA, et al (2012) The inositol 5-phosphatase SHIP1 is a nucleo-cytoplasmic shuttling protein and enzymatically active in cell nuclei. Cell Signal 24:621–8. doi: 10.1016/j.cellsig.2011.07.012

Ndakong I, Jones DR, Lapko H, Divecha N, Avramova Z (2010) Phosphatidylinositol 5-phosphate links dehydration stress to the activity of ARABIDOPSIS TRITHORAX-LIKE factor ATX1. Plos One 5:e13396.

Neri LM, Milani D, Bertolaso L, et al (1994) Nuclear translocation of phosphatidylinositol 3-kinase in rat pheochromocytoma PC 12 cells after treatment with nerve growth factor. Cell Mol Biol (Noisy-le-grand) 40:619–26.

Obrdlik A and Percipalle P (2011) The F-actin severing protein cofilin-1 is required for RNA polymerase II transcription elongation. Nucleus 2(1): 72–79. doi: 10.4161/nucl.2.1.14508

Osborne SL, Thomas CL, Gschmeissner S, Schiavo G (2001) Nuclear PtdIns(4,5)P2 assembles in a mitotically regulated particle involved in pre-mRNA splicing. J Cell Sci 114:2501–11.

Oppelt A, Lobert VH, Haglund K, Mackey AM, Rameh LE, Liestøl K, Schink KO, Pedersen NM, Wenzel EM, Haugsten EM, Brech A, Rusten TE, Stenmark H, Wesche J (2013) Production of phosphatidylinositol 5-phosphate via PIKfyve and MTMR3 regulates cell migration. EMBO Rep 14:57-64.

Papamichos-Chronakis M, Petrakis T, Ktistaki E, Topalidou I, Tzamarias D (2002) Cti6, a PHD domain protein, bridges the Cyc8-Tup1 corepressor and the SAGA coactivator to overcome repression at GAL1. Mol Cell 9:1297-305

Patki V, Lawe DC, Corvera S, et al (1998) A functional PtdIns(3)P-binding motif. Nature 394:433–4. doi: 10.1038/28771

Pollard, T.D and Borisy, G.G (2003) Cellular motility driven by assembly and disassembly of actin filaments. Cell 112:453–46.

Posor Y, Eichhorn-Gruenig M, Puchkov D, et al (2013) Spatiotemporal control of endocytosis by phosphatidylinositol-3,4-bisphosphate. Nature 499:233–7. doi: 10.1038/nature12360

Rajakumara E,Wang Z, Ma H, Hu L, Chen H, Lin Y, Guo R,Wu F, Li H, Lan F, Shi YG, Xu Y, Patel DJ, Shi Y (2011) PHD finger recognition of unmodified histone H3R2 links UHRF1 to regulation of euchromatic gene expression. Mol Cell 43:275-284.

Rando OJ, Zhao K, Janmey P, Crabtree GR (2002) Phosphatidylinositol-dependent actin filament binding by the SWI/SNF-like BAF chromatin remodeling complex. Proc Natl Acad Sci U S A 99:2824–9. doi: 10.1073/pnas.032662899

Resnick AC, Snowman AM, Kang BN, et al (2005) Inositol polyphosphate multikinase is a nuclear PI3-kinase with transcriptional regulatory activity. Proc Natl Acad Sci U S A 102:12783–8. doi: 10.1073/pnas.0506184102

Richardson JP, Wang M, Clarke JH, et al (2007) Genomic tagging of endogenous type IIbeta phosphatidylinositol 5-phosphate 4-kinase in DT40 cells reveals a nuclear localisation. Cell Signal 19:1309–14. doi: 10.1016/j.cellsig.2007.01.010

Roberts HF, Clarke JH, Letcher AJ, Irvine RF, Hinchliffe KA (2005) Effects of lipid kinase expression and cellular stimuli on phosphatidylinositol 5-phosphate levels in mammalian cell lines. FEBS Lett 579:2868-2872.

Rose HG, Frenster JH (1965) Composition and metabolism of lipids within repressed and active chromatin of interphase lymphocytes. Biochim Biophys Acta 106: 577-91.

Rutherford AC, Traer C, Wassmer T, et al (2006) The mammalian phosphatidylinositol 3-phosphate 5-kinase (PIKfyve) regulates endosome-to-TGN retrograde transport. J Cell Sci 119:3944–57. doi: 10.1242/jcs.03153

Salamon RS, Backer JM (2013) Phosphatidylinositol-3,4,5-trisphosphate: Tool of choice for class I PI 3-kinases. BioEssays 35:602–611. doi: 10.1002/bies.201200176

Sarkes D, Rameh LE (2010) A novel HPLC-based approach makes possible the spatial characterization of cellular PtdIns5P and other phosphoinositides. Biochem J 428:375–84.

doi: 10.1042/BJ20100129
Sbrissa D, Ikonomov OC, Strakova J, Shisheva A (2004) Role for a novel signaling intermediate, phosphatidylinositol 5-phosphate, in insulin-regulated F-actin stress fiber breakdown and GLUT4 translocation. Endocrinology 145:4853–65. doi: 10.1210/en.2004-0489
Shah ZH, Jones DR, Sommer L, et al (2013) Nuclear phosphoinositides and their impact on nuclear functions. FEBS J 280:6295–6310. doi: 10.1111/febs.12543
Shen X, Xiao H, Ranallo R,Wu WH, Wu C (2003) Modulation of ATP-dependent chromatin-remodeling complexes by inositol polyphosphates. Science 299:112-114.
Shi X, Hong T, Walter KL, Ewalt M, Michishita E, Hung T, Carney D, Peña P, Lan F, Kaadige MR, Lacoste N, Cayrou C, Davrazou F, Saha A, Cairns BR, Ayer DE, Kutateladze TG, Shi Y, Côté J, Chua KF, Gozani O (2006) ING2 PHD domain links histone H3 lysine 4 methylation to active gene repression. Nature 442:96-99.
Schill NJ, Anderson RA (2009) Two novel phosphatidylinositol-4-phosphate 5-kinase type Igamma splice variants expressed in human cells display distinctive cellular targeting. Biochem J 422:473–82. doi: 10.1042/BJ20090638
Sindić A, Aleksandrova A, Fields AP, et al (2001) Presence and activation of nuclear phosphoinositide 3-kinase C2beta during compensatory liver growth. J Biol Chem 276:17754–61. doi: 10.1074/jbc.M006533200
Slessareva JE, Routt SM, Temple B, et al (2006) Activation of the Phosphatidylinositol 3-Kinase Vps34 by a G Protein α Subunit at the Endosome. Cell 126:191–203. doi: 10.1016/j.cell.2006.04.045.
Sobol M, Philimonenko V V, Marášek P, et al (2016) Nuclear PIP2 islets contribute to efficient DNA transcription.
Sobol M, Yildirim S, Philimonenko V V, et al (2013) UBF complexes with phosphatidylinositol 4,5-bisphosphate in nucleolar organizer regions regardless of ongoing RNA polymerase I activity. Nucleus 4:478–86. doi: 10.4161/nucl.27154
Spector DL, Lamond AI (2011) Nuclear speckles. Cold Spring Harb Perspect Biol 3:a000646–. doi: 10.1101/cshperspect.a000646
Stallings JD, Tall EG, Pentyala S, Rebecchi MJ (2005) Nuclear translocation of phospholipase C-delta1 is linked to the cell cycle and nuclear phosphatidylinositol 4,5-bisphosphate. J Biol Chem 280:22060-22069.
Stephens L.R, Huges K.T, Irvine R.F (1991) Pathway of phosphatidylinositol(3,4,5)-trisphosphate synthesis in activated neutrophils. Nature 351:33-39.
Strahl T, Hama H, DeWald DB, Thorner J (2005) Yeast phosphatidylinositol 4-kinase, Pik1, has essential roles at the Golgi and in the nucleus. J Cell Biol 171:967–979. doi: 10.1083/jcb.200504104
Su K, Xu T, Yu Z, Zhu J, Zhang Y, Wu M, Xiong Y, Liu J, Xu J (2017) Structure of the PX domain of SNX25 reveals a novel phospholipid recognition model by dimerization in the PX domain. FEBS Lett 591(13):2011-2018. doi: 10.1002/1873-3468.12688.
Suh BC, Hille B (2005) Regulation of ion channels by phosphatidylinositol 4,5-bisphosphate. Curr Opin Neurobiol 15:370-8
Tanaka K, Horiguchi K, Yoshida T, et al (1999) Evidence That a Phosphatidylinositol 3,4,5-Trisphosphate-binding Protein Can Function in Nucleus. J Biol Chem 274 :3919–3922. doi: 10.1074/jbc.274.7.3919
Toska E, Campbell HA, Shandilya J, et al (2012) Repression of Transcription by WT1-BASP1 Requires the Myristoylation of BASP1 and the PIP2-Dependent Recruitment of Histone Deacetylase. Cell Rep 2:462–469. doi: 10.1016/j.celrep.2012.08.005
Ungewickell A, Hugge C, Kisseleva M, et al (2005) The identification and characterization of

two phosphatidylinositol-4,5-bisphosphate 4-phosphatases. Proc Natl Acad Sci U S A 102:18854–9. doi: 10.1073/pnas.0509740102

Vann LR, Wooding FB, Irvine RF, Divecha N (1997) Metabolism and possible compartmentalization of inositol lipids in isolated rat-liver nuclei. Biochem J 327 (Pt 2:569–576.

Viaud J, Mansour R, Antkowiak A, et al (2015) Phosphoinositides: Important lipids in the coordination of cell dynamics. Biochimie. doi: 10.1016/j.biochi.2015.09.005

Viiri KM, Jänis J, Siggers T, Heinonen TY, Valjakka J, Bulyk ML, Mäki M, Lohi O (2009) DNA-binding and -bending activities of SAP30L and SAP30 are mediated by a zinc-dependent module and monophosphoinositides. Mol Cell Biol 29:342-56. doi: 10.1128/MCB.01213-08

Wang M, Bond NJ, Letcher AJ, et al (2010) Genomic tagging reveals a random association of endogenous PtdIns5P 4-kinases IIalpha and IIbeta and a partial nuclear localization of the IIalpha isoform. Biochem J 430:215–21. doi: 10.1042/BJ20100340

Wang YJ, Wang J, Sun HQ, et al (2003) Phosphatidylinositol 4 Phosphate Regulates Targeting of Clathrin Adaptor AP-1 Complexes to the Golgi. Cell 114:299–310. doi: 10.1016/S0092-8674(03)00603-2

Weinkove D, Bastiani M, Chessa T.A.M, Joshi D, Hauth L, Cooke F.T, Divecha N, Kim S (2008) Overexpression of PPK-1, the C. elegans Type 1 PIP kinase, inhibits growth cone collapse in the developing nervous system and causes axonal degeneration in adults. Dev Biol 313:384–397.

Whetstine JR, Nottke A, Lan F, Huarte M, Smolikov S, Chen Z, Spooner E, Li E, Zhang G, Colaiacovo M, Shi Y (2006) Reversal of histone lysine trimethylation by the JMJD2 family of histone demethylases. Cell 125(3):467-81. doi:10.1016/j.cell.2006.03.028

Wilcox A, Hinchliffe KA (2008) Regulation of extranuclear PtdIns5P production by phosphatidylinositol phosphate 4-kinase 2alpha. FEBS Lett 582:1391–4. doi: 10.1016/j.febslet.2008.03.022

Xu Y, Hortsman H, Seet L, et al (2001) SNX3 regulates endosomal function through its PX-domain-mediated interaction with PtdIns(3)P. Nat Cell Biol 3:658–66. doi: 10.1038/35083051

Xu X, Guo H, Wycuff D.L, Lee M (2007) Role of phosphatidylinositol-4-phosphate 5′ kinase (ppk-1) in ovulation of Caenorhabditis elegans. Experimental Cell Research 313:2465-2475.

Yamaga M, Fujii M, Kamata H, et al (1999) Phospholipase C-delta1 contains a functional nuclear export signal sequence. J Biol Chem 274:28537–41.

Ye J, Zhao J, Hoffmann-Rohrer U, Grummt I (2008) Nuclear myosin I acts in concert with polymeric actin to drive RNA polymerase I transcription. Genes Dev 22:322–30. doi: 10.1101/gad.455908

Yildirim S, Castano E, Sobol M, et al (2013) Involvement of phosphatidylinositol 4,5-bisphosphate in RNA polymerase I transcription. J Cell Sci 126:2730–9. doi: 10.1242/jcs.123661

Yin H.L, Janmey PA (2003) Phosphoinositide regulation of the actin cytoskeleton. Annu Rev Physiol 65:761-789.

Yoda A, Oda S, Shikano T, et al (2004) Ca2+ oscillation-inducing phospholipase C zeta expressed in mouse eggs is accumulated to the pronucleus during egg activation. Dev Biol 268:245–57. doi: 10.1016/j.ydbio.2003.12.028

Yokogawa T.S, Nagata ., Nishio T, Tsutsumi S, Ihara R, Shirai K, Morita M, Umeda, Y, Shirai N, Saitoh *et al.* (2000). Evidence that 3'-phosphorylated polyphosphoinositides are generated at the nuclear surface: use of immunostaining technique with monoclonal antibodies specific for PI 3,4-P(2). FEBS Lett 47*3*:222-226.

Yoo Y, Wu X, Guan J-L (2007) A Novel Role of the Actin-nucleating Arp2/3 Complex in the Regulation of RNA Polymerase II-dependent Transcription. J Biol Chem 282(10):7616–7623. doi: 10.1074/jbc.M607596200

Yu H, Fukami K, Watanabe Y, et al (1998) Phosphatidylinositol 4,5-bisphosphate reverses the inhibition of RNA transcription caused by histone H1. Eur J Biochem 251:281–287.

Yuan T, Cantley LC (2008) PI3K pathway alterations in cancer: variations on a theme. Oncogene 27:5497-5510.

Zhang Y, Zolov SN, Chow CY, et al (2007) Loss of Vac14, a regulator of the signaling lipid phosphatidylinositol 3,5-bisphosphate, results in neurodegeneration in mice. Proc Natl Acad Sci U S A 104:17518–23. doi: 10.1073/pnas.0702275104

Zhang Y, Akinmade D, Hamburger AW (2005) The ErbB3 binding protein Ebp1 interacts with Sin3A to repress E2F1 and AR-mediated transcription. Nucleic Acid Res 33:6024-6033.

Zhao K, Wang W, Rando OJ, et al (1998) Rapid and phosphoinositol-dependent binding of the SWI/SNF-like BAF complex to chromatin after T lymphocyte receptor signaling. Cell 95:625–636. doi: 10.1016/S0092-8674(00)81633-5

Zhu Z, Wang Y, Li X, Xu L, Wang X, Sun T, Dong X, Chen L, Mao H, Yu Y *et al.* (2010). PHF8 is a histone H3K9me2 demethylase regulating rRNA synthesis. Cell Res 20:794-801.

Zini N, Ognibene A, Bavelloni A, et al (1996) Cytoplasmic and nuclear localization sites of phosphatidylinositol 3-kinase in human osteosarcoma sensitive and multidrug-resistant Saos-2 cells. Histochem Cell Biol 106:457–64.

Zou J, Marjanovic J, Kisseleva M V, et al (2007) Type I phosphatidylinositol-4,5-bisphosphate 4-phosphatase regulates stress-induced apoptosis. Proc Natl Acad Sci U S A 104:16834–16839. doi: 10.1073/pnas.0708189104